

Spin effects in the phasing formula of eccentric compact binary inspirals till the third post-Newtonian order

Omkar Sridhar^{①,*}, Soham Bhattacharyya^{①,†}, Kaushik Paul^{①,‡} and Chandra Kant Mishra^{①,§}

Department of Physics, Indian Institute of Technology Madras, Chennai 600036, India and

Centre for Strings, Gravitation and Cosmology, Department of Physics,

Indian Institute of Technology Madras, Chennai 600036, India

(Dated: December 17, 2024)

Compact binary sources that emit gravitational waves (GW) are expected to be both spinning and have eccentric orbits. To date, there has been no closed-form expression for the phasing of GWs that contain information from both spin and eccentricity. The introduction of eccentricity can slow waveform generation, as obtaining closed-form expressions for the waveform phase is unattainable due to the complexity of the differential equations involved, often requiring slower numerical methods. However, closed-form expressions for the waveform phase can be obtained when eccentricity is treated as a small parameter, enabling quick waveform generation. In this paper, closed-form expressions for the GW phasing in the form of Taylor approximants up to the eighth power in initial eccentricity (e_0) are obtained while also including aligned spins up to the third post-Newtonian order. The phasing is obtained in both time and frequency domains. The TaylorT2 phasing is also resummed for usage in scenarios where initial eccentricities are as high as 0.5. Finally, a waveform is constructed using the e_0^2 expanded TaylorF2 phasing for aligned-spin systems added to `TaylorF2Ecc`. We perform mismatch computation between this model and `TaylorF2Ecc`. The findings indicate that for eccentricities $\gtrsim 0.15$ (defined at 10 Hz) and small spins (~ 0.2), the mismatches can be higher than 1%. This leads to an overall loss in signal-to-noise ratio and lower detection efficiency of GWs coming from eccentric spinning compact binary inspirals if the combined effects of eccentricity and aligned spins are neglected in the waveforms.

I. INTRODUCTION

Gravitational wave (GW) detections from binary black hole (BBH) [1], binary neutron star (BNS) [2, 3], and neutron-star-black hole [4] mergers by the ground-based network of LIGO [5] and Virgo [6] detectors have opened a new avenue for exploring astrophysical phenomena in the Universe. Nearly 90 compact binary coalescence (CBC) events [7–10] have been detected by the LIGO-Virgo detector network until the end of the third observing run (O3). The detection of GWs relies on a technique known as matched filtering [11–13]. In this method, the observed data is cross-correlated with simulated copies of pre-computed waveforms (also known as templates). Its accuracy heavily depends on how closely the templates match the signal hidden within the detector’s noisy data. Typically, the disagreement between the templates and the signal should be no larger than $\sim 3\%$ for detection purposes and $\sim 1\%$ for parameter estimation studies [14].

The evolution of CBC systems can be divided into three distinct phases: the low-frequency, weak field inspiral phase can be modelled accurately using post-Newtonian (PN) theory (for a detailed review on this, see Ref. [15]), while the high-frequency, strong field merger and ringdown can be described using Numerical relativity (NR) [16–18] and black hole perturbation theory (BHPT)

(see Ref. [19] for a review). The inspiralling compact binaries shed eccentricity, and their orbits are expected to circularize due to the emission of GWs [20, 21]. However, compact binaries formed via dynamical interactions in dense stellar environments or through Kozai-Lidov processes [22, 23] can have large enough residual eccentricities ($e_0 \gtrsim 0.1$) while entering the frequency band of the current ground-based detectors. Additionally, eccentricity is the cleanest signature to know about the binary formation channels and various astrophysical processes, such as the evolution of binaries in globular clusters and in galactic nuclei [24–36]. Besides, a small eccentricity does not mean that its exclusion in waveform modelling will go unpunished while doing matched filtering [37], as was found in Ref. [38, 39]. Ref. [40] demonstrates that even small initial eccentricities (e.g., 6×10^{-3} at 10 Hz) can significantly bias source parameter estimates if GW models used for matched filtering neglect eccentricity.

Current pipelines might have reduced sensitivity to eccentric binaries, potentially leading to missed detections, particularly for systems with larger eccentricities [41]. The orbits of CBC systems are expected to have eccentricities, and the components themselves have spins. Electromagnetic observations like Ref. [42] have revealed that black holes have dimensionless spins close to 0.9. Spins of individual compact objects significantly change the shape and length of the GW signal. As can be seen in Ref. [43] (see Fig. 3-6 there), the positive (negative) aligned spins about the orbital angular momentum vector largely elongate (shorten) the GW waveform. If the combined effects due to spins and eccentricity are excluded from the template bank, it can lead to biases in param-

* omkarnm1401@gmail.com

† xeonese@gmail.com

‡ kpaul.gw@gmail.com

§ ckm@physics.iitm.ac.in

eter estimation or missed event detections [41, 44, 45]. Therefore, it is crucial to include both spins and eccentricity in GW templates to avoid any biases in binary parameters in the parameter estimation and low detection efficiency of GWs coming from spinning eccentric sources.

Though progress in waveform modelling including effects due to eccentricity and spins in inspiral-only [46–54] and full inspiral-merger-ringdown (IMR) [39, 55–62] models have been made, higher PN order corrections including the combined effects of spin and eccentricity in the gravitational waveform is needed to improve their accuracy. Over the past several decades, significant progress has been made in computing spin and eccentricity effects in GW amplitude and phase at high PN orders. We highlight those here. Earlier work on GW amplitude for non-spinning but eccentric binaries was performed in Ref. [63], where the instantaneous (the part of GW radiation that depends on the state of the source at a given retarded time) contributions to the spherical harmonic modes till the 3PN order was presented. Spin effects were introduced for quasi-circular orbits in modes at the 1.5PN and 2PN order in Refs. [64] and [65] respectively. This was extended to 3.5PN, including both instantaneous and hereditary (the part of GW radiation which depends on the entire past history of the source) contributions in modes by Ref. [66]. The combined effect of spin and eccentricity in energy loss rate and GW radiation were calculated in Refs. [67, 68] up to 2PN and 2.5PN order, respectively. Additionally, Refs. [69, 70] and Refs. [54, 71] calculated the GW polarizations and modes till 1.5PN and 2PN order respectively. The modes computation was pushed to 3PN by Ref. [72]. Earlier works on GW phasing in quasi-circular binaries can be found in Ref. [73] where they calculated the 2PN phasing from the energy loss of the binary. However, the 3PN extension was a formidable task completed almost a decade later in Ref. [74]. Recently, the same group calculated the phasing for quasi-circular binaries till 4.5PN in Ref. [75]. Previous work on the phasing of GWs in eccentric systems can be found in Ref. [13], where they computed the Newtonian part of the phase. The work was then extended to 2PN in Ref. [40]. Finally, Ref. [76] extended the computation of non-spinning eccentric binaries to 3PN.

This paper is an update to the non-spinning 3PN (e_0^2 expanded) eccentric phasing of Ref. [76]. Here, we include aligned-spin effects to the small eccentricity expanded time and frequency domain phases of Ref. [76]. We use inputs from Ref. [72] to calculate various Taylor approximants or the phasing formulae. The phasing formulae/approximants are functions of intrinsic orbital parameters like mass ratios, spins, deformability factors, etc. While Ref. [76] provides results accurate to second power of initial eccentricity ($\mathcal{O}(e_0^2)$), we extend it to $\mathcal{O}(e_0^8)$.

A. Summary of the current work

In this work, we have calculated the phasing of GWs for eccentric aligned-spinning compact binary inspirals. We have obtained closed-form expressions for the phasing involving the eccentricity in the form of Taylor approximants in both the time and frequency domains. Like Ref. [76], we utilized the smallness of the eccentricity to obtain the closed-form phasing expressions. The main challenge in obtaining closed-form expression of Taylor approximants is that the differential equation governing the evolution of the eccentricity with respect to the instantaneous orbital frequency is highly non-linear and complex. The only respite, as was shown by Ref. [76] is to Taylor expand the above mentioned evolution equation with respect to the eccentricity about zero. At the e^2 order, the differential equation is separable and can be solved exactly. In this study, we extend the formalism such that the evolution equation of eccentricity can be solved till any arbitrary order following a perturbative method. We describe the method to perturbatively solve the first order differential equation towards the end of Sec. III A, and give the solution in Sec. IV A till e_0^8 , where e_0 is the eccentricity at some reference instantaneous frequency or time. We then substitute our eccentricity solution to the formula for the secular part of the adiabatic approximated TaylorT2 or the time domain phasing in Eq. (13a), and then obtain the same in Eq. (23). At the same time, we also obtain the relationship between the time to coalescence and the instantaneous frequency in Eq. (21). We also obtain other time domain Taylor approximants such as TaylorT1, TaylorT3, and TaylorT4 in Appendix C.

We utilized the stationary phase approximation (SPA) to obtain the frequency domain phasing formula or TaylorF2 in Sec. IV C. We assess the importance of the newly computed spinning eccentric corrections expanded in eccentricity up to $\mathcal{O}(e_0^2)$ in TaylorF2 phase by comparing these newly computed terms added to TaylorF2Ecc [76, 77] with TaylorF2Ecc - which is a frequency domain, inspiral-only waveform model having non-spinning eccentric and spinning quasi-circular corrections in phase. Additionally, we define $\kappa_s = (\kappa_1 + \kappa_2)/2$ and $\kappa_a = (\kappa_1 - \kappa_2)/2$, where κ_1 and κ_2 are the spin-induced quadrupole moment (SIQM) parameters [78, 79]. Both κ_1 and κ_2 are equal to one for black holes. Note that, following TaylorF2Ecc, we too set κ_1 and κ_2 equal to one while performing the comparison study. As a first validation step, we computed mismatches (defined in Eq. (30)) between the two models in chirp mass (M_{chirp}), mass ratio (q), eccentricity at 10 Hz (e_{10}), effective spin parameter (χ_{eff}) planes. In Fig. 1 and 2, we show the mismatch (denoted as color-bar) as a function of e_{10} and q , e_{10} and M_{chirp} , e_{10} and χ_{eff} (left, middle and right panels of Fig. 1, respectively), and χ_{eff} and M_{chirp} in Fig. 2. We denote the 96.5% and 99% match regions on the parameter space with solid black contours. These contours help us to distinguish the pa-

parameter space where these newly computed terms become important over `TaylorF2Ecc`. For instance, above the 99% match contour, we will not find any difference in parameter estimation results between the two models. Hence, the parameter space beyond this 99% contour is the region where these corrections will play a crucial role in identifying spinning eccentric GW signals. As it can be observed from Figs. 1 and 2, the mismatches for e_{10} vs. q , M_{chirp} , and χ_{eff} achieves a maximum value of 13%, it is highest in $\chi_{\text{eff}} - M_{\text{chirp}}$ plane reaching up to $\sim 15\%$. This indicates the need to include spin and eccentricity effects in waveform templates for spinning eccentric GW searches. In Sec. IV D, we perform a resummation of the TaylorT2 phasing with respect to the eccentricity and show in Fig. 3 that while the e^2 expanded phasing is applicable only for initial eccentricities less than 0.1, the e^8 resummed TaylorT2 phasing takes the validity of the model to initial eccentricities as high as 0.5.

This paper is organized as follows. We give a broad summary and snapshots of results in Sec. II. We explain the methods used to calculate the 3PN spin-aligned and small eccentricity expanded phase of the GWs in Section III. In Sec. IV, we calculate various PN approximants like TaylorT1-TaylorT4 (the time domain phases) and TaylorF2 (the frequency domain phase) till 3PN, which is e_0^8 expanded in eccentricity. Although we present Taylor approximants only till e^2 in the main text, we provide expressions for TaylorT2 and TaylorF2 till e_0^8 in a supplementary file. In Sec. IV B 1, we calculate the number of cycles each PN order contributes to the GW, which provides a useful measure of the relative importance of each PN order to the phasing. This study is previewed in Table I, which displays the number of cycles contributed by the spinning section of the TaylorT2 phasing for a specific spin, mass and initial eccentricity setting. In Sec. IV D, we compare the small eccentricity expanded analytical results with the numerically solved results. Finally, in Sec. V, we discuss some of the pertinent features of this study and motivate future work. We use the notations of Ref. [76] unless otherwise mentioned. Throughout the paper we set $G = c = 1$.

II. SPIN EFFECTS IN THE PHASING FORMULA

Our current work extends earlier work of Ref. [76], which calculates the small initial eccentricity expanded (till e_0^2) 3PN Taylor approximants. Our work takes in-

puts from Ref. [72], which calculates the evolution of quasi-Keplerian (QK) orbital elements due to radiation reaction. Using the QK formalism, one can define a gauge invariant orbital frequency, which, when scaled properly, becomes a dimensionless frequency that can be used as a PN parameter. Combining the information from the evolution of the PN parameter with the eccentricity evolution, we obtain the evolution of the eccentricity with respect to the PN parameter (or the orbital frequency). We expanded the eccentricity evolution equation with respect to the PN parameter till the eighth order of initial eccentricity e_0 and have solved the differential equation, obtaining the eccentricity as a function of the orbital frequency (or the PN parameter).

To calculate the orbital phasing using the eccentricity evolution equations, we utilized the adiabatic approximation in which radiation reaction time-scale is much longer compared to orbital and precessional time scales associated with eccentric orbits [80]. For calculating the Taylor approximants, we have once again used inputs from Ref. [72] to calculate the evolution of a modified PN parameter that was first defined in Ref. [81] to account for the convergence of the PN series when eccentricities are present. This, along with the analytical eccentricity solution, helped us write down the TaylorT1 approximants where we have calculated the energy flux and orbital energy as a function of the modified PN parameter and constants such as the initial eccentricity and initial orbital frequency at which the initial eccentricity is to be measured.

We have calculated the time domain orbital phase, also known as the TaylorT2 phase, as a function of both the gauge invariant PN parameter x and a gauge dependent PN parameter y where

$$x = \left(\frac{GM\omega}{c^3} \right)^{2/3}, \quad (1)$$

$$y = \left(\frac{x}{1 - e_t^2} \right)^{1/2}. \quad (2)$$

Here, G is universal gravitational constant, M is the total mass of the binary, ω is the instantaneous orbital frequency defined in Appendix A as a product of two gauge invariant QK parameters, c is the speed of light, and $e_t \equiv e$ is the time eccentricity that appears as a QK parameter in Appendix A. The TaylorT2 phasing was found to have the following form in the v parametrization (where $v = \sqrt{x}$)

$$\begin{aligned} \phi = \phi_c - \frac{1}{32\nu v^5} & \left\{ 1 + (\dots) v^2 + \frac{565}{24} \left[\delta\chi_a + (\dots) \chi_s \right] v^3 + \dots + \mathcal{O}(v^7) \right. \\ & - \frac{785}{272} e_0^2 \left(\frac{v_0}{v} \right)^{19/3} \left[1 + (\dots) v^2 + (\dots) v_0^2 - \frac{157}{54} \left[\delta\chi_a + \chi_s (\dots) \right] v_0^3 \right. \\ & \left. \left. + \frac{208012}{21195} \left[\delta\chi_a + \chi_s (\dots) \right] v^3 + \dots + \mathcal{O}(v^6) \right] \right\}, \end{aligned} \quad (3)$$

where, $\nu = \frac{m_1 m_2}{M^2}$ is the symmetric mass ratio and $\delta = \frac{m_1 - m_2}{M}$. Here, $M = m_1 + m_2$ where m_1 and m_2 are the binary component masses. v_0 is the value of the scaled dimensionless PN parameter at a reference frequency ω_0 . ϕ_c is phase of the GW signal at the time of coalescence. For the spinning sector, we have $\chi_s = \frac{\chi_1 + \chi_2}{2}$, $\chi_a = \frac{\chi_1 - \chi_2}{2}$, where $\chi_A = \frac{cS_A}{Gm_A^2}$ for $A = 1, 2$ are the dimensionless spins. S_1 and S_2 are constant magnitude spins.

Using the inverse of the modified PN parameter evolution, we found an updated relationship between the coalescence time and the modified PN parameter (which is also a monotonic function of the orbital frequency). The TaylorT3 approximant was then found by inverting the time as a function of frequency to frequency as a function of time. Using this, the TaylorT2 phase was written as a function of time instead of a function of the modified PN parameter. We finally calculated the evolution of the modified PN parameter with respect to time as a function of the modified PN parameter itself, which forms the TaylorT4 approximant.

Parameter estimation requires the computation of a match between the detected GW signal and a theoretical waveform template. This procedure occurs in the frequency space; hence, constructing waveforms in the frequency space is important. We utilized the stationary phase approximation (SPA), introduced for GW calculations in Ref. [82], valid in the early inspiral when various time scales are well separated, that is

$$t_{\text{orb}} \ll t_{\text{rr}} \quad (4)$$

where t_{orb} is the orbital timescale and t_{rr} is the radiation reaction timescale. The SPA allows one to write the Fourier domain orbital phase as linear combinations of the time domain TaylorT2 phase and the coalescence time (expressed as a function of the scaled dimensionless orbital frequency).

Throughout our Taylor approximant calculations, we have only concentrated on the secular part of the time and frequency domain phase. However, eccentricity introduces oscillatory behaviour in the phase apart from its secular evolution. However, it was shown in Ref. [76] that the oscillatory part of the phase quickly dies away with time (or the instantaneous frequency). Here, we show that the same is true for eccentric spinning systems in Appendix B.

We have calculated the number of GW cycles that occur in a GW signal when the frequency of the wave sweeps the LIGO and Virgo (and other detector) bands. For each PN order, we have determined the number of cycles that accumulate in the waveform. We found that eccentricity always reduces the signal duration in the LIGO band by taking away several cycles. On the other hand, spins can either contribute or take away cycles from a GW signal depending on whether they are aligned or anti-aligned to each other and the orbital angular momentum. For a simple extension of Table I of Ref. [76], that is at the e_0^2

level, refer to Table I for a demonstration of the same. Furthermore, we have demonstrated that our resummed analytic solution, which is faster to compute, matches the exact eccentricity numerical solution well in the small eccentricity limit, with initial eccentricities as high as 0.5. We also calculate in Appendix B the number of GW cycles contributed by the oscillatory part of the phase for different detectors.

PN order	ΔN_{cyc}
0PN (circ)	16031
0PN (ecc)	-463
1PN (circ)	439
1PN (ecc)	-15.8
1.5PN (circ)	-208 (-156)
1.5PN (ecc)	1.67 (1.25)
2PN (circ)	9.54 (7.89)
2PN (ecc)	-0.215 (-0.207)
2.5PN (circ)	-10.6 (-3.9)
2.5PN (ecc)	0.0443 (0.0167)
3PN (circ)	2.02 (-0.21)
3PN (ecc)	0.00200 (0.00369)
3.5PN (circ)	-0.662
Total	15785 (15840)

Table I. Post-Newtonian contributions to the number of GW cycles by the non-spinning (non-spinning+spinning) sections of the TaylorT2 phase for $\chi_1 = \chi_2 = 0.4$ assuming an initial eccentricity $e_0 = e(f_0) = 0.1$ for an equal mass $m_1 = m_2 = 1.4M_\odot$ system. This is computed using $\Delta N_{\text{cyc}} = [\phi(f_2) - \phi(f_1)]/\pi$. In the first column, the term ‘‘circ’’ corresponds to the contribution of the circular term at that PN order, while ‘‘ecc’’ implies the corresponding eccentric term. Since there are no spinning contributions at 0PN, 1PN and 3.5PN, the parentheses at these orders have been omitted. The binary enters the LIGO band at $f_1 = 10$ Hz. Since this is a low-mass system, the innermost stable circular orbit frequency (f_{isco}) extends beyond the LIGO band ($f_{\text{max}} = 1000$ Hz), and hence we curtail the signal at $f_2 = 1000$ Hz. The total cycles in the last row are the sum of all non-spinning (spinning) contributions. Note that these orbit calculations were done using TaylorT2 phasing expressed in the PN parameter x , while the y parameterization is used in the detailed expressions listed in Sec. IV. Also to be noted is that, in the spirit of Table I of Ref. [76], we use the phasing expression curtailed to e_0^2 order, while the expressions listed in Sec. IV are extended till e_0^8 order.

The paper’s results, including the eccentricity evolution and Taylor approximants, have been divided into three categories: non-spinning (NS), spin-orbit (SO), and spin-spin (SS) coupling terms. However, we have only presented the leading PN order NS results in this paper, as they are already available in Ref. [76].

III. METHODS

In this section, we will explain the methods and tools used to calculate the time domain and frequency domain secular phase of an eccentric orbit based on intrinsic source parameters such as binary's masses and spins. First, we will provide a brief description of the inputs used to construct the phases. To describe an eccentric orbit, we need to parameterize the orbit by relating one of the angles of the orbit (which can be the phase of the orbit or the more commonly used eccentric anomaly) with the distance of separation between the centre of masses (COM) of the two constituents in the binary system. This is called the Keplerian formalism (or its relativistic counterpart, the quasi-Keplerian formalism).

A. Eccentricity evolution

We denote the set $O \equiv \{a_r, e_r, e_t, e_\phi, n, k, f_\phi, f_t, g_\phi, g_t\}$ as orbital elements, as defined in Appendix A. All of the elements of the set O are PN functions of the energy and angular momentum and can be found in both the ADM and harmonic gauge in Ref. [83] for non-spinning systems. For spin-aligned systems, refer to Ref. [72], where O is given in one of the supplementary files as functions of the energy and angular momentum. Therefore, the time evolution of a single element of the set O can be found by the chain rule of calculus

$$\dot{O}_i = \frac{\partial O_i}{\partial E} \dot{E} + \frac{\partial O_i}{\partial L} \dot{L}. \quad (5)$$

We start by rewriting the evolution equations for eccentricity $e_t \equiv e$ and the PN parameter y . The evolution equations of x and e can be found in Ref. [72], where they write down the evolution equations in a resummed (with respect to the eccentricity) form. However, for our usage, we expand the resummed form in a Taylor expansion in eccentricity to find closed-form solutions of the Taylor approximants in an eccentricity Taylor series. Upon Taylor expanding the evolution equations of x and

e in Ref. [72] in e , and then converting from x to y using the relation in Eq. (2) we find the following evolution equations of y and e :

$$\frac{dy}{dt} = (1 - e^2)^{3/2} \nu y^9 [a_{\text{NS}} + a_{\text{SO}} + a_{\text{SS}}], \quad (6a)$$

$$\frac{de^2}{dt} = - (1 - e^2)^{3/2} \nu y^8 [b_{\text{NS}} + b_{\text{SO}} + b_{\text{SS}}]. \quad (6b)$$

The coefficients a and b are PN series, such that

$$a_{\text{NS}} = \sum_{i=0}^6 a_{\text{NS}}^i y^i, \quad (7a)$$

$$a_{\text{SO}} = \sum_{i=3}^6 a_{\text{SO}}^i y^i, \quad (7b)$$

$$a_{\text{SS}} = \sum_{i=4}^6 a_{\text{SS}}^i y^i, \quad (7c)$$

and similarly for b . For our purposes (*i.e.* while working with small eccentricities), the gauge-invariant parameter x could also have been used to express the results; however, it was observed in previous studies (for instance, in Ref. [81]) that the use of the parameter y over x helps with the convergence of PN series when dealing with cases with relatively high eccentricities. Hence, although we obtain our inputs from Ref. [72] where x has been used instead of y , we convert their results to y for our convenience and for the above reasons.

One can now use the chain rule of calculus to find the rate of change of eccentricity with respect to the PN parameter y . One obtains, for small eccentricities, that is till $\mathcal{O}(e^8)$

$$\frac{de^2}{dy} = -\frac{19e^2}{3y} (c_{\text{NS}} + c_{\text{SO}} + c_{\text{SS}}) + \frac{e^4}{y} (\dots) + \dots + \mathcal{O}(e^8), \quad (8)$$

where coefficients c_{NS} can be found in Ref. [76]. The spin-orbit and the spin-spin coefficients of the e^2 part are given by

$$c_{\text{SO}}^{1.5\text{PN}} = \left(\frac{55\nu}{57} - \frac{157}{114} \right) \chi_s - \frac{157\delta\chi_a}{114}, \quad (9a)$$

$$c_{\text{SO}}^{2.5\text{PN}} = \left(\frac{1631\delta\nu}{228} - \frac{373867\delta}{19152} \right) \chi_a + \left(-\frac{1195\nu^2}{228} + \frac{586343\nu}{19152} - \frac{373867}{19152} \right) \chi_s, \quad (9b)$$

$$c_{\text{SO}}^{3\text{PN}} = \frac{8857\pi\delta\chi_a}{1824} + \left(\frac{8857\pi}{1824} - \frac{141\pi\nu}{152} \right) \chi_s, \quad (9c)$$

$$c_{\text{SS}}^{2\text{PN}} = \chi_a^2 \left[\frac{89\delta\kappa_a}{304} + \kappa_s \left(\frac{89}{304} - \frac{89\nu}{152} \right) - \frac{623\nu}{152} + \frac{293}{304} \right] + \chi_a \chi_s \left[\frac{89\delta\kappa_s}{152} + \frac{293\delta}{152} + \kappa_a \left(\frac{89}{152} - \frac{89\nu}{76} \right) \right] + \chi_s^2 \left[\frac{89\delta\kappa_a}{304} \right]$$

$$+\kappa_s \left(\frac{89}{304} - \frac{89\nu}{152} \right) + \frac{37\nu}{152} + \frac{293}{304} \Big], \quad (9d)$$

$$\begin{aligned} c_{\text{SS}}^{3\text{PN}} = & \chi_a^2 \left[\kappa_a \left(\frac{326983\delta}{102144} - \frac{10549\delta\nu}{3648} \right) + \kappa_s \left(\frac{1123\nu^2}{608} - \frac{158223\nu}{17024} + \frac{326983}{102144} \right) + \frac{7861\nu^2}{608} - \frac{1373687\nu}{21888} + \frac{4320187}{306432} \right] \\ & + \chi_a \chi_s \left[\kappa_s \left(\frac{326983\delta}{51072} - \frac{10549\delta\nu}{1824} \right) - \frac{189737\delta\nu}{5472} + \frac{4320187\delta}{153216} + \kappa_a \left(\frac{1123\nu^2}{304} - \frac{158223\nu}{8512} + \frac{326983}{51072} \right) \right] \\ & + \chi_s^2 \left[\kappa_a \left(\frac{326983\delta}{102144} - \frac{10549\delta\nu}{3648} \right) + \kappa_s \left(\frac{1123\nu^2}{608} - \frac{158223\nu}{17024} + \frac{326983}{102144} \right) + \frac{24269\nu^2}{5472} - \frac{4337201\nu}{153216} + \frac{4320187}{306432} \right], \end{aligned} \quad (9e)$$

where γ is the Euler-Mascheroni constant.

Eq. (8) is a first-order differential equation and can be solved assuming y and e as small parameters. Note that, since we are extending our calculations to higher orders in eccentricity (the justification and benefit of which will be described in subsequent sections), Eq. (8) is not separable in nature, and a perturbative method needs to be devised to solve it. Here, we solve Eq. (8) by successively increasing the order of eccentricity we consider and using the previous order solution to maintain a quasi-separable form of the equation. For example, till e^2 order, the equation begins off as a separable equation. Now when extending to e^4 order, we maintain separability by first dividing by e^2 and then applying the e^2 order solution to the equation. We further extend this process to e^8 order. The detailed expression for the eccentricity evolution has been provided in Sec. IV A.

B. Taylor approximants or the phase of the GW waveform

Evolution of the orbital phase for binaries in quasi-circular orbits under the adiabatic approximation (i.e., the binary's orbital timescale is much shorter than the radiation reaction timescale) is given by the following differential equations,

$$\frac{d\phi}{dt} = \frac{x^{3/2}}{M}, \quad (10a)$$

$$\frac{dx}{dt} = -\frac{\mathcal{F}(x)}{dE(x)/dx}, \quad (10b)$$

where x is a gauge invariant PN parameter which was defined in Eq. (A3), $\mathcal{F}(x)$ is the GW luminosity and $E(x)$ is the orbital energy.

For eccentric orbits, the orbital phase includes oscillatory terms, as was found in Eq. (A1c) and (A1e), apart from those evolving over radiation reaction time scales and hence Eq. (10) need to be modified. However, it was shown (in the case of binaries with compact components without spins) that these oscillatory terms contribute negligibly to the orbital phase in Ref. [76] as long as the eccentricities are small which is also the case with

the present study. We show that the oscillatory terms decay away quickly with the frequency (or time) in Appendix B. While these terms can be formally included in these phase evolution equations, in the current work, we simply work with neglecting such contributions, and this leaves simply solving Eq. (10) even for binaries in quasi-elliptical orbits. Different approaches for solving these differential equations are referred to as different PN *approximants* (see, for instance, Refs. [76, 84]). While it might be interesting to work through different schemes of finding these approximants, we intend to provide four such approximants (TaylorT1, TaylorT2, TaylorT3, and TaylorT4) for which closed-form analytical expressions can be obtained.

To approximate the TaylorT1 series up to a specific PN order, we require the energy and energy flux expressed in terms of the PN parameter up to that PN order. In one of the supplementary files of Ref. [72], we can find the mean motion n , periastron advance k , and time eccentricity e_t in terms of the binary's conserved energy and angular momentum. We observe that the orbital frequency ω is defined in Eq. (A2), and the corresponding dimensionless PN parameter is defined in Eq. (A3). By multiplying the mean motion series with the periastron advance series in Ref. [72] and truncating it to 3PN, we can find ω in terms of energy and angular momentum. Transforming from ω to x using Eq. (A3) is straightforward. As a result, we now have x and e_t in terms of the energy and angular momentum. Inverting the two series leads to the energy and angular momentum expressed in terms of x and e_t . By transforming the energy to the PN parameter y , substituting the solution of e_t from Eq. (20), and truncating it to 3PN, we have obtained the energy per unit mass \mathcal{E} and the energy flux \mathcal{F} in terms of e_0 , y_0 , and y and have shown it in Appendix C. Similarly, the TaylorT2 approximant is obtained by performing a series expansion of the ratio on the RHS of Eq. (10b) and then solving the following set of equations by integration (see, for instance Sec. VIB of Ref. [76])

Eq. (6a) can now be inverted to obtain the evolution of time with respect to the PN frequency parameter y . After its inversion from $\frac{dy}{dt}$ to $\frac{dt}{dy}$, the RHS is expanded both with respect to the PN parameter y and eccentricity e . Then the solution for the eccentricity, that is Eq. (20)

is replaced in the place of e and the whole of the RHS is again expanded, now in terms of y , y_0 , and e_0 , up to

3PN and $\mathcal{O}(e_0^8)$. One then obtains

$$\frac{dt}{dy} = \frac{5M}{32y^9\nu} (T_{\text{NS}} + T_{\text{SO}} + T_{\text{SS}}), \quad (11)$$

where,

$$T_{\text{NS}} = 1 + \frac{5e_0^2}{8} \left(\frac{y_0}{y}\right)^{19/3} + \mathcal{O}(y^2, e_0^4), \quad (12a)$$

$$T_{\text{SO}}^{1.5\text{PN}} = y^3 \left[\frac{113\delta\chi_a}{12} + \left(\frac{113}{12} - \frac{19\nu}{3}\right)\chi_s \right] + e_0^2 \left(\frac{y_0}{y}\right)^{19/3} \left\{ y^3 \left[\frac{611\delta\chi_a}{27} + \left(\frac{611}{27} - \frac{1319\nu}{216}\right)\chi_s \right] + y_0^3 \left[\left(\frac{275\nu}{216} - \frac{785}{432}\right)\chi_s - \frac{785\delta\chi_a}{432} \right] \right\} + \mathcal{O}(e_0^4), \quad (12b)$$

$$T_{\text{SS}}^{2\text{PN}} = y^4 \left[\chi_a^2 \left\{ -5\delta\kappa_a + (10\nu - 5)\kappa_s + 10\nu - \frac{1}{16} \right\} + \chi_a\chi_s \left\{ (20\nu - 10)\kappa_a - 10\delta\kappa_s - \frac{\delta}{8} \right\} + \chi_s^2 \left\{ -5\delta\kappa_a + (10\nu - 5)\kappa_s - \frac{39\nu}{4} - \frac{1}{16} \right\} \right] + e_0^2 \left(\frac{y_0}{y}\right)^{19/3} \left[y^4 \left\{ \chi_a^2 \left[-\frac{5149\delta\kappa_a}{384} + \frac{5149\nu}{192} + \left(\frac{5149\nu}{192} - \frac{5149}{384}\right)\kappa_s - \frac{197}{768} \right] + \chi_a\chi_s \left[\left(\frac{5149\nu}{96} - \frac{5149}{192}\right)\kappa_a - \frac{197\delta}{384} - \frac{5149\delta\kappa_s}{192} \right] + \chi_s^2 \left[-\frac{5149\delta\kappa_a}{384} - \frac{619\nu}{24} + \left(\frac{5149\nu}{192} - \frac{5149}{384}\right)\kappa_s - \frac{197}{768} \right] \right\} + y_0^4 \left\{ \chi_a^2 \left[\frac{445\delta\kappa_a}{384} - \frac{445\nu}{192} + \left(\frac{445}{384} - \frac{445\nu}{192}\right)\kappa_s + \frac{65}{768} \right] + \chi_a\chi_s \left[\left(\frac{445}{192} - \frac{445\nu}{96}\right)\kappa_a + \frac{65\delta}{384} + \frac{445\delta\kappa_s}{192} \right] + \chi_s^2 \left[\frac{445\delta\kappa_a}{384} + \frac{95\nu}{48} + \left(\frac{445}{384} - \frac{445\nu}{192}\right)\kappa_s + \frac{65}{768} \right] \right\} \right] + \mathcal{O}(e_0^4), \quad (12c)$$

$$T_{\text{SO}}^{2.5\text{PN}} = y^5 \left[\chi_a \left(\frac{7\delta\nu}{2} + \frac{146597\delta}{2016} \right) + \left(-\frac{17\nu^2}{2} - \frac{1213\nu}{18} + \frac{146597}{2016} \right)\chi_s \right] + e_0^2 \left(\frac{y_0}{y}\right)^{19/3} \left[y^5 \left\{ \chi_a \left(\frac{1203689\delta\nu}{5184} - \frac{13842365\delta}{435456} \right) + \left(-\frac{39331\nu^2}{324} + \frac{19696429\nu}{108864} - \frac{13842365}{435456} \right)\chi_s \right\} + y_0^2 y^3 \left\{ \chi_a \left(\frac{1730963\delta}{27216} - \frac{120367\delta\nu}{972} \right) + \left(\frac{259843\nu^2}{7776} - \frac{30698935\nu}{217728} + \frac{1730963}{27216} \right)\chi_s \right\} + y_0^3 y^2 \left\{ \chi_a \left(\frac{26089475\delta}{435456} - \frac{316355\delta\nu}{5184} \right) + \left(\frac{110825\nu^2}{2592} - \frac{22426535\nu}{217728} + \frac{26089475}{435456} \right)\chi_s \right\} + y_0^5 \left\{ \chi_a \left(\frac{242719\delta\nu}{15552} - \frac{1279073\delta}{62208} \right) + \left(-\frac{10805\nu^2}{972} + \frac{146807\nu}{3888} - \frac{1279073}{62208} \right)\chi_s \right\} \right] + \mathcal{O}(e_0^4), \quad (12d)$$

$$T_{\text{SO}}^{3\text{PN}} = y^6 \left[\left(26\pi\nu - \frac{227\pi}{6} \right)\chi_s - \frac{227}{6}\pi\delta\chi_a \right] + e_0^2 \left(\frac{y_0}{y}\right)^{19/3} \left[y^6 \left\{ \left(\frac{4052537\pi\nu}{31104} - \frac{31241125\pi}{124416} \right)\chi_s - \frac{31241125\pi\delta\chi_a}{124416} \right\} + y_0^3 y^3 \left\{ \frac{4987553\pi\delta\chi_a}{31104} + \left(\frac{4987553\pi}{31104} - \frac{476689\pi\nu}{7776} \right)\chi_s \right\} + y_0^6 \left\{ \left(\frac{188315\pi\nu}{31104} - \frac{785215\pi}{124416} \right)\chi_s - \frac{785215\pi\delta\chi_a}{124416} \right\} \right] + \mathcal{O}(e_0^4), \quad (12e)$$

$$T_{\text{SS}}^{3\text{PN}} = y^6 \left[\chi_a^2 \left\{ \kappa_a \left(\frac{299\delta\nu}{24} - \frac{5203\delta}{112} \right) + 12\nu^2 - \frac{53563\nu}{1008} + \left(12\nu^2 + \frac{8851\nu}{84} - \frac{5203}{112} \right)\kappa_s + \frac{268895}{8064} \right\} + \chi_a\chi_s \left\{ \left(24\nu^2 + \frac{8851\nu}{42} - \frac{5203}{56} \right)\kappa_a - \frac{149\delta\nu}{72} + \frac{268895\delta}{4032} + \left(\frac{299\delta\nu}{12} - \frac{5203\delta}{56} \right)\kappa_s \right\} + \chi_s^2 \left\{ \kappa_a \left(\frac{299\delta\nu}{24} - \frac{5203\delta}{112} \right) - \frac{683\nu^2}{36} - \frac{165941\nu}{2016} + \left(12\nu^2 + \frac{8851\nu}{84} - \frac{5203}{112} \right)\kappa_s + \frac{268895}{8064} \right\} \right]$$

$$\begin{aligned}
& + e_0^2 \left(\frac{y_0}{y} \right)^{19/3} \left[y^6 \left\{ \chi_a^2 \left[\kappa_a \left(-\frac{836147\delta\nu}{13824} - \frac{4689653\delta}{129024} \right) + \frac{197635\nu^2}{768} - \frac{819409469\nu}{1306368} + \left(\frac{197635\nu^2}{768} + \frac{2362901\nu}{193536} \right. \right. \right. \\
& \left. \left. \left. - \frac{4689653}{129024} \right) \kappa_s + \frac{3345863285}{20901888} \right] + \chi_a \chi_s \left[\left(\frac{197635\nu^2}{384} + \frac{2362901\nu}{96768} - \frac{4689653}{64512} \right) \kappa_a - \frac{13785319\delta\nu}{373248} \right. \right. \\
& \left. \left. + \frac{3345863285\delta}{10450944} + \left(-\frac{836147\delta\nu}{6912} - \frac{4689653\delta}{64512} \right) \kappa_s \right] + \chi_s^2 \left[\kappa_a \left(-\frac{836147\delta\nu}{13824} - \frac{4689653\delta}{129024} \right) - \frac{25616525\nu^2}{93312} \right. \right. \\
& \left. \left. - \frac{37317125\nu}{746496} + \left(\frac{197635\nu^2}{768} + \frac{2362901\nu}{193536} - \frac{4689653}{129024} \right) \kappa_s + \frac{3345863285}{20901888} \right] \right\} + y_0^2 y^4 \left\{ \chi_a^2 \left[\kappa_a \left(\frac{1014353\delta\nu}{13824} \right. \right. \right. \\
& \left. \left. \left. - \frac{14587117\delta}{387072} \right) - \frac{1014353\nu^2}{6912} + \frac{3714695\nu}{48384} + \left(-\frac{1014353\nu^2}{6912} + \frac{28788059\nu}{193536} - \frac{14587117}{387072} \right) \kappa_s - \frac{558101}{774144} \right] \right. \\
& \left. + \chi_a \chi_s \left[\left(-\frac{1014353\nu^2}{3456} + \frac{28788059\nu}{96768} - \frac{14587117}{193536} \right) \kappa_a + \frac{38809\delta\nu}{13824} - \frac{558101\delta}{387072} + \left(\frac{1014353\delta\nu}{6912} - \frac{14587117\delta}{193536} \right) \kappa_s \right] \right. \\
& \left. + \chi_s^2 \left[\kappa_a \left(\frac{1014353\delta\nu}{13824} - \frac{14587117\delta}{387072} \right) + \frac{121943\nu^2}{864} - \frac{13757353\nu}{193536} + \left(-\frac{1014353\nu^2}{6912} + \frac{28788059\nu}{193536} - \frac{14587117}{387072} \right) \kappa_s \right. \right. \\
& \left. \left. - \frac{558101}{774144} \right] \right\} + y_0^3 y^3 \left\{ \left(\frac{191854\nu}{729} - \frac{95927}{1458} \right) \chi_a^2 + \chi_a \left(\frac{744763\delta\nu}{11664} - \frac{95927\delta}{729} \right) \chi_s + \left(-\frac{72545\nu^2}{5832} + \frac{744763\nu}{11664} \right. \right. \\
& \left. \left. - \frac{95927}{1458} \right) \chi_s^2 \right\} + y_0^4 y^2 \left\{ \chi_a^2 \left[\kappa_a \left(\frac{179335\delta\nu}{4608} - \frac{14789575\delta}{387072} \right) - \frac{179335\nu^2}{2304} + \frac{7669835\nu}{96768} + \left(-\frac{179335\nu^2}{2304} \right. \right. \right. \\
& \left. \left. \left. + \frac{22321645\nu}{193536} - \frac{14789575}{387072} \right) \kappa_s - \frac{2160275}{774144} \right] + \chi_a \chi_s \left[\left(-\frac{179335\nu^2}{1152} + \frac{22321645\nu}{96768} - \frac{14789575}{193536} \right) \kappa_a \right. \right. \\
& \left. \left. + \frac{26195\delta\nu}{4608} - \frac{2160275\delta}{387072} + \left(\frac{179335\delta\nu}{2304} - \frac{14789575\delta}{193536} \right) \kappa_s \right] + \chi_s^2 \left[\kappa_a \left(\frac{179335\delta\nu}{4608} - \frac{14789575\delta}{387072} \right) + \frac{38285\nu^2}{576} \right. \right. \\
& \left. \left. - \frac{12079205\nu}{193536} + \left(-\frac{179335\nu^2}{2304} + \frac{22321645\nu}{193536} - \frac{14789575}{387072} \right) \kappa_s - \frac{2160275}{774144} \right] \right\} + y_0^6 \left\{ \chi_a^2 \left[\kappa_a \left(\frac{4530515\delta}{387072} \right. \right. \right. \\
& \left. \left. \left. - \frac{64385\delta\nu}{4608} \right) + \frac{121355\nu^2}{6912} - \frac{105953815\nu}{2612736} + \left(\frac{121355\nu^2}{6912} - \frac{7234685\nu}{193536} + \frac{4530515}{387072} \right) \kappa_s + \frac{122165975}{20901888} \right] \right. \\
& \left. + \chi_a \chi_s \left[\left(\frac{121355\nu^2}{3456} - \frac{7234685\nu}{96768} + \frac{4530515}{193536} \right) \kappa_a - \frac{5993155\delta\nu}{373248} + \frac{122165975\delta}{10450944} + \left(\frac{4530515\delta}{193536} - \frac{64385\delta\nu}{2304} \right) \kappa_s \right] \right. \\
& \left. + \chi_s^2 \left[\kappa_a \left(\frac{4530515\delta}{387072} - \frac{64385\delta\nu}{4608} \right) - \frac{957695\nu^2}{93312} + \frac{5837485\nu}{5225472} + \left(\frac{121355\nu^2}{6912} - \frac{7234685\nu}{193536} + \frac{4530515}{387072} \right) \kappa_s \right. \right. \\
& \left. \left. + \frac{122165975}{20901888} \right] \right\} \Big] + \mathcal{O}(e_0^4). \tag{12f}
\end{aligned}$$

The coalescence time t can be obtained by integrating $dt = dy/(dy/dt)$. Now that we have already inverted Eq. (6a), we can obtain the time to coalescence as a function of initial eccentricity and PN parameter y by directly integrating Eq. (11). The evolution equation of the TaylorT2 phasing can be written as follows

$$\frac{d\langle\phi\rangle}{dy} = \frac{d\langle\phi\rangle}{dt} \frac{dt}{dy} = (1 - e_t^2)^{3/2} \frac{y^3}{M} \frac{dt}{dy}, \tag{13a}$$

$$\frac{dt}{dy} = -\frac{dE(y, e_t)/dy}{\langle\mathcal{F}(y, e_t)\rangle}, \tag{13b}$$

where $\langle\cdot\rangle$ represent averaged quantities.¹

Further, Eq. (11) can directly be used in Eq. (13a), which can be integrated to obtain the TaylorT2 phasing as a function of e_0 and y . This then gives us the desired parametric solution for TaylorT2, i.e. $\{t(y, y_0, e_0), \phi(y, y_0, e_0)\}$. They're given by,

$$\begin{aligned}
t = & -\frac{5M}{256\nu y^8} \left\{ t_{\text{circ}} + \frac{15}{43} e_0^2 \left(\frac{y_0}{y} \right)^{19/3} \left[t_{\text{SO, ecc}} + t_{\text{SS, ecc}} \right] \right. \\
& \left. + \frac{2175}{13072} e_0^4 \left(\frac{y_0}{y} \right)^{19/3} \left[\dots + \mathcal{O}(y^6) \right] + \dots + \mathcal{O}(e_0^8) \right\}, \tag{14a}
\end{aligned}$$

¹ Note, $\phi \simeq \langle\phi\rangle$ over radiation reaction time-scales.

$$\phi = -\frac{1}{32\nu y^5} \left\{ \phi_{\text{circ}} - \frac{105}{272} e_0^2 \left(\frac{y_0}{y} \right)^{19/3} \left[\phi_{\text{SO,ecc}} + \phi_{\text{SS,ecc}} \right] - \frac{15225}{82688} e_0^4 \left(\frac{y_0}{y} \right)^{19/3} \left[\dots + \mathcal{O}(y^6) \right] + \dots + \mathcal{O}(e_0^8) \right\}, \quad (14b)$$

The TaylorT3 approximant is derived following the exact process followed by Ref. [76] in Sec VI. C. To recapitulate, $y(t)$ is obtained by performing a series inversion of $t(y)$ using an ansatz. Then, there is a simultaneous transformation of variables from y to $F = y^3(1 - e^2)/(\pi M)$ and t to $\theta = [\eta(t_c - t)/5M]^{-1/8}$. This gives us an expression for $F(\theta)$, including spins up to 3PN of the following form

$$F = \frac{\theta^3}{8M\pi} \left\{ F_{\text{circ}} - \frac{471}{344} e_0^2 \left(\frac{\theta_0}{\theta} \right)^{19/3} \left[F_{\text{SO,ecc}} + F_{\text{SS,ecc}} \right] \right\}, \quad (15a)$$

$$\langle \phi \rangle - \phi_c = -\frac{1}{\nu \theta^5} \left\{ \phi_{\text{circ}} - \frac{7065}{11696} e_0^2 \left(\frac{\theta_0}{\theta} \right)^{19/3} \left[\phi_{\text{SO,ecc}} + \phi_{\text{SS,ecc}} \right] \right\}. \quad (15b)$$

It must be noted that, as has been described in Sec. VI C of Ref. [76] and further elaborated upon in Ref. [84], the TaylorT3 approximant behaves in a non-monotonic manner at certain PN orders. This renders its usage in practical applications ill-advised, and we have provided their detailed expressions in Appendix C for the sake of completeness.

The TaylorT4 approximant is computed by expanding Eq. (6a) in y till 3PN and in eccentricity till $\mathcal{O}(e^8)$, using the eccentricity solution from Eq. (20) and then re-expanding till 3PN. The expression for dy/dt with spinning terms up to $\mathcal{O}(y^6)$ is provided in Appendix C and is of the functional form

$$\frac{dy}{dt} = \frac{32y^9\nu}{5M} \left\{ \rho_{\text{circ}} - \frac{5}{8} e_0^2 \left(\frac{y_0}{y} \right)^{19/3} \left[\rho_{\text{SO,ecc}} + \rho_{\text{SS,ecc}} \right] - \frac{725}{2432} e_0^4 \left(\frac{y_0}{y} \right)^{19/3} \left[\dots + \mathcal{O}(y^6) \right] + \mathcal{O}(e_0^8) \right\}. \quad (16)$$

We also calculate the spinning eccentric corrections in the Fourier domain TaylorF2 phase by performing a sta-

tionary phase approximation (SPA) of a time domain waveform [76]. The frequency domain SPA waveform is widely used for fast parameter estimation and template bank generation and, hence, is a crucial part of this analysis. We have put the exact form of the TaylorF2 phasing in Sec. IV C 1. The TaylorF2 phase can be written in terms of the coalescence time t and the TaylorT2 phase ϕ as was shown in Ref. [76]

$$\Psi = 2\pi f t(f) - 2\phi[t(f)] + 2\Phi_0 - \frac{\pi}{4}, \quad (17)$$

where Ψ has a structure given by

$$\Psi = \frac{3}{128\nu y^5} \left\{ \Psi_{\text{circ}} + \frac{650}{731} e_0^2 \left(\frac{y_0}{y} \right)^{19/3} \left[\Psi_{\text{SO,ecc}} + \Psi_{\text{SS,ecc}} \right] + \frac{47125}{111112} e_0^4 \left(\frac{y_0}{y} \right)^{19/3} \left[\dots + \mathcal{O}(y^6) \right] + \dots + \mathcal{O}(e_0^8) \right\}. \quad (18)$$

IV. SPIN EFFECTS IN GRAVITATIONAL WAVEFORMS: (ANTI-)ALIGNED SPINS

In this section, we display the eccentricity evolution and phase of the orbit of a spin-aligned eccentric binary system using the PN approximants in the time domain (TaylorT2) and in the frequency domain (TaylorF2), respectively. Additionally, we also quantify the effect of newly computed spinning eccentric corrections expanded in eccentricity up to $\mathcal{O}(e_0^2)$ in TaylorF2 phase by performing a mismatch study between TaylorF2Ecc [76, 77] and all these terms added to TaylorF2Ecc. We also calculate a resummed version of TaylorT2 in this section. We give the Taylor approximants TaylorT1, TaylorT3, and TaylorT4 in Appendix C.

A. Eccentricity evolution

Solving Eq. (8) order by order in both e and y , as described in Sec. III A, one finds the structure of the eccentricity solution $e(y)$ in terms of an initial eccentricity e_0 at some initial frequency $y_0 = y(t_0)$ (where t_0 is some initial reference time) as

$$e^2(y, y_0; e_0) = e_0^2 \left(\frac{y_0}{y} \right)^{19/3} \left[d_{\text{NS}} + d_{\text{SO}} + d_{\text{SS}} \right] + e_0^4 \left(\frac{y_0}{y} \right)^{19/3} \left[\dots + \left(\frac{y_0}{y} \right)^{19/3} (\dots) \right] + \dots + \mathcal{O}(e_0^8). \quad (19)$$

The non-spinning coefficient d_{NS} till 3PN can be found in Ref. [76]. The SO and SS coefficients are given by

$$d_{\text{SO}}^{1.5\text{PN}} = y^3 \left[\frac{157\delta\chi_a}{54} + \left(\frac{157}{54} - \frac{55\nu}{27} \right) \chi_s \right] + y_0^3 \left[\left(\frac{55\nu}{27} - \frac{157}{54} \right) \chi_s - \frac{157\delta\chi_a}{54} \right], \quad (20a)$$

$$d_{\text{SO}}^{2.5\text{PN}} = y^5 \left[\chi_a \left(\frac{66571\delta\nu}{9720} + \frac{4505701\delta}{272160} \right) + \left(-\frac{2191\nu^2}{486} - \frac{1166491\nu}{68040} + \frac{4505701}{272160} \right) \chi_s \right] + y_0^5 \left[\chi_a \left(\frac{242719\delta\nu}{9720} - \frac{1279073\delta}{38880} \right) + \left(-\frac{4322\nu^2}{243} + \frac{146807\nu}{2430} - \frac{1279073}{38880} \right) \chi_s \right] + y^2 y_0^3 \left[\chi_a \left(\frac{444781\delta}{54432} - \frac{30929\delta\nu}{1944} \right) + \left(\frac{10835\nu^2}{972} - \frac{588821\nu}{27216} + \frac{444781}{54432} \right) \chi_s \right] + y^3 y_0^2 \left[\chi_a \left(\frac{444781\delta}{54432} - \frac{30929\delta\nu}{1944} \right) + \left(\frac{10835\nu^2}{972} - \frac{588821\nu}{27216} + \frac{444781}{54432} \right) \chi_s \right], \quad (20b)$$

$$d_{\text{SO}}^{3\text{PN}} = y^6 \left[\left(\frac{45277\pi\nu}{3888} - \frac{316469\pi}{15552} \right) \chi_s - \frac{316469\pi\delta\chi_a}{15552} \right] + y_0^6 \left[\left(\frac{37663\pi\nu}{3888} - \frac{157043\pi}{15552} \right) \chi_s - \frac{157043\pi\delta\chi_a}{15552} \right] + y^3 y_0^3 \left[\frac{59189\pi\delta\chi_a}{1944} + \left(\frac{59189\pi}{1944} - \frac{20735\pi\nu}{972} \right) \chi_s \right], \quad (20c)$$

$$d_{\text{SS}}^{2\text{PN}} = y^4 \left\{ \chi_a^2 \left[-\frac{89\delta\kappa_a}{192} + \kappa_s \left(\frac{89\nu}{96} - \frac{89}{192} \right) + \frac{623\nu}{96} - \frac{293}{192} \right] + \chi_a \chi_s \left[-\frac{89\delta\kappa_s}{96} - \frac{293\delta}{96} + \kappa_a \left(\frac{89\nu}{48} - \frac{89}{96} \right) \right] + \chi_s^2 \left[-\frac{89\delta\kappa_a}{192} + \kappa_s \left(\frac{89\nu}{96} - \frac{89}{192} \right) - \frac{37\nu}{96} - \frac{293}{192} \right] \right\} + y_0^4 \left\{ \chi_a^2 \left[\frac{89\delta\kappa_a}{192} + \kappa_s \left(\frac{89}{192} - \frac{89\nu}{96} \right) - \frac{623\nu}{96} + \frac{293}{192} \right] + \chi_a \chi_s \left[\frac{89\delta\kappa_s}{96} + \frac{293\delta}{96} + \kappa_a \left(\frac{89}{96} - \frac{89\nu}{48} \right) \right] + \chi_s^2 \left[\frac{89\delta\kappa_a}{192} + \kappa_s \left(\frac{89}{192} - \frac{89\nu}{96} \right) + \frac{37\nu}{96} + \frac{293}{192} \right] \right\}, \quad (20d)$$

$$d_{\text{SS}}^{3\text{PN}} = y^6 \left\{ \chi_a^2 \left[\kappa_a \left(\frac{3565\delta\nu}{6912} - \frac{133943\delta}{64512} \right) + \kappa_s \left(\frac{10795\nu^2}{3456} + \frac{451739\nu}{96768} - \frac{133943}{64512} \right) + \frac{75565\nu^2}{3456} + \frac{8491589\nu}{373248} - \frac{33265999}{5225472} \right] + \chi_a \chi_s \left[\kappa_s \left(\frac{3565\delta\nu}{3456} - \frac{133943\delta}{32256} \right) + \frac{1304159\delta\nu}{93312} - \frac{33265999\delta}{2612736} + \kappa_a \left(\frac{10795\nu^2}{1728} + \frac{451739\nu}{48384} - \frac{133943}{32256} \right) \right] + \chi_s^2 \left[\kappa_a \left(\frac{3565\delta\nu}{6912} - \frac{133943\delta}{64512} \right) + \kappa_s \left(\frac{10795\nu^2}{3456} + \frac{451739\nu}{96768} - \frac{133943}{64512} \right) - \frac{440045\nu^2}{93312} + \frac{43607327\nu}{2612736} - \frac{33265999}{5225472} \right] \right\} + y_0^6 \left\{ \chi_a^2 \left[\kappa_a \left(\frac{906103\delta}{193536} - \frac{12877\delta\nu}{2304} \right) + \kappa_s \left(\frac{24271\nu^2}{3456} - \frac{1446937\nu}{96768} + \frac{906103}{193536} \right) + \frac{169897\nu^2}{3456} - \frac{40961143\nu}{373248} + \frac{17465819}{746496} \right] + \chi_a \chi_s \left[\kappa_s \left(\frac{906103\delta}{96768} - \frac{12877\delta\nu}{1152} \right) - \frac{5526373\delta\nu}{93312} + \frac{17465819\delta}{373248} + \kappa_a \left(\frac{24271\nu^2}{1728} - \frac{1446937\nu}{48384} + \frac{906103}{96768} \right) \right] + \chi_s^2 \left[\kappa_a \left(\frac{906103\delta}{193536} - \frac{12877\delta\nu}{2304} \right) + \kappa_s \left(\frac{24271\nu^2}{3456} - \frac{1446937\nu}{96768} + \frac{906103}{193536} \right) + \frac{433639\nu^2}{93312} - \frac{16075987\nu}{373248} + \frac{17465819}{746496} \right] \right\} + y^2 y_0^4 \left\{ \chi_a^2 \left[\kappa_a \left(\frac{17533\delta\nu}{6912} - \frac{252137\delta}{193536} \right) + \kappa_s \left(-\frac{17533\nu^2}{3456} + \frac{497599\nu}{96768} - \frac{252137}{193536} \right) - \frac{122731\nu^2}{3456} + \frac{367579\nu}{13824} - \frac{830069}{193536} \right] + \chi_a \chi_s \left[\kappa_s \left(\frac{17533\delta\nu}{3456} - \frac{252137\delta}{96768} \right) + \frac{57721\delta\nu}{3456} - \frac{830069\delta}{96768} + \kappa_a \left(-\frac{17533\nu^2}{1728} + \frac{497599\nu}{48384} - \frac{252137}{96768} \right) \right] + \chi_s^2 \left[\kappa_a \left(\frac{17533\delta\nu}{6912} - \frac{252137\delta}{193536} \right) + \kappa_s \left(-\frac{17533\nu^2}{3456} + \frac{497599\nu}{96768} - \frac{252137}{193536} \right) + \frac{7289\nu^2}{3456} + \frac{703273\nu}{96768} - \frac{830069}{193536} \right] \right\} + y^3 y_0^3 \left\{ \chi_a \chi_s \left(\frac{8635\delta\nu}{729} - \frac{24649\delta}{1458} \right) + \left(-\frac{3025\nu^2}{729} + \frac{8635\nu}{729} - \frac{24649}{2916} \right) \chi_s^2 + \left(\frac{24649\nu}{729} - \frac{24649}{2916} \right) \chi_a^2 \right\} + y^4 y_0^2 \left\{ \chi_a^2 \left[\kappa_a \left(\frac{17533\delta\nu}{6912} - \frac{252137\delta}{193536} \right) + \kappa_s \left(-\frac{17533\nu^2}{3456} + \frac{497599\nu}{96768} - \frac{252137}{193536} \right) - \frac{122731\nu^2}{3456} + \frac{367579\nu}{13824} - \frac{830069}{193536} \right] + \chi_a \chi_s \left[\kappa_s \left(\frac{17533\delta\nu}{3456} - \frac{252137\delta}{96768} \right) + \frac{57721\delta\nu}{3456} - \frac{830069\delta}{96768} + \kappa_a \left(-\frac{17533\nu^2}{1728} + \frac{497599\nu}{48384} - \frac{252137}{96768} \right) \right] + \chi_s^2 \left[\kappa_a \left(\frac{17533\delta\nu}{6912} - \frac{252137\delta}{193536} \right) + \kappa_s \left(-\frac{17533\nu^2}{3456} + \frac{497599\nu}{96768} - \frac{252137}{193536} \right) + \frac{7289\nu^2}{3456} + \frac{703273\nu}{96768} - \frac{830069}{193536} \right] \right\} + \frac{703273\nu}{96768} - \frac{830069}{193536} \right\}. \quad (20e)$$

B. Spin effects in TaylorT2

The coalescence time as a function of the modified orbital frequency y can be found out by integrating both sides of Eq. (11) with respect to y , as described in Sec. III B. The structure of the coalescence time, and the corresponding SO and SS coefficients read as

$$t = -\frac{5M}{256\nu y^8} \left\{ t_{\text{circ}} + \frac{15}{43} e_0^2 \left(\frac{y_0}{y} \right)^{19/3} \left[t_{\text{SO,ecc}} + t_{\text{SS,ecc}} \right] + \frac{2175}{13072} e_0^4 \left(\frac{y_0}{y} \right)^{19/3} \left[\dots + \mathcal{O}(y^6) + \frac{21543}{8990} \left(\frac{y_0}{y} \right)^{19/3} \left[\dots + \mathcal{O}(y^6) \right] \right] + \dots + \mathcal{O}(e_0^8) \right\}, \quad (21)$$

where,

$$t_{\text{NS}} = 1 + \frac{15}{43} e_0^2 \left(\frac{y_0}{y} \right)^{19/3} + \frac{2175}{13072} e_0^4 \left(\frac{y_0}{y} \right)^{19/3} \left[1 + \frac{21543}{8990} \left(\frac{y_0}{y} \right)^{19/3} \right] + \dots + \mathcal{O}(e_0^8), \quad (22a)$$

$$t_{\text{SO,ecc}}^{1.5\text{PN}} = y^3 \left[\frac{105092\delta\chi_a}{2295} + \frac{105092}{2295} \left(1 - \frac{1319\nu}{4888} \right) \chi_s \right] + y_0^3 \left[-\frac{157\delta\chi_a}{54} - \frac{157}{54} \left(1 - \frac{110\nu}{157} \right) \chi_s \right], \quad (22b)$$

$$t_{\text{SS,ecc}}^{2\text{PN}} = y_0^4 \left\{ \left[\frac{13}{96} + \frac{89\delta\kappa_a}{48} + \frac{89}{48} \kappa_s (1 - 2\nu) - \frac{89\nu}{24} \right] \chi_a^2 + \left[\delta \left(\frac{13}{48} + \frac{89\kappa_s}{24} \right) + \frac{89}{24} \kappa_a (1 - 2\nu) \right] \chi_a \chi_s + \left[\frac{13}{96} + \frac{89\delta\kappa_a}{48} + \frac{89}{48} \kappa_s (1 - 2\nu) + \frac{19\nu}{6} \right] \chi_s^2 \right\} + y^4 \left\{ \chi_a \chi_s \left[\delta \left(-\frac{8471}{7440} - \frac{221407\kappa_s}{3720} \right) - \frac{221407}{3720} (1 - 2\nu) \kappa_a \right] + \chi_s^2 \left[-\frac{8471}{14880} - \frac{221407\delta\kappa_a}{7440} - \frac{26617\nu}{465} - \frac{221407}{7440} (1 - 2\nu) \kappa_s \right] + \chi_a^2 \left[-\frac{8471}{14880} - \frac{221407\delta\kappa_a}{7440} - \frac{221407\nu}{3720} - \frac{221407}{7440} (1 - 2\nu) \kappa_s \right] \right\}, \quad (22c)$$

$$t_{\text{SO,ecc}}^{2.5\text{PN}} = y^2 y_0^3 \left[\frac{224369485}{2013984} \left(1 - \frac{33852\nu}{33235} \right) \delta\chi_a + \frac{224369485}{2013984} \left(1 - \frac{8970614\nu}{5217895} + \frac{744744\nu^2}{1043579} \right) \chi_s \right] + y^3 y_0^2 \left[\frac{74431409}{578340} \left(1 - \frac{5516\nu}{2833} \right) \delta\chi_a + \frac{74431409}{578340} \left(1 - \frac{30698935\nu}{13847704} + \frac{1818901\nu^2}{3461926} \right) \chi_s \right] + y_0^5 \left[-\frac{1279073}{38880} \left(1 - \frac{2348912\nu}{1279073} + \frac{691520\nu^2}{1279073} \right) \chi_s - \frac{1279073}{38880} \left(1 - \frac{970876\nu}{1279073} \right) \delta\chi_a \right] + y^5 \left[-\frac{119044339}{1524096} \left(1 - \frac{78785716\nu}{13842365} + \frac{52860864\nu^2}{13842365} \right) \chi_s - \frac{119044339}{1524096} \left(1 - \frac{101109876\nu}{13842365} \right) \delta\chi_a \right], \quad (22d)$$

$$t_{\text{SO,ecc}}^{3\text{PN}} = y_0^6 \left[-\frac{157043\pi\delta\chi_a}{15552} - \frac{157043\pi}{15552} \left(1 - \frac{150652\nu}{157043} \right) \chi_s \right] + y^3 y_0^3 \left[\frac{214464779\pi\delta\chi_a}{660960} + \frac{214464779\pi}{660960} \left(1 - \frac{1906756\nu}{4987553} \right) \chi_s \right] + y^6 \left[-\frac{10746947\pi\delta\chi_a}{15552} - \frac{10746947\pi}{15552} \left(1 - \frac{16210148\nu}{31241125} \right) \chi_s \right], \quad (22e)$$

$$t_{\text{SS,ecc}}^{3\text{PN}} = y^3 y_0^3 \left\{ -\frac{8249722}{61965} (1 - 4\nu) \chi_a^2 - \frac{16499444\delta}{61965} \left(1 - \frac{744763\nu}{1534832} \right) \chi_a \chi_s - \frac{8249722}{61965} \left(1 - \frac{744763\nu}{767416} + \frac{72545\nu^2}{383708} \right) \chi_s^2 \right\} + y^4 y_0^2 \left\{ \left[-\frac{23998343}{14999040} \left(1 - \frac{59435120\nu}{558101} + \frac{576688\nu^2}{2833} \right) - \frac{627246031\delta}{7499520} \left(1 - \frac{5516\nu}{2833} \right) \kappa_a - \frac{627246031}{7499520} \left(1 - \frac{11182\nu}{2833} + \frac{11032\nu^2}{2833} \right) \kappa_s \right] \chi_a^2 + \left[-\frac{23998343\delta}{7499520} \left(1 - \frac{5516\nu}{2833} \right) - \frac{627246031}{3749760} \left(1 - \frac{11182\nu}{2833} + \frac{11032\nu^2}{2833} \right) \kappa_a - \frac{627246031\delta}{3749760} \left(1 - \frac{5516\nu}{2833} \right) \kappa_s \right] \chi_a \chi_s + \left[-\frac{23998343}{14999040} \left(1 + \frac{55029412\nu}{558101} - \frac{554624\nu^2}{2833} \right) - \frac{627246031\delta}{7499520} \left(1 - \frac{5516\nu}{2833} \right) \kappa_a - \frac{627246031}{7499520} \left(1 - \frac{11182\nu}{2833} + \frac{11032\nu^2}{2833} \right) \kappa_s \right] \chi_s^2 \right\} + y^2 y_0^4 \left\{ \left[-\frac{18578365}{3580416} \left(1 - \frac{11182\nu}{2833} + \frac{11032\nu^2}{2833} \right) \kappa_s \right] \chi_s^2 + \left[-\frac{18578365}{3580416} \left(1 - \frac{11182\nu}{2833} + \frac{11032\nu^2}{2833} \right) \kappa_s \right] \chi_s^2 \right\}$$

$$\begin{aligned}
& - \frac{12271736\nu}{432055} + \frac{927024\nu^2}{33235} \Big) - \frac{127190345\delta}{1790208} \left(1 - \frac{33852\nu}{33235} \right) \kappa_a - \frac{127190345}{1790208} \left(1 - \frac{100322\nu}{33235} + \frac{67704\nu^2}{33235} \right) \kappa_s \Big] \chi_a^2 \\
& + \left[- \frac{18578365\delta}{1790208} \left(1 - \frac{33852\nu}{33235} \right) - \frac{127190345}{895104} \left(1 - \frac{100322\nu}{33235} + \frac{67704\nu^2}{33235} \right) \kappa_a - \frac{127190345\delta}{895104} \left(1 \right. \right. \\
& \left. \left. - \frac{33852\nu}{33235} \right) \kappa_s \right] \chi_a \chi_s + \left[- \frac{18578365}{3580416} \left(1 + \frac{9663364\nu}{432055} - \frac{791616\nu^2}{33235} \right) - \frac{127190345\delta}{1790208} \left(1 - \frac{33852\nu}{33235} \right) \kappa_a \right. \\
& \left. - \frac{127190345}{1790208} \left(1 - \frac{100322\nu}{33235} + \frac{67704\nu^2}{33235} \right) \kappa_s \right] \chi_s^2 \Big\} + y_0^6 \left\{ \left[\frac{24433195}{2612736} \left(1 - \frac{169526104\nu}{24433195} + \frac{73395504\nu^2}{24433195} \right) \right. \right. \\
& \left. \left. + \frac{906103\delta}{48384} \left(1 - \frac{1081668\nu}{906103} \right) \kappa_a + \frac{906103}{48384} \left(1 - \frac{2893874\nu}{906103} + \frac{1359176\nu^2}{906103} \right) \kappa_s \right] \chi_a^2 + \left[\frac{24433195\delta}{1306368} \left(1 \right. \right. \right. \\
& \left. \left. - \frac{33561668\nu}{24433195} \right) + \frac{906103}{24192} \left(1 - \frac{2893874\nu}{906103} + \frac{1359176\nu^2}{906103} \right) \kappa_a + \frac{906103\delta}{24192} \left(1 - \frac{1081668\nu}{906103} \right) \kappa_s \right] \chi_a \chi_s \\
& \left. + \left[\frac{24433195}{2612736} \left(1 + \frac{4669988\nu}{24433195} - \frac{42904736\nu^2}{24433195} \right) + \frac{906103\delta}{48384} \left(1 - \frac{1081668\nu}{906103} \right) \kappa_a + \frac{906103}{48384} \left(1 - \frac{2893874\nu}{906103} \right. \right. \right. \\
& \left. \left. + \frac{1359176\nu^2}{906103} \right) \kappa_s \right] \chi_s^2 \Big\} + y_0^6 \left\{ \left[\frac{28774424251}{65318400} \left(1 - \frac{13110551504\nu}{3345863285} + \frac{1075766832\nu^2}{669172657} \right) - \frac{201655079\delta}{2016000} \left(1 \right. \right. \right. \\
& \left. \left. + \frac{23412116\nu}{14068959} \right) \kappa_a - \frac{201655079}{2016000} \left(1 - \frac{4725802\nu}{14068959} - \frac{33202680\nu^2}{4689653} \right) \kappa_s \right] \chi_a^2 + \left[\frac{28774424251\delta}{32659200} \left(1 - \frac{385988932\nu}{3345863285} \right) \right. \\
& \left. - \frac{201655079}{1008000} \left(1 - \frac{4725802\nu}{14068959} - \frac{33202680\nu^2}{4689653} \right) \kappa_a - \frac{201655079\delta}{1008000} \left(1 + \frac{23412116\nu}{14068959} \right) \kappa_s \right] \chi_a \chi_s \\
& \left. + \left[\frac{28774424251}{65318400} \left(1 - \frac{208975900\nu}{669172657} - \frac{1147620320\nu^2}{669172657} \right) - \frac{201655079\delta}{2016000} \left(1 + \frac{23412116\nu}{14068959} \right) \kappa_a - \frac{201655079}{2016000} \left(1 \right. \right. \right. \\
& \left. \left. - \frac{4725802\nu}{14068959} - \frac{33202680\nu^2}{4689653} \right) \kappa_s \right] \chi_s^2 \Big\}. \tag{22f}
\end{aligned}$$

The TaylorT2 phase can then be obtained by integrating both sides of Eq. (13a) with respect to y , as described in Sec. III B. This is the time domain orbital phasing formula and is given by the following form, which is followed by the various coefficients of the eccentric SO and SS terms, as they appear in the structure of the phase

$$\begin{aligned}
\phi = & - \frac{1}{32\nu y^5} \left\{ \phi_{\text{circ}} - \frac{105}{272} e_0^2 \left(\frac{y_0}{y} \right)^{19/3} \left[\phi_{\text{SO,ecc}} + \phi_{\text{SS,ecc}} \right] \right. \\
& \left. - \frac{15225}{82688} e_0^4 \left(\frac{y_0}{y} \right)^{19/3} \left[\dots + \mathcal{O}(y^6) - \frac{13974}{7685} \left(\frac{y_0}{y} \right)^{19/3} \left[\dots + \mathcal{O}(y^6) \right] \right] + \dots + \mathcal{O}(e_0^8) \right\}, \tag{23}
\end{aligned}$$

where,

$$\phi_{\text{NS}} = 1 - \frac{105}{272} e_0^2 \left(\frac{y_0}{y} \right)^{19/3} - \frac{15225}{82688} e_0^4 \left(\frac{y_0}{y} \right)^{19/3} \left[1 - \frac{13974}{7685} \left(\frac{y_0}{y} \right)^{19/3} \right] + \dots + \mathcal{O}(e_0^8), \tag{24a}$$

$$\phi_{\text{SO,ecc}}^{1.5\text{PN}} = y_0^3 \left[- \frac{157\delta\chi_a}{54} - \frac{157\chi_s}{54} \left(1 - \frac{110\nu}{157} \right) \right] + y^3 \left[- \frac{6086\delta\chi_a}{945} - \frac{6086\chi_s}{945} \left(1 + \frac{1393\nu}{895} \right) \right], \tag{24b}$$

$$\begin{aligned}
\phi_{\text{SS,ecc}}^{2\text{PN}} = & y_0^4 \left\{ \left[\frac{293}{192} \left(1 - \frac{1246\nu}{293} \right) + \frac{89\delta\kappa_a}{192} + \frac{89}{192} (1 - 2\nu)\kappa_s \right] \chi_a^2 + \left[\frac{89}{96} (1 - 2\nu)\kappa_a + \delta \left(\frac{293}{96} + \frac{89\kappa_s}{96} \right) \right] \chi_a \chi_s \right. \\
& + \left[\frac{293}{192} \left(1 + \frac{74\nu}{293} \right) + \frac{89\delta\kappa_a}{192} + \frac{89}{192} (1 - 2\nu)\kappa_s \right] \chi_s^2 \Big\} + y^4 \left\{ \left[\frac{60197}{14784} \left(1 - \frac{16814\nu}{3541} \right) + \frac{20417\delta\kappa_a}{14784} \right. \right. \\
& + \frac{20417}{14784} (1 - 2\nu)\kappa_s \Big] \chi_a^2 + \left[\frac{20417}{7392} (1 - 2\nu)\kappa_a + \delta \left(\frac{60197}{7392} + \frac{20417\kappa_s}{7392} \right) \right] \chi_a \chi_s + \left[\frac{60197}{14784} \left(1 + \frac{2650\nu}{3541} \right) \right. \\
& \left. + \frac{20417\delta\kappa_a}{14784} + \frac{20417}{14784} (1 - 2\nu)\kappa_s \right] \chi_s^2 \Big\}, \tag{24c}
\end{aligned}$$

$$\phi_{\text{SO,ecc}}^{2.5\text{PN}} = y_0^5 \left[- \frac{1279073}{38880} \left(1 - \frac{970876\nu}{1279073} \right) \delta\chi_a - \frac{1279073}{38880} \left(1 - \frac{2348912\nu}{1279073} + \frac{691520\nu^2}{1279073} \right) \chi_s \right]$$

$$\begin{aligned}
& + y^5 \left[\frac{717229337}{2585520} \left(1 - \frac{39620772\nu}{42189961} \right) \delta\chi_a + \frac{717229337}{2585520} \left(1 - \frac{432179708\nu}{295329727} + \frac{12905280\nu^2}{42189961} \right) \chi_s \right] \\
& + y^3 y_0^2 \left[-\frac{8620819}{476280} \left(1 - \frac{5516\nu}{2833} \right) \delta\chi_a - \frac{8620819}{476280} \left(1 - \frac{990451\nu}{2535535} - \frac{7683788\nu^2}{2535535} \right) \chi_s \right] \\
& + y^2 y_0^3 \left[-\frac{424176163}{5334336} \left(1 - \frac{69804\nu}{158927} \right) \delta\chi_a - \frac{424176163}{5334336} \left(1 - \frac{28441198\nu}{24951539} + \frac{7678440\nu^2}{24951539} \right) \chi_s \right], \tag{24d}
\end{aligned}$$

$$\begin{aligned}
\phi_{\text{SO,ecc}}^{\text{3PN}} & = y_0^6 \left[-\frac{157043\pi\delta\chi_a}{15552} - \frac{157043\pi}{15552} \left(1 - \frac{150652\nu}{157043} \right) \chi_s \right] - y^3 y_0^3 \left[\frac{12307507\pi\delta\chi_a}{340200} \right. \\
& \left. + \frac{12307507\pi}{340200} \left(1 + \frac{1015892\nu}{723971} \right) \chi_s \right] + y^6 \left[\frac{153181985\pi\delta\chi_a}{870912} + \frac{153181985\pi}{870912} \left(1 - \frac{1475156\nu}{9010705} \right) \chi_s \right], \tag{24e}
\end{aligned}$$

$$\begin{aligned}
\phi_{\text{SS,ecc}}^{\text{3PN}} & = y^3 y_0^3 \left[\frac{477751}{25515} (1 - 4\nu) \chi_a^2 + \frac{955502}{25515} \left(1 + \frac{120251\nu}{281030} \right) \delta\chi_a \chi_s + \frac{477751}{25515} \left(1 + \frac{120251\nu}{140515} - \frac{30646\nu^2}{28103} \right) \chi_s^2 \right] \\
& + y^2 y_0^4 \left\{ \left[\frac{35122867}{9483264} \left(1 - \frac{57485464\nu}{2066051} + \frac{24850224\nu^2}{2066051} \right) + \frac{240456551}{4741632} \left(1 - \frac{69804\nu}{158927} \right) \delta\kappa_a \right. \right. \\
& + \frac{240456551}{4741632} \left(1 - \frac{387658\nu}{158927} + \frac{139608\nu^2}{158927} \right) \kappa_s \left. \right] \chi_a^2 + \left[\frac{240456551}{2370816} \left(1 - \frac{387658\nu}{158927} + \frac{139608\nu^2}{158927} \right) \kappa_a \right. \\
& + \delta \left[\frac{35122867}{4741632} \left(1 - \frac{69804\nu}{158927} \right) + \frac{240456551}{2370816} \left(1 - \frac{69804\nu}{158927} \right) \kappa_s \right] \chi_a \chi_s + \left[\frac{35122867}{9483264} \left(1 + \frac{47406356\nu}{2066051} \right. \right. \\
& \left. \left. - \frac{21220416\nu^2}{2066051} \right) + \frac{240456551}{4741632} \left(1 - \frac{69804\nu}{158927} \right) \delta\kappa_a + \frac{240456551}{4741632} \left(1 - \frac{387658\nu}{158927} + \frac{139608\nu^2}{158927} \right) \kappa_s \right] \chi_s^2 \left. \right\} \\
& + y_0^6 \left\{ \left[\frac{24433195}{2612736} \left(1 - \frac{169526104\nu}{24433195} + \frac{73395504\nu^2}{24433195} \right) + \frac{906103}{48384} \left(1 - \frac{1081668\nu}{906103} \right) \delta\kappa_a \right. \right. \\
& + \frac{906103}{48384} \left(1 - \frac{2893874\nu}{906103} + \frac{1359176\nu^2}{906103} \right) \kappa_s \left. \right] \chi_a^2 + \left[\frac{906103}{24192} \left(1 - \frac{2893874\nu}{906103} + \frac{1359176\nu^2}{906103} \right) \kappa_a \right. \\
& + \delta \left[\frac{24433195}{1306368} \left(1 - \frac{33561668\nu}{24433195} \right) + \frac{906103}{24192} \left(1 - \frac{1081668\nu}{906103} \right) \kappa_s \right] \chi_a \chi_s + \left[\frac{24433195}{2612736} \left(1 + \frac{4669988\nu}{24433195} \right. \right. \\
& \left. \left. - \frac{42904736\nu^2}{24433195} \right) + \frac{906103}{48384} \left(1 - \frac{1081668\nu}{906103} \right) \delta\kappa_a + \frac{906103}{48384} \left(1 - \frac{2893874\nu}{906103} + \frac{1359176\nu^2}{906103} \right) \kappa_s \right] \chi_s^2 \left. \right\} \\
& + y^6 \left\{ \left[-\frac{24653523709}{146313216} \left(1 - \frac{7638735632\nu}{1450207277} + \frac{2575441008\nu^2}{1450207277} \right) - \frac{67698947}{903168} \left(1 - \frac{12996788\nu}{11946873} \right) \delta\kappa_a \right. \right. \\
& - \frac{67698947}{903168} \left(1 - \frac{36890534\nu}{11946873} + \frac{15897784\nu^2}{3982291} \right) \kappa_s \left. \right] \chi_a^2 + \left[-\frac{67698947}{451584} \left(1 - \frac{36890534\nu}{11946873} + \frac{15897784\nu^2}{3982291} \right) \kappa_a \right. \\
& + \delta \left[-\frac{24653523709}{73156608} \left(1 + \frac{87630620\nu}{1450207277} \right) - \frac{67698947}{451584} \left(1 - \frac{12996788\nu}{11946873} \right) \kappa_s \right] \chi_a \chi_s \\
& + \left[-\frac{24653523709}{146313216} \left(1 + \frac{2013167764\nu}{1450207277} - \frac{3160271968\nu^2}{1450207277} \right) - \frac{67698947}{903168} \left(1 - \frac{12996788\nu}{11946873} \right) \delta\kappa_a \right. \\
& \left. \left. - \frac{67698947}{903168} \left(1 - \frac{36890534\nu}{11946873} + \frac{15897784\nu^2}{3982291} \right) \kappa_s \right] \chi_s^2 \right\} + y^4 y_0^2 \left\{ \left[-\frac{1492991}{7451136} \left(1 + \frac{13438736\nu}{87823} - \frac{26498864\nu^2}{87823} \right) \right. \right. \\
& + \frac{57841361}{3725568} \left(1 - \frac{5516\nu}{2833} \right) \delta\kappa_a + \frac{57841361}{3725568} \left(1 - \frac{11182\nu}{2833} + \frac{11032\nu^2}{2833} \right) \kappa_s \left. \right] \chi_a^2 + \left[\frac{57841361}{1862784} \left(1 - \frac{11182\nu}{2833} \right. \right. \\
& + \frac{11032\nu^2}{2833} \left. \right) \kappa_a + \delta \left[-\frac{1492991}{3725568} \left(1 - \frac{5516\nu}{2833} \right) + \frac{57841361}{1862784} \left(1 - \frac{5516\nu}{2833} \right) \kappa_s \right] \chi_a \chi_s + \left[-\frac{1492991}{7451136} \left(1 \right. \right. \\
& \left. \left. - \frac{14132020\nu}{87823} + \frac{27182848\nu^2}{87823} \right) + \frac{57841361}{3725568} \left(1 - \frac{5516\nu}{2833} \right) \delta\kappa_a + \frac{57841361}{3725568} \left(1 - \frac{11182\nu}{2833} + \frac{11032\nu^2}{2833} \right) \kappa_s \right] \chi_s^2 \left. \right\}. \tag{24f}
\end{aligned}$$

1. PN contribution to the number of GW cycles

Now that TaylorT2 has been constructed, we can compute the number of GW cycles the time-domain wave-

form sweeps from an initial frequency f_1 to a final fre-

Detector	LIGO/Virgo		3G			DECIGO		LISA	
Masses (M_\odot)	1.4 + 1.4	10 + 10	1.4 + 1.4	50 + 50	500 + 500	500 + 500	5000 + 5000	$10^5 + 10^5$	$10^7 + 10^7$
PN order	cumulative number of cycles								
1.5PN (circ)	51.9072	28.8143	250.7890	48.2115	7.0857	232.0150	48.2115	149.0670	2.9067
1.5PN (ecc)	-1.7260	-1.0468	-8.0115	-1.6621	-0.3493	-7.7149	-1.6621	-4.8601	-0.1916
2PN (circ)	-1.6502	-3.5553	-4.1416	-4.9924	-1.2597	-11.7745	-4.9924	-9.9381	-0.5927
2PN (ecc)	0.0334	0.0878	0.0720	0.1107	0.0491	0.2385	0.1107	0.1893	0.0321
2.5PN (circ)	6.7599	10.2069	10.8024	12.4962	4.8913	15.2098	12.4962	17.8117	2.6020
2.5PN (ecc)	-0.1148	-0.2577	-0.1148	-0.2581	-0.2418	-0.2582	-0.2581	-0.2583	-0.1921
3PN (circ)	-2.2268	-4.9561	-3.0152	-5.5237	-3.0028	-3.6909	-5.5237	-6.4303	-1.7800
3PN (ecc)	0.0070	0.0385	0.0033	0.0309	0.0515	0.0144	0.0309	0.0182	0.0330
Total	52.9898	29.3315	246.384	48.4129	7.2239	224.0390	48.4129	145.5990	2.8173

Table II. Contribution of each PN order to the total number of accumulated cycles by the spinning section of the phase inside the detector’s frequency band, for typical eccentric spinning ($e_0 = 0.2$; $\chi_1 = \chi_2 = 0.4$ for BNS and $\chi_1 = \chi_2 = 0.9$ for BBH) compact binaries observed by current and future detectors. We have approximated the frequency bands of LIGO/Virgo A+, Einstein Telescope (ET/CE/3G), DECIGO, and LISA with step functions, respectively between $[10 \text{ Hz}, 10^3 \text{ Hz}]$, $[1 \text{ Hz}, 10^4 \text{ Hz}]$, $[10^{-2} \text{ Hz}, 1 \text{ Hz}]$ and $[10^{-4} \text{ Hz}, 10^{-1} \text{ Hz}]$.

quency f_2 . The final frequency is taken to be the minimum of the upper limit of a particular detector band (for example, $f_2 = 1000 \text{ Hz}$ for the LIGO band) and f_{ISCO} (where the PN formalism is supposed to break down), given by the following

$$f_{\text{ISCO}} = \frac{c^3}{6^{3/2}\pi GM}. \quad (25)$$

We will take $f_1 = 10 \text{ Hz}$ as the lower end of the LIGO sensitivity bucket. We also quote the number of cycles

accumulated in 3G, DECIGO, and LISA bands by utilizing different ranges of f_1 and f_2 . The number of accumulated GW cycles between f_1 and f_2 can be defined as

$$N_{\text{cyc}} = \frac{1}{\pi} [\phi(f_2) - \phi(f_1)]. \quad (26)$$

Table II shows the PN breakup of N_{cyc} for a fixed initial eccentricity and spins for various detector and mass configurations.

From Table II we can now draw the following conclusions

- (a) The number of accumulated GW cycles contributed by the circular part of the phasing always has a relative negative sign with respect to the number of cycles contributed by the eccentric part. This is evident from the TaylorT2 phasing formula in Eq. (23) that the eccentric part of the phasing has a relative negative sign with respect to the circular part. Moreover, it is expected that the presence of eccentricity will take away several cycles from an inspiral in general, even though for certain PN orders, it does not hold, as can be seen in the LIGO/Virgo column in Table II for the 2PN (as well as 3PN) circular and eccentric cases.
- (b) From Table I and II it is to be noted that the spin-orbit effect for aligned spinning binaries contributes positively to the number of accumulated GW cycles (they make the waveform longer/elongates the inspiral process). It is also to be noted that anti-alignment of spins with respect to the orbital angular momentum works reversely, i.e. they take away the number of cycles (makes the binary merge faster compared to the non-spinning case).
- (c) While the spin-orbit coupling positively contributes to the number of GW cycles for aligned spins, the spin-spin coupling, however, owing to the relative sign difference between the spin-orbit and spin-spin sections of Eq. (23), contributes negatively to the number of cycles. This can also be seen in Table II for the 2PN (circular) row. However, since the spin-spin coupling is a subdominant effect (owing to its quadratic nature), the number of cycles contributed by the spin-orbit case (owing to its linear nature) trumps the number of cycles taken away by the spin-spin case.
- (d) The combined presence of eccentricity and spins has a subdominant effect on the number of GW cycles. For the leading order spin-orbit spin-aligned case, as seen from Table II, some cycles, ranging from -0.1 to -8 for various total mass ranges, are taken away. The same holds for the leading order spin-spin spin-aligned case where a negligible num-

ber of cycles gets added to the net waveform.

- (e) For the mixed spin case (where one spin is parallel to the orbital angular momentum and the other is anti-parallel to the orbital angular momentum), the numbers entirely depend on the relative magnitude of positive and negative spins. If the aligned-spin magnitude is greater than that of the anti-aligned spin, or equivalently if $\chi_{\text{eff}} > 0$, it follows the trends of both spin-aligned cases. But for the opposite scenario, when $\chi_{\text{eff}} < 0$, it follows the anti-aligned case. However, the magnitude of cycles accumulated is (predictably) lower than the corresponding spin-aligned and spin-anti-aligned cases.
- (f) The importance of an effect while using the GW cycles metric can be judged by whether or not the

corresponding $N_{\text{cyc}} > 1$. A general analysis of the total cycles in each table indicates that the eccentric spinning contributions (the new addition of our study to TaylorT2) have become increasingly important for larger spinning systems, especially those with aligned/anti-aligned spin configurations.

C. Spin effects in TaylorF2 approximant (SPA)

1. TaylorF2 phase

Using the parametric Eq. (21) and (23) given in terms of the PN parameter y , we can then write our final result for the eccentric spinning SPA phase in the following form.

$$\begin{aligned} \Psi = & \frac{3}{128\nu y^5} \left\{ \Psi_{\text{circ}} + \frac{650}{731} e_0^2 \left(\frac{y_0}{y} \right)^{19/3} \left[\Psi_{\text{SO,ecc}} + \Psi_{\text{SS,ecc}} \right] \right. \\ & \left. + \frac{47125}{111112} e_0^4 \left(\frac{y_0}{y} \right)^{19/3} \left[\dots + \mathcal{O}(y^6) - \frac{52361377}{30970550} \left(\frac{y_0}{y} \right)^{19/3} \left[\dots + \mathcal{O}(y^6) \right] \right] + \dots + \mathcal{O}(e_0^8) \right\}, \end{aligned} \quad (27)$$

where,

$$\Psi_{\text{NS}} = 1 + \frac{650}{731} e_0^2 \left(\frac{y_0}{y} \right)^{19/3} + \frac{47125}{111112} e_0^4 \left(\frac{y_0}{y} \right)^{19/3} \left[1 - \frac{52361377}{30970550} \left(\frac{y_0}{y} \right)^{19/3} \right] + \dots + \mathcal{O}(e_0^8), \quad (28a)$$

$$\Psi_{\text{SO,ecc}}^{1.5\text{PN}} = y^3 \left[\frac{1969099\delta\chi_a}{70200} + \frac{1969099}{70200} \left(1 - \frac{118636\nu}{228965} \right) \chi_s \right] + y_0^3 \left[-\frac{157\delta\chi_a}{54} - \frac{157}{54} \left(1 - \frac{110\nu}{157} \right) \chi_s \right], \quad (28b)$$

$$\begin{aligned} \Psi_{\text{SS,ecc}}^{2\text{PN}} = & y_0^4 \left[\chi_a \chi_s \left[\delta \left(\frac{13}{48} + \frac{89\kappa_s}{24} \right) + \frac{89}{24} (1 - 2\nu) \kappa_a \right] + \chi_a^2 \left[\frac{13}{96} + \frac{89\delta\kappa_a}{48} - \frac{89\nu}{24} + \frac{89}{48} (1 - 2\nu) \kappa_s \right] \right. \\ & \left. + \chi_s^2 \left[\frac{13}{96} + \frac{89\delta\kappa_a}{48} + \frac{19\nu}{6} + \frac{89}{48} (1 - 2\nu) \kappa_s \right] \right] + y^4 \left[\chi_a \chi_s \left[\delta \left(-\frac{236113}{425568} - \frac{43122421\kappa_s}{1063920} \right) \right. \right. \\ & \left. \left. - \frac{43122421}{1063920} (1 - 2\nu) \kappa_a \right] + \chi_s^2 \left[-\frac{236113}{851136} - \frac{43122421\delta\kappa_a}{2127840} - \frac{238306\nu}{6045} - \frac{43122421}{2127840} (1 - 2\nu) \kappa_s \right] \right. \\ & \left. + \chi_a^2 \left[-\frac{236113}{851136} - \frac{43122421\delta\kappa_a}{2127840} + \frac{43122421\nu}{1063920} - \frac{43122421}{2127840} (1 - 2\nu) \kappa_s \right] \right], \end{aligned} \quad (28c)$$

$$\begin{aligned} \Psi_{\text{SO,ecc}}^{2.5\text{PN}} = & y_0^5 \left[-\frac{1279073}{38880} \left(1 - \frac{2348912\nu}{1279073} + \frac{691520\nu^2}{1279073} \right) \chi_s - \frac{1279073}{38880} \left(1 - \frac{970876\nu}{1279073} \right) \delta\chi_a \right] \\ & + y^2 y_0^3 \left[\frac{132601447499}{7330901760} \left(1 - \frac{2615284\nu}{1155397} \right) \delta\chi_a + \frac{132601447499}{7330901760} \left(1 - \frac{537693258\nu}{181397329} + \frac{287681240\nu^2}{181397329} \right) \chi_s \right] \\ & + y^3 y_0^2 \left[\frac{5578457467}{70761600} \left(1 - \frac{5516\nu}{2833} \right) \delta\chi_a + \frac{5578457467}{70761600} \left(1 - \frac{1599066728\nu}{648657845} + \frac{654396176\nu^2}{648657845} \right) \chi_s \right] \\ & + y^5 \left[\frac{4267187295851}{18822585600} \left(1 + \frac{6072295628\nu}{5837465521} \right) \delta\chi_a + \frac{4267187295851}{18822585600} \left(1 - \frac{1266783204\nu}{5837465521} - \frac{4030104736\nu^2}{5837465521} \right) \chi_s \right], \end{aligned} \quad (28d)$$

$$\begin{aligned} \Psi_{\text{SO,ecc}}^{3\text{PN}} = & y_0^6 \left[-\frac{157043\pi\delta\chi_a}{15552} - \frac{157043\pi}{15552} \left(1 - \frac{150652\nu}{157043} \right) \chi_s \right] + y^3 y_0^3 \left[\frac{4787739497\pi\delta\chi_a}{25272000} \right. \\ & \left. + \frac{4787739497\pi}{25272000} \left(1 - \frac{62257792\nu}{111342779} \right) \chi_s \right] + y^6 \left[-\frac{82262188063\pi\delta\chi_a}{161740800} - \frac{82262188063\pi}{161740800} \left(1 - \frac{342805652\nu}{562668865} \right) \chi_s \right], \end{aligned} \quad (28e)$$

$$\begin{aligned}
\Psi_{\text{SS,ecc}}^{\text{3PN}} = & y^4 y_0^2 \left\{ \chi_a \chi_s \left[-\frac{122165818693}{1072431360} \left(1 - \frac{11182\nu}{2833} + \frac{11032\nu^2}{2833} \right) \kappa_a - \frac{668908129\delta}{428972544} \left(1 - \frac{5516\nu}{2833} \right) \right. \right. \\
& - \frac{122165818693\delta}{1072431360} \left(1 - \frac{5516\nu}{2833} \right) \kappa_s \left. \right] + \chi_a^2 \left[-\frac{122165818693}{2144862720} \left(1 - \frac{11182\nu}{2833} + \frac{11032\nu^2}{2833} \right) \kappa_s \right. \\
& - \frac{122165818693\delta}{2144862720} \left(1 - \frac{5516\nu}{2833} \right) \kappa_a - \frac{668908129}{857945088} \left(1 - \frac{677394352\nu}{4575295} + \frac{1301577424\nu^2}{4575295} \right) \left. \right] \\
& + \chi_s^2 \left[-\frac{122165818693}{2144862720} \left(1 - \frac{11182\nu}{2833} + \frac{11032\nu^2}{2833} \right) \kappa_s - \frac{122165818693\delta}{2144862720} \left(1 - \frac{5516\nu}{2833} \right) \kappa_a \right. \\
& - \frac{668908129}{857945088} \left(1 + \frac{641276492\nu}{4575295} - \frac{1265944064\nu^2}{4575295} \right) \left. \right] \left. \right\} + y^2 y_0^4 \left\{ \chi_a \chi_s \left[-\frac{75168973423}{3258178560} \left(1 - \frac{4926078\nu}{1155397} \right) \right. \right. \\
& + \frac{5230568\nu^2}{1155397} \kappa_a - \frac{844595207\delta}{501258240} \left(1 - \frac{2615284\nu}{1155397} \right) - \frac{75168973423\delta}{3258178560} \left(1 - \frac{2615284\nu}{1155397} \right) \kappa_s \left. \right] \\
& + \chi_a^2 \left[-\frac{75168973423}{6516357120} \left(1 - \frac{4926078\nu}{1155397} + \frac{5230568\nu^2}{1155397} \right) \kappa_s - \frac{75168973423\delta}{6516357120} \left(1 - \frac{2615284\nu}{1155397} \right) \kappa_a \right. \\
& - \frac{844595207}{1002516480} \left(1 - \frac{445320024\nu}{15020161} + \frac{931041104\nu^2}{15020161} \right) \left. \right] + \chi_s^2 \left[-\frac{75168973423}{6516357120} \left(1 - \frac{4926078\nu}{1155397} + \frac{5230568\nu^2}{1155397} \right) \kappa_s \right. \\
& - \frac{75168973423\delta}{6516357120} \left(1 - \frac{2615284\nu}{1155397} \right) \kappa_a - \frac{844595207}{1002516480} \left(1 + \frac{317241996\nu}{15020161} - \frac{795046336\nu^2}{15020161} \right) \left. \right] \left. \right\} \\
& + y_0^6 \left\{ \chi_a^2 \left[\frac{906103}{48384} \left(1 - \frac{2893874\nu}{906103} + \frac{1359176\nu^2}{906103} \right) \kappa_s + \frac{906103\delta}{48384} \left(1 - \frac{1081668\nu}{906103} \right) \kappa_a + \frac{24433195}{2612736} \left(1 \right. \right. \right. \\
& - \frac{169526104\nu}{24433195} + \frac{73395504\nu^2}{24433195} \left. \right) \left. \right] + \chi_a \chi_s \left(\frac{906103}{24192} \left(1 - \frac{2893874\nu}{906103} + \frac{1359176\nu^2}{906103} \right) \kappa_a + \frac{906103\delta}{24192} \left(1 \right. \right. \right. \\
& - \frac{1081668\nu}{906103} \left. \right) \kappa_s + \frac{24433195\delta}{1306368} \left(1 - \frac{33561668\nu}{24433195} \right) \left. \right) + \chi_s^2 \left[\frac{906103}{48384} \left(1 - \frac{2893874\nu}{906103} + \frac{1359176\nu^2}{906103} \right) \kappa_s \right. \\
& + \frac{906103\delta}{48384} \left(1 - \frac{1081668\nu}{906103} \right) \kappa_a + \frac{24433195}{2612736} \left(1 + \frac{4669988\nu}{24433195} - \frac{42904736\nu^2}{24433195} \right) \left. \right] \left. \right\} \\
& + y^6 \left\{ \chi_a^2 \left[-\frac{830182833661\delta}{2515968000} \left(1 + \frac{43459444\nu}{1135681031} \right) \kappa_a - \frac{830182833661}{2515968000} \left(1 - \frac{2227902618\nu}{1135681031} - \frac{1374645160\nu^2}{1135681031} \right) \kappa_s \right. \right. \\
& + \frac{10996032441971}{27172454400} \left(1 - \frac{203534409296\nu}{75212260205} + \frac{14846167728\nu^2}{15042452041} \right) \left. \right] + \chi_s^2 \left[-\frac{830182833661\delta}{2515968000} \left(1 + \frac{43459444\nu}{1135681031} \right) \kappa_a \right. \\
& - \frac{830182833661}{2515968000} \left(1 - \frac{2227902618\nu}{1135681031} - \frac{1374645160\nu^2}{1135681031} \right) \kappa_s + \frac{10996032441971}{27172454400} \left(1 - \frac{22377479356\nu}{15042452041} \right. \\
& - \frac{17050930400\nu^2}{15042452041} \left. \right) \left. \right] + \chi_a \chi_s \left[-\frac{830182833661\delta}{1257984000} \left(1 + \frac{43459444\nu}{1135681031} \right) \kappa_s - \frac{830182833661}{1257984000} \left(1 - \frac{2227902618\nu}{1135681031} \right. \right. \\
& - \frac{1374645160\nu^2}{1135681031} \left. \right) \kappa_a + \frac{10996032441971\delta}{13586227200} \left(1 - \frac{7286382628\nu}{75212260205} \right) \left. \right] \left. \right\} + y^3 y_0^3 \left[-\frac{309148543\delta}{1895400} \left(1 \right. \right. \\
& - \frac{21906001\nu}{35947505} \left. \right) \chi_a \chi_s - \frac{309148543}{3790800} \left(1 - \frac{43812002\nu}{35947505} + \frac{237272\nu^2}{653591} \right) \chi_s^2 - \frac{309148543}{3790800} (1 - 4\nu) \chi_a^2 \left. \right]. \quad (28f)
\end{aligned}$$

Note that we only list the leading (Newtonian) non-spinning term here. The full 3PN expression for the non-spinning part of the phase is listed as Eq. (6.26) of Ref. [76]. Also, while we haven't explicitly listed it here, we provide full expressions for all the Taylor approximants, including the spinning part up to $\mathcal{O}(e_0^8)$ till 3PN, which we compute here as additional material.

2. Waveform systematics

To estimate the effects due to newly computed spinning eccentric corrections, we start by defining the scalar product between any two waveforms h_1 and h_2 , as,

$$(h_1|h_2) \equiv 4\Re \left[\int_{f_{\text{low}}}^{f_{\text{high}}} \frac{\tilde{h}_1(f)\tilde{h}_2^*(f)}{S_n(f)} df \right], \quad (29)$$

where, $\tilde{h}_1(f)$, $\tilde{h}_2(f)$ are the Fourier transforms of h_1 , h_2 , f_{low} , f_{high} , $S_n(f)$ are lower and upper cutoff frequencies, and one-sided power-spectral density (PSD) of the detector noise, respectively. The $*$ denotes the complex conjugate of the quantity. The natural way of quantifying the agreement between two waveforms is to compute the *match* (also known as *overlap*), defined as [85],

$$\mathcal{M}(h_1, h_2) \equiv \max_{\phi_c, t_c} \frac{(e^{i(\phi_c + 2\pi f t_c)} h_1 | h_2)}{\sqrt{(h_1 | h_1)(h_2 | h_2)}}. \quad (30)$$

The quantity $1 - \mathcal{M}$ is referred to as the *mismatch* between the two waveforms h_1 and h_2 . The numerical value of mismatch is used extensively in GW modelling and parameter estimation studies to denote the disagreement between two waveforms.

Following the discussion above, we, too, compute and quote mismatch values between `TaylorF2Ecc` [76, 77] and with the newly computed spinning eccentric corrections in `TaylorF2` phase up to 3PN and expanded in second power in eccentricity added in `TaylorF2Ecc`. We perform the mismatch study in the parameter space of total mass (M) = $(5 - 100)M_\odot$, mass ratio (q) = $1 - 4$, initial eccentricity at 10Hz (e_{10}) = $0.1 - 0.3$, and dimensionless spins of $(\chi_1, \chi_2) = 0.0 - 0.9$. Instead of dealing with M and individual dimensionless spins (χ_1, χ_2) of the binary, we define two parameters related to component masses (m_1, m_2) and spins of the binary called the *chirp mass* (M_{chirp}) and *effective spin parameter* (χ_{eff}), defined as,

$$M_{\text{chirp}} = \frac{(m_1 m_2)^{3/5}}{(m_1 + m_2)^{1/5}}, \quad \chi_{\text{eff}} = \frac{m_1 \chi_1 + m_2 \chi_2}{M}. \quad (31)$$

In Fig. 1, we show the mismatch (denoted as color bar) in (a) $e_{10} - q$ (left), (b) $e_{10} - M_{\text{chirp}}$ (middle), (c) $e_{10} - \chi_{\text{eff}}$ (right) panels, respectively. We show the mismatch as a function of χ_{eff} and M_{chirp} separately in Fig. 2. We fix various parameters while performing the mismatch study in different parameter planes. For instance, total mass (M) is fixed to $10M_\odot$ in the left and right figures of Fig. 1, q is fixed to 4 for middle, right figures of Fig. 1 and in Fig. 2. The dimensionless spins are fixed to $(0.9, 0.9)$ for the left and middle figures of Fig. 1. Further, e_{10} is fixed to 0.3 in Fig. 2. We denote the 96.5% and 99% match values between the two waveforms using contours (denoted by solid black curves) to identify the region of parameter space where these spinning eccentric terms become important and can't be ignored. In $e_{10} - q$ plane, though the mismatches are negligible ($\lesssim 1\%$) up to $e_{10} \sim 0.15$ for all mass ratios, it becomes as large as $\sim 11\%$ for $e_{10} = 0.3$ and $q = 4$. Next, in $e_{10} - M_{\text{chirp}}$ plane, the effect of these corrections is mostly negligible up to $e_{10} \sim 0.18$ for $M_{\text{chirp}} > 10M_\odot$. The mismatch achieves a value of 13% for lower chirp mass ($M_{\text{chirp}} < 10M_\odot$) and higher eccentricity ($e_{10} \gtrsim 0.25$) value. Further, the mismatch variation due to eccentricity and spins can be quantified by looking at the panel's right figure. The mismatches between the two can be as high as $\sim 11\%$ for high spin ($\sim (0.9, 0.9)$) and high

(~ 0.3) eccentricity value. Finally, the mismatches attain an even larger value in $\chi_{\text{eff}} - M_{\text{chirp}}$ plane (shown in Fig. 2). For systems with $\chi_{\text{eff}} \gtrsim 0.2$ shows a mismatch of $> 1\%$ for all M_{chirp} , while for lighter ($M_{\text{chirp}} \sim 2M_\odot$) and maximally spinning systems ($\chi_{\text{eff}} \gtrsim 0.8$) the mismatch can achieve a value $\sim 15\%$. This observation is consistent as lower mass positive aligned systems will have more cycles than a high mass case in the frequency band of current ground-based detectors. This will lead to a larger accumulation of mismatches in the inspiral cycles for lighter mass cases compared to the heavier ones. All these observations point to the importance of including effects due to eccentricity and spins in the waveform templates while doing parameter estimation and searches for spinning eccentric GW signals.

D. Resummation of the Taylor T2 phase

Since the current study deals with an extension of Ref. [76] both in terms of an increase in eccentricity order and spins, it is natural to ask about the validity (in terms of the eccentricity) of the current model. Since Ref. [76] deals with $\mathcal{O}(e_0^2)$ in eccentricity, and the current model deals with $\mathcal{O}(e_0^8)$ the extent in eccentricity to which the current model is applicable is naturally higher than the previous works. To quantify that, we compare the $\mathcal{O}(e_0^2)$, $\mathcal{O}(e_0^4)$, $\mathcal{O}(e_0^6)$, $\mathcal{O}(e_0^8)$, and a resummed version of the $\mathcal{O}(e_0^4)$ and $\mathcal{O}(e_0^8)$ TaylorT2 phase with the numerically calculated TaylorT2 that is valid for arbitrary initial eccentricities ($e_0 < 1$). We use only the secularly increasing parts of the phase, ignoring the oscillatory pieces (which will be discussed in Appendix B). We plot in Fig. 3 the difference between the number of cycles, that is

$$\Delta N_{\text{cyc}} = N_{\text{cyc, numerical}} - N_{\text{cyc, analytical}}, \quad (32)$$

as a function of the eccentricity. The figure indicates that as the initial eccentricity increases, the difference in the number of cycles between the numerical and the analytical increases. It shows that the $\mathcal{O}(e_0^2)$ solution is valid only for initial eccentricities around 0.07, whereas for the $\mathcal{O}(e_0^8)$ solution, the validity increases to about 0.45. The validity is further improved up to close to 0.55 for the $\mathcal{O}(e_0^8)$ resummed version.

Since an eccentricity expanded phase will naturally only be valid for a small range of initial eccentricities, we attempt to increase its accuracy by performing a simple resummation, as highlighted in Sec. III D of Ref. [72]. To do this, we choose a resummation ansatz of the form

$$\phi_{\text{ans}}^{(\text{resum})} = x^{-5/2} (1 - e_0^2)^3 (d + f e_0^2 + g e_0^4 + h e_0^6 + l e_0^8). \quad (33)$$

Note that in Eq. (33), the exponent of the $(1 - e_0^2)$ segment was arrived at by experimenting with various powers, and we finally settled with the cubic power since it proved to

accumulate the smallest error in the number of cycles vis-a-vis the numerical solution.

This resummation ansatz is then expanded once again in e_0 and compared with the PN version of the phase to determine the ansatz coefficients d , f , g , h and l . Fig. 3 includes comparing the resummed analytical expression with numerical phase results. The resummed phase was

found to have the following structure

$$\begin{aligned} \phi^{(\text{resum})} = & -\frac{(1-e_0^2)^3}{32\nu y^5} \left\{ \phi_{\text{NS}}^{(\text{resum})} + \phi_{\text{SO}}^{(\text{resum})} + \phi_{\text{SS}}^{(\text{resum})} \right. \\ & + 3e_0^2 \left[\phi_{\text{SO,ecc}}^{(\text{resum})} + \phi_{\text{SS,ecc}}^{(\text{resum})} \right] + 6e_0^4 \left[\dots + \mathcal{O}(y^6) \right] \\ & \left. + \dots + \mathcal{O}(e_0^8) \right\}, \end{aligned} \quad (34)$$

where the various pieces were found to be as follows

$$\phi_{\text{NS}}^{(\text{resum})} = 1 + 3e_0^2 \left[1 - \frac{35}{272} \left(\frac{y_0}{y} \right)^{19/3} \right] + 6e_0^4 \left[1 - \frac{36995}{165376} \left(\frac{y_0}{y} \right)^{19/3} + \frac{14385}{257792} \left(\frac{y_0}{y} \right)^{38/3} \right] + \dots + \mathcal{O}(e_0^8), \quad (35a)$$

$$\phi_{\text{SO}}^{(\text{resum})1.5\text{PN}} = y^3 \left[\frac{565\delta\chi_a}{24} + \frac{565}{24} \left(1 - \frac{76\nu}{113} \right) \chi_s \right], \quad (35b)$$

$$\begin{aligned} \phi_{\text{SO,ecc}}^{(\text{resum})1.5\text{PN}} = & y^3 \left[\frac{565\delta\chi_a}{24} + \frac{565}{24} \left(1 - \frac{76\nu}{113} \right) \chi_s \right] - \frac{35}{272} \left(\frac{y_0}{y} \right)^{19/3} \left\{ y_0^3 \left[-\frac{157\delta\chi_a}{54} - \frac{157}{54} \left(1 - \frac{110\nu}{157} \right) \chi_s \right] \right. \\ & \left. + y^3 \left[-\frac{6086\delta\chi_a}{945} - \frac{6086}{945} \left(1 + \frac{1393\nu}{895} \right) \chi_s \right] \right\}, \end{aligned} \quad (35c)$$

$$\begin{aligned} \phi_{\text{SS}}^{(\text{resum})2\text{PN}} = & y^4 \left\{ \left[-\frac{5}{16} (1 - 160\nu) - 25\delta\kappa_a - 25(1 - 2\nu)\kappa_s \right] \chi_a^2 + \left[-50(1 - 2\nu)\kappa_a + \delta \left(-\frac{5}{8} - 50\kappa_s \right) \right] \chi_a \chi_s \right. \\ & \left. + \left[-\frac{5}{16} (1 + 156\nu) - 25\delta\kappa_a - 25(1 - 2\nu)\kappa_s \right] \chi_s^2 \right\}, \end{aligned} \quad (35d)$$

$$\begin{aligned} \phi_{\text{SS,ecc}}^{(\text{resum})2\text{PN}} = & y^4 \left\{ \left[-\frac{5}{16} (1 - 160\nu) - 25\delta\kappa_a - 25(1 - 2\nu)\kappa_s \right] \chi_a^2 + \left[-50(1 - 2\nu)\kappa_a + \delta \left(-\frac{5}{8} - 50\kappa_s \right) \right] \chi_a \chi_s \right. \\ & + \left[-\frac{5}{16} (1 + 156\nu) - 25\delta\kappa_a - 25(1 - 2\nu)\kappa_s \right] \chi_s^2 \left. - \frac{35}{272} \left(\frac{y_0}{y} \right)^{19/3} \left\{ y_0^4 \left[\left[\frac{13}{96} \left(1 - \frac{356\nu}{13} \right) + \frac{89\delta\kappa_a}{48} \right. \right. \right. \right. \\ & + \left. \frac{89}{48} (1 - 2\nu)\kappa_s \right] \chi_a^2 + \left[\frac{89}{24} (1 - 2\nu)\kappa_a + \delta \left(\frac{13}{48} + \frac{89\kappa_s}{24} \right) \right] \chi_a \chi_s + \left[\frac{13}{96} \left(1 + \frac{304\nu}{13} \right) + \frac{89\delta\kappa_a}{48} \right. \\ & + \left. \left. \frac{89}{48} (1 - 2\nu)\kappa_s \right] \chi_s^2 \right. + y^4 \left[\left[-\frac{527}{7392} \left(1 + \frac{4804\nu}{31} \right) + \frac{20417\delta\kappa_a}{3696} + \frac{20417}{3696} (1 - 2\nu)\kappa_s \right] \chi_a^2 \right. \\ & + \left[\frac{20417}{1848} (1 - 2\nu)\kappa_a + \delta \left(-\frac{527}{3696} + \frac{20417\kappa_s}{1848} \right) \right] \chi_a \chi_s + \left[-\frac{527}{7392} \left(1 - \frac{4928\nu}{31} \right) + \frac{20417\delta\kappa_a}{3696} \right. \\ & \left. \left. + \frac{20417}{3696} (1 - 2\nu)\kappa_s \right] \chi_s^2 \right\}, \end{aligned} \quad (35e)$$

$$\phi_{\text{SO}}^{(\text{resum})2.5\text{PN}} = -\frac{732985}{2016} y^5 \log(y) \left[\left(1 + \frac{7056\nu}{146597} \right) \delta\chi_a + \left(1 - \frac{135856\nu}{146597} - \frac{17136\nu^2}{146597} \right) \chi_s \right], \quad (35f)$$

$$\begin{aligned} \phi_{\text{SO,ecc}}^{(\text{resum})2.5\text{PN}} = & -\frac{732985}{2016} y^5 \log(y) \left[\left(1 + \frac{7056\nu}{146597} \right) \delta\chi_a + \left(1 - \frac{135856\nu}{146597} - \frac{17136\nu^2}{146597} \right) \chi_s \right] \\ & - \frac{35}{272} \left(\frac{y_0}{y} \right)^{19/3} \left\{ y_0^5 \left[-\frac{1279073}{38880} \left(1 - \frac{970876\nu}{1279073} \right) \delta\chi_a - \frac{1279073}{38880} \left(1 - \frac{2348912\nu}{1279073} + \frac{691520\nu^2}{1279073} \right) \chi_s \right] \right. \\ & + y^5 \left[\frac{717229337}{2585520} \left(1 - \frac{39620772\nu}{42189961} \right) \delta\chi_a + \frac{717229337}{2585520} \left(1 - \frac{432179708\nu}{295329727} + \frac{12905280\nu^2}{42189961} \right) \chi_s \right] \\ & + y^3 y_0^2 \left[-\frac{8620819}{476280} \left(1 - \frac{5516\nu}{2833} \right) \delta\chi_a - \frac{8620819}{476280} \left(1 - \frac{990451\nu}{2535535} - \frac{7683788\nu^2}{2535535} \right) \chi_s \right] \\ & \left. + y^2 y_0^3 \left[-\frac{424176163}{5334336} \left(1 - \frac{69804\nu}{158927} \right) \delta\chi_a - \frac{424176163}{5334336} \left(1 - \frac{28441198\nu}{24951539} + \frac{7678440\nu^2}{24951539} \right) \chi_s \right] \right\}, \end{aligned} \quad (35g)$$

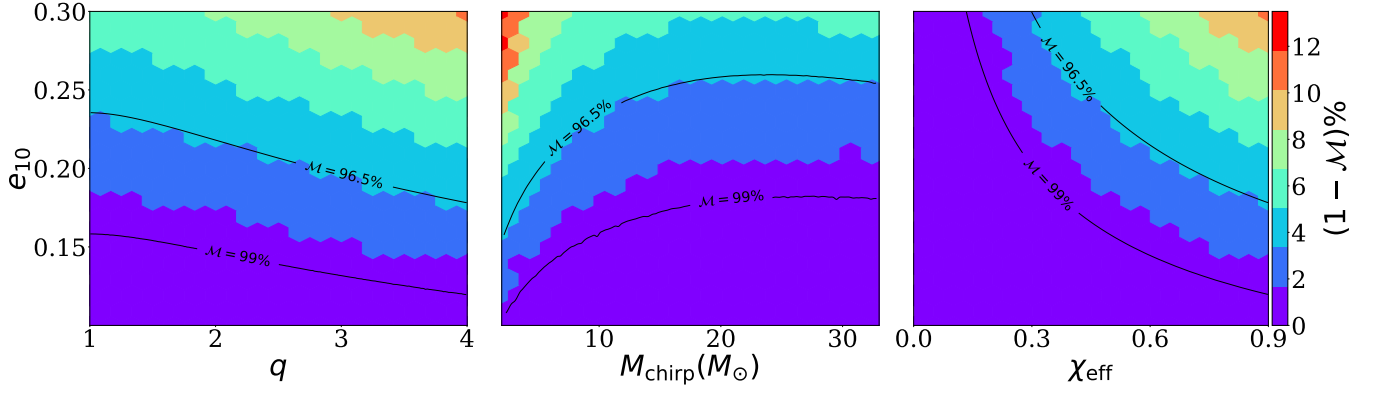


Figure 1. The comparison of **TaylorF2Ecc** [76, 77] with the spinning eccentric corrections in TaylorF2 up to 3PN order, expanded in eccentricity up to second power in eccentricity added in **TaylorF2Ecc** is shown here. We compute mismatch $(1 - \mathcal{M})\%$ between the two waveforms in various parameter planes, such as (a) eccentricity at 10Hz (e_{10}) - mass-ratio (q) (left), (b) e_{10} - chirp mass (M_{chirp}) (middle), (c) e_{10} - effective spin parameter (χ_{eff}) (right), respectively. The total mass (M) is fixed to $10M_{\odot}$ (left and right), q is fixed to 4 (middle and right), the z -component of dimensionless spins (χ_{1z}, χ_{2z}) are fixed to $(0.9, 0.9)$ (left and middle). The 96.5% and 99% match contours (as indicated by the solid black curves) are shown in each figure. The mismatch is performed using a lower cutoff frequency 10Hz, choosing Schwarzschild ISCO frequency (defined in Eq. (25)) as the upper cutoff frequency, and using advanced LIGO (aLIGO) zero-detuned high-power PSD.

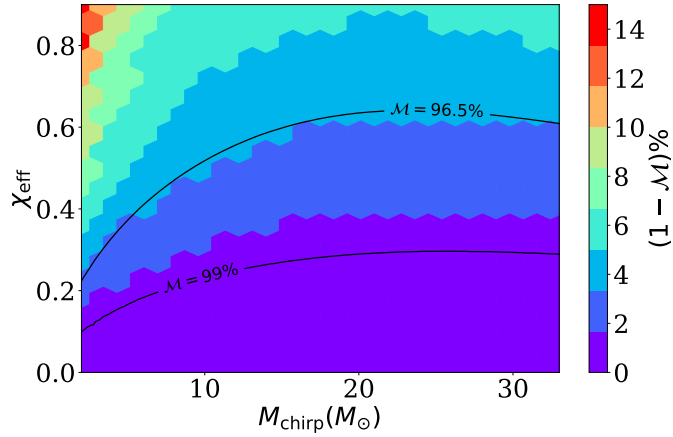


Figure 2. Similar to Fig. 1, here we show the mismatch $(1 - \mathcal{M})\%$ as a function of χ_{eff} and M_{chirp} . q and e_{10} are fixed to 4 and 0.3, respectively. The 96.5% and 99% match contours (as indicated by the solid black curves) are shown in the figure. The mismatch is performed using a lower cutoff frequency 10Hz, choosing Schwarzschild ISCO frequency (defined in Eq. (25)) as the upper cutoff frequency, and using advanced LIGO (aLIGO) zero-detuned high-power PSD.

$$\phi_{\text{SO}}^{(\text{resum})3\text{PN}} = y^6 \left[\frac{1135}{6} \pi \delta \chi_a + \frac{1135\pi}{6} \left(1 - \frac{156\nu}{227} \right) \chi_s \right], \quad (35h)$$

$$\begin{aligned} \phi_{\text{SO,ecc}}^{(\text{resum})3\text{PN}} = & y^6 \left[\frac{1135}{6} \pi \delta \chi_a + \frac{1135\pi}{6} \left(1 - \frac{156\nu}{227} \right) \chi_s \right] + \frac{35}{272} \left(\frac{y_0}{y} \right)^{19/3} \left\{ y_0^6 \left[\frac{157043\pi \delta \chi_a}{15552} + \frac{157043\pi}{15552} \left(1 - \frac{150652\nu}{157043} \right) \chi_s \right] \right. \\ & + y^3 y_0^3 \left[\frac{12307507\pi \delta \chi_a}{340200} + \frac{12307507\pi}{340200} \left(1 + \frac{1015892\nu}{723971} \right) \chi_s \right] \\ & \left. - y^6 \left[\frac{153181985\pi \delta \chi_a}{870912} + \frac{153181985\pi}{870912} \left(1 - \frac{1475156\nu}{9010705} \right) \chi_s \right] \right\}, \quad (35i) \end{aligned}$$

$$\begin{aligned} \phi_{\text{SS}}^{(\text{resum})3\text{PN}} = & y^6 \left\{ \left[-\frac{1344475}{8064} \left(1 - \frac{428504\nu}{268895} + \frac{96768\nu^2}{268895} \right) + \frac{26015}{112} \left[\left(1 - \frac{4186\nu}{15609} \right) \delta \kappa_a + \left(1 - \frac{35404\nu}{15609} - \frac{1344\nu^2}{5203} \right) \kappa_s \right] \right] \chi_a^2 \right. \\ & \left. + \left[\frac{26015}{56} \left(1 - \frac{35404\nu}{15609} - \frac{1344\nu^2}{5203} \right) \kappa_a + \delta \left[-\frac{1344475}{4032} \left(1 - \frac{8344\nu}{268895} \right) \right] \right] \chi_a \right\} \end{aligned}$$

$$\begin{aligned}
& + \frac{26015}{56} \left(1 - \frac{4186\nu}{15609}\right) \kappa_s \Big] \chi_a \chi_s + \left[-\frac{1344475}{8064} \left(1 - \frac{663764\nu}{268895} - \frac{152992\nu^2}{268895}\right) + \frac{26015}{112} \left[\left(1 - \frac{4186\nu}{15609}\right) \delta\kappa_a + \left(1 - \frac{35404\nu}{15609} - \frac{1344\nu^2}{5203}\right) \kappa_s \right] \chi_s^2 \right\}, \tag{35j} \\
\phi_{\text{SS,ecc}}^{(\text{resum})3\text{PN}} = & y^6 \left\{ \left[-\frac{1344475}{8064} \left(1 - \frac{428504\nu}{268895} + \frac{96768\nu^2}{268895}\right) + \frac{26015}{112} \left[\left(1 - \frac{4186\nu}{15609}\right) \delta\kappa_a + \left(1 - \frac{35404\nu}{15609} - \frac{1344\nu^2}{5203}\right) \kappa_s \right] \chi_a^2 + \left[\frac{26015}{56} \left(1 - \frac{35404\nu}{15609} - \frac{1344\nu^2}{5203}\right) \kappa_a + \delta \left[-\frac{1344475}{4032} \left(1 - \frac{8344\nu}{268895}\right) + \frac{26015}{56} \left(1 - \frac{4186\nu}{15609}\right) \kappa_s \right] \chi_a \chi_s + \left[-\frac{1344475}{8064} \left(1 - \frac{663764\nu}{268895} - \frac{152992\nu^2}{268895}\right) + \frac{26015}{112} \left[\left(1 - \frac{4186\nu}{15609}\right) \delta\kappa_a + \left(1 - \frac{35404\nu}{15609} - \frac{1344\nu^2}{5203}\right) \kappa_s \right] \chi_s^2 \right\} - \frac{35}{272} \left(\frac{y_0}{y}\right)^{19/3} \left\{ y^3 y_0^3 \left[\frac{477751}{25515} (1 - 4\nu) \chi_a^2 + \frac{955502}{25515} \left(1 + \frac{120251\nu}{281030}\right) \delta\chi_a \chi_s + \frac{477751}{25515} \left(1 + \frac{120251\nu}{140515} - \frac{30646\nu^2}{28103}\right) \chi_s^2 \right] + y^4 y_0^2 \left[\left[-\frac{1492991}{7451136} \left(1 + \frac{13438736\nu}{87823} - \frac{26498864\nu^2}{87823}\right) + \frac{57841361}{3725568} \left(1 - \frac{5516\nu}{2833}\right) \delta\kappa_a + \frac{57841361}{3725568} \left(1 - \frac{11182\nu}{2833} + \frac{11032\nu^2}{2833}\right) \kappa_s \right] \chi_a^2 + \left[\frac{57841361}{1862784} \left(1 - \frac{11182\nu}{2833} + \frac{11032\nu^2}{2833}\right) \kappa_a + \delta \left[-\frac{1492991}{3725568} \left(1 - \frac{5516\nu}{2833}\right) + \frac{57841361}{1862784} \left(1 - \frac{5516\nu}{2833}\right) \kappa_s \right] \chi_a \chi_s + \left[-\frac{1492991}{7451136} \left(1 - \frac{14132020\nu}{87823} + \frac{27182848\nu^2}{87823}\right) + \frac{57841361}{3725568} \left(1 - \frac{5516\nu}{2833}\right) \delta\kappa_a + \frac{57841361}{3725568} \left(1 - \frac{11182\nu}{2833} + \frac{11032\nu^2}{2833}\right) \kappa_s \right] \chi_s^2 + y^2 y_0^4 \left[\left[\frac{35122867}{9483264} \left(1 - \frac{57485464\nu}{2066051} + \frac{24850224\nu^2}{2066051}\right) + \frac{240456551}{4741632} \left(1 - \frac{69804\nu}{158927}\right) \delta\kappa_a + \frac{240456551}{4741632} \left(1 - \frac{387658\nu}{158927} + \frac{139608\nu^2}{158927}\right) \kappa_s \right] \chi_a^2 + \left[\frac{240456551}{2370816} \left(1 - \frac{387658\nu}{158927} + \frac{139608\nu^2}{158927}\right) \kappa_a + \delta \left[\frac{35122867}{4741632} \left(1 - \frac{69804\nu}{158927}\right) + \frac{240456551}{2370816} \left(1 - \frac{69804\nu}{158927}\right) \kappa_s \right] \chi_a \chi_s + \left[\frac{35122867}{9483264} \left(1 + \frac{47406356\nu}{2066051} - \frac{21220416\nu^2}{2066051}\right) + \frac{240456551}{4741632} \left(1 - \frac{69804\nu}{158927}\right) \delta\kappa_a + \frac{240456551}{4741632} \left(1 - \frac{387658\nu}{158927} + \frac{139608\nu^2}{158927}\right) \kappa_s \right] \chi_s^2 \right\} + y_0^6 \left[\left[\frac{24433195}{2612736} \left(1 - \frac{169526104\nu}{24433195} + \frac{73395504\nu^2}{24433195}\right) + \frac{906103}{48384} \left(1 - \frac{1081668\nu}{906103}\right) \delta\kappa_a + \frac{906103}{48384} \left(1 - \frac{2893874\nu}{906103} + \frac{1359176\nu^2}{906103}\right) \kappa_s \right] \chi_a^2 + \left[\frac{906103}{24192} \left(1 - \frac{2893874\nu}{906103} + \frac{1359176\nu^2}{906103}\right) \kappa_a + \delta \left[\frac{24433195}{1306368} \left(1 - \frac{33561668\nu}{24433195}\right) + \frac{906103}{24192} \left(1 - \frac{1081668\nu}{906103}\right) \kappa_s \right] \chi_a \chi_s + \left[\frac{24433195}{2612736} \left(1 + \frac{4669988\nu}{24433195} - \frac{42904736\nu^2}{24433195}\right) + \frac{906103}{48384} \left(1 - \frac{1081668\nu}{906103}\right) \delta\kappa_a + \frac{906103}{48384} \left(1 - \frac{2893874\nu}{906103} + \frac{1359176\nu^2}{906103}\right) \kappa_s \right] \chi_s^2 + y^6 \left[\left[-\frac{24653523709}{146313216} \left(1 - \frac{7638735632\nu}{1450207277} + \frac{2575441008\nu^2}{1450207277}\right) - \frac{67698947}{903168} \left(1 - \frac{12996788\nu}{11946873}\right) \delta\kappa_a + \left(-\frac{67698947}{903168} \left(1 - \frac{36890534\nu}{11946873} + \frac{15897784\nu^2}{3982291}\right) \kappa_s \right] \chi_a^2 + \left[-\frac{67698947}{451584} \left(1 - \frac{36890534\nu}{11946873} + \frac{15897784\nu^2}{3982291}\right) \kappa_a + \delta \left[-\frac{24653523709}{73156608} \left(1 + \frac{87630620\nu}{1450207277}\right) - \frac{67698947}{451584} \left(1 - \frac{12996788\nu}{11946873}\right) \kappa_s \right] \chi_a \chi_s + \left[-\frac{24653523709}{146313216} \left(1 + \frac{2013167764\nu}{1450207277} \right. \right.
\end{aligned}$$

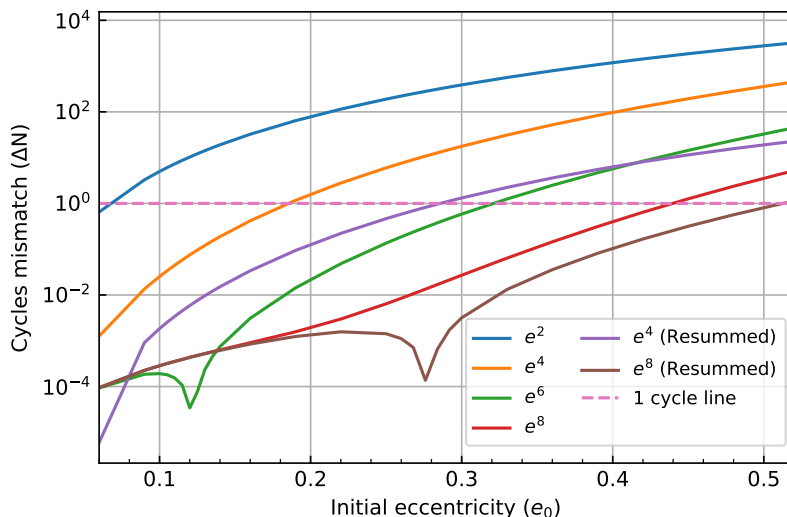


Figure 3. Difference in the number of GW cycles between a numerical evolution of ϕ (valid for any initial eccentricity e_0) and the analytical ϕ derived above, plotted using Eq. (32). The 1-cycle line roughly represents where the phase error between the exact eccentricity solution and the analytical low eccentricity solution becomes significant and our approximation breaks down. Further, the analytical resummed expressions (as in Eq. 35) for the e_0^4 , e_0^6 and e_0^8 expanded phase are also shown. The plot has been made for a system with spins $\chi_1 = 0.7$, $\chi_2 = 0.8$ and with component masses $m_1 = m_2 = 1.4 M_\odot$.

$$\begin{aligned}
 & - \frac{3160271968\nu^2}{1450207277} \Big) - \frac{67698947}{903168} \left(1 - \frac{12996788\nu}{11946873} \right) \delta\kappa_a - \frac{67698947}{903168} \left(1 - \frac{36890534\nu}{11946873} \right. \\
 & \left. + \frac{15897784\nu^2}{3982291} \right) \kappa_s \Big] \chi_s^2 \Big\}. \tag{35k}
 \end{aligned}$$

V. CONCLUSIONS AND DISCUSSIONS

The main objective of our work has been to include spinning eccentric corrections, as well as higher-order eccentricity ($\mathcal{O}(e_0^8)$) corrections to the existing analytical inspiral-only Taylor approximants derived in Ref. [76]. We perform this task and give the reader a prescription to calculate the eccentricity evolution to any arbitrary eccentricity order of e_0 . Although we only quote low eccentricity solution and Taylor approximants (till e_0^2) in the main paper, we provide the full e_0^8 solution in a supplementary file.

We estimate the importance of the newly computed spinning eccentric expressions reported in the TaylorF2 phase. To do so, we compute mismatch (defined in Eq. (30)) between TaylorF2Ecc [76, 77] and spinning eccentric corrections in TaylorF2 phase expanded in eccentricity up to $\mathcal{O}(e_0^2)$ added in TaylorF2Ecc in Figs. 1 and 2. We show the mismatch in eccentricity at 10 Hz (e_{10}), chirp mass (M_{chirp}), effective spin parameter (χ_{eff}) (defined in Eq. (31)), mass ratio (q) parameter space.

While our study primarily focuses on the secular contribution to the orbit and waveform in terms of the TaylorT2 approximants, we also provide a derivation of the oscillatory part of the phase, $W(f)$, in Appendix B. It

has also been shown that the eccentric spinning section of the oscillatory terms contributes negligibly to the total GW cycles for $e_0 = 0.1$ and any spin setting. To be precise, the oscillatory contribution does not exceed 0.06 GW cycles for $e_0 = 0.1$ at 10 Hz for any configuration of spins.

While we include eccentricity corrections to $\mathcal{O}(e_0^8)$ to the phasing approximants, we do not consider eccentricity corrections to the waveform amplitude. But, our low-eccentricity approximation has been compared in Sec. IV D with a numerically calculated solution to the evolution equations (Eq. (6)), which is exact in eccentricity. For most spin systems, our analytic expressions are valid up to $e_0 \lesssim 0.45$ (arrived at by setting the threshold of accumulated cycles difference to $\Delta N_{\text{cyc}} \leq 1$), and the resummed expressions extend this validity up to $e_0 \lesssim 0.55$. This validity is subject to the specific settings of the system under consideration.

We quantify the relative importance of the low eccentricity spinning corrections to the secular phasing in Sec. IV B 1 through Table II by defining a measure (used in Ref. [76]) called number of cumulative GW cycles, defined in Eq. (26). This particular measure quantifies the length of the GW signal in a particular frequency band. We first gauge the importance of each PN term's contri-

bution to the number of GW cycles in Table II, where we find particular trends due to the addition of spinning eccentric effects to the phasing formula. From Table II, we can draw certain conclusions on the effects of spins and eccentricity taken together.

In this study, we calculated both time and frequency domain phasing for spin-aligned and eccentric compact binary systems. An immediate consequence of this study will be the estimation of source parameters of GWs coming from spinning and eccentric binary systems. The results of this study can be used to create new inspiral waveform templates or augment existing waveform models. The inclusion of the combined effect of spins and orbital eccentricity in waveform models will lead to lesser systematic biases in the estimation of GW source properties and can possibly lead to more detections because of a better match between a template waveform and the data, leading to an increase in the signal-to-noise ratio. A possible extension of this study is to include the effects of misaligned spins on the spherical harmonic modes and the phasing of compact binary mergers with eccentric orbits. In such systems, there is a precession of the orbit due to spin misalignment, which leads to amplitude modulation of the GW signal since the plane of the orbit keeps changing with respect to the line connecting the source and the detector. In the absence of matter (for example, accretion disks), spin-misaligned eccentric systems form the most general situation a compact binary system can be in. Hence, we hope to include the combined effect of spin precession and eccentricity in GW waveforms in a future study.

ACKNOWLEDGMENTS

We thank Prayush Kumar for insightful discussions on waveform related issues. We also thank Guillaume Faye for key inputs throughout the course of this study. C.K.M. acknowledges the support of SERB's Core Research Grant No. CRG/2022/007959. K.P. acknowledges the hospitality of the International Centre for Theoretical Sciences (ICTS) during the final stages of writing the paper. This document has LIGO preprint number LIGO-P2400592. We thank Anuradha Gupta for useful comments and suggestions on our manuscript.

Appendix A: Quasi-Keplerian (QK) parametrization

The energy and angular momentum emitted by an inspiralling compact binary system can be written as functions of the distance of separation r , the orbital phase ϕ , and their derivatives. Looking only at the conservative problem, the derivatives of r and ϕ can be written instead as a function of the energy and angular momentum. Treating the energy and angular momentum as constants in the conservative problem, these two first-order differential equations can be used to find the following 3PN

relations between the r and the eccentric anomaly u and the relationship between various other angles. In the following, we have reproduced the set of QK equations from Ref. [76] for the reader's advantage.

$$r = S(l; n, e_t) = a_r(1 - e_r \cos u), \quad (\text{A1a})$$

$$\dot{r} = n \frac{\partial S}{\partial l}(l; n, e_t), \quad (\text{A1b})$$

$$\phi = \lambda + W(l; n, e_t), \quad (\text{A1c})$$

$$\lambda = (1 + k)n(t - t_0) + c_\lambda, \quad (\text{A1d})$$

$$\begin{aligned} W(l; n, e_t) = & (1 + k)(v - l) + \left(\frac{f_{4\phi}}{c^4} + \frac{f_{6\phi}}{c^6} \right) \sin 2v \\ & + \left(\frac{g_{4\phi}}{c^4} + \frac{g_{6\phi}}{c^6} \right) \sin 3v + \frac{i_{6\phi}}{c^6} \sin 4v \\ & + \frac{h_{6\phi}}{c^6} \sin 5v, \end{aligned} \quad (\text{A1e})$$

$$\dot{\phi} = (1 + k)n + n \frac{\partial W}{\partial l}(l; n, e_t), \quad (\text{A1f})$$

$$\begin{aligned} l = & n(t - t_0) + c_l = u - e_t \sin u \\ & + \left(\frac{g_{4t}}{c^4} + \frac{g_{6t}}{c^6} \right) (v - u) + \left(\frac{f_{4t}}{c^4} + \frac{f_{6t}}{c^6} \right) \sin v \\ & + \frac{i_{6t}}{c^6} \sin 2v + \frac{h_{6t}}{c^6} \sin 3v, \end{aligned} \quad (\text{A1g})$$

$$v = V(u) \equiv 2 \arctan \left[\left(\frac{1 + e_\phi}{1 - e_\phi} \right)^{1/2} \tan \left(\frac{u}{2} \right) \right]. \quad (\text{A1h})$$

In the above, the various symbols have a corresponding PN series, which are energy and angular momentum functions. A non-exhaustive list of the meanings of the symbols in Eqs. (A1a)-(A1h) are given as follows

- a_r : Semi-major axis
- e_r : Radial eccentricity
- u : Eccentric anomaly
- λ : Secularly increasing part of the orbital phase
- W : Oscillatory part of the orbital phase
- k : Periastron precession under a single orbit
- v : True anomaly
- l : Mean anomaly
- $n = \frac{2\pi}{P}$: Mean motion
- P : Radial orbital period
- e_t : time eccentricity
- e_ϕ : phase eccentricity

It is to be noted that while all the quantities are gauge-dependent objects, the mean motion and the periastron advance are gauge-invariant. It is also to be noted that the orbital frequency ω is defined as follows

$$\omega = (1 + k) n, \quad (\text{A2})$$

which is also a gauge-invariant quantity. Hence, one can define a dimensionless and gauge-invariant quantity x that is given by

$$x = \left(\frac{GM\omega}{c^3} \right)^{2/3}, \quad (\text{A3})$$

which is a monotonic and increasing function of time and can be used as a substitute of time itself.

Appendix B: Oscillatory part of the orbital phase till e^2

One finds the oscillatory part of the phase from Eq. (A1e). To obtain it as a function of the GW frequency, however, one needs to calculate quantities like the periastron precession (k), the true anomaly (v), the mean anomaly (l), and f_ϕ, g_ϕ, i_ϕ and h_ϕ as a function of the PN parameter or the GW frequency.

Considering a binary with no radiation reaction, differentiation of Eq. (A1g) with respect to time yields the following equation for the mean anomaly evolution

$$\frac{dl}{dt} = n. \quad (\text{B1})$$

Again, using the chain rule, we rewrite the l evolution with respect to time as l evolution with respect to the PN parameter y , that is

$$\frac{dl}{dy} = \frac{n}{\frac{dy}{dt}}, \quad (\text{B2})$$

where $\frac{dy}{dt}$ was given in Eq. (6a), and we obtain n from the supplementary material of Ref. [72]. Rewriting n as y , and integrating both sides of Eq. (B2), we obtain l as follows

$$l = -\frac{1}{32y^5\nu} (\mathcal{L}_{\text{NS}} + \mathcal{L}_{\text{SO}} + \mathcal{L}_{\text{SS}}), \quad (\text{B3})$$

where,

$$\mathcal{L}_{\text{NS}} = 1 - e_0^2 \frac{105}{272} \left(\frac{y_0}{y} \right)^{19/3} + \mathcal{O}(y^2, e_0^4), \quad (\text{B4a})$$

$$\mathcal{L}_{\text{SO,circ}}^{1.5\text{PN}} = y^3 \left[\frac{805\delta\chi_a}{24} + \left(\frac{805}{24} - \frac{125\nu}{6} \right) \chi_s \right], \quad (\text{B4b})$$

$$\mathcal{L}_{\text{SO,ecc}}^{1.5\text{PN}} = -e_0^2 \frac{105}{272} \left(\frac{y_0}{y} \right)^{19/3} \left\{ y^3 \left[\left(-\frac{8602\nu}{675} - \frac{4726}{4725} \right) \chi_s - \frac{4726\delta\chi_a}{4725} \right] + y_0^3 \left[\left(\frac{55\nu}{27} - \frac{157}{54} \right) \chi_s - \frac{157\delta\chi_a}{54} \right] \right\}, \quad (\text{B4c})$$

$$\begin{aligned} \mathcal{L}_{\text{SS,circ}}^{2\text{PN}} &= y^4 \left\{ \chi_a^2 \left[-\frac{65\delta\kappa_a}{2} + \kappa_s \left(65\nu - \frac{65}{2} \right) + 65\nu - \frac{5}{16} \right] + \chi_a \chi_s \left[-65\delta\kappa_s - \frac{5\delta}{8} + \kappa_a(130\nu - 65) \right] \right. \\ &\quad \left. + \chi_s^2 \left[-\frac{65\delta\kappa_a}{2} + \kappa_s \left(65\nu - \frac{65}{2} \right) - \frac{255\nu}{4} - \frac{5}{16} \right] \right\}, \quad (\text{B4d}) \end{aligned}$$

$$\begin{aligned} \mathcal{L}_{\text{SS,ecc}}^{2\text{PN}} &= -e_0^2 \frac{105}{272} \left(\frac{y_0}{y} \right)^{19/3} \left(y^4 \left\{ \chi_a^2 \left[\frac{461873\delta\kappa_a}{14784} + \kappa_s \left(\frac{461873}{14784} - \frac{461873\nu}{7392} \right) + \frac{33371\nu}{672} - \frac{415531}{14784} \right] \right. \right. \\ &\quad \left. \left. + \chi_a \chi_s \left[\frac{461873\delta\kappa_s}{7392} - \frac{415531\delta}{7392} + \kappa_a \left(\frac{461873}{7392} - \frac{461873\nu}{3696} \right) \right] + \chi_s^2 \left[\frac{461873\delta\kappa_a}{14784} + \kappa_s \left(\frac{461873}{14784} - \frac{461873\nu}{7392} \right) \right. \right. \right. \\ &\quad \left. \left. \left. + \frac{66283\nu}{1056} - \frac{415531}{14784} \right] \right\} + y_0^4 \left\{ \chi_a^2 \left[\frac{89\delta\kappa_a}{192} + \kappa_s \left(\frac{89}{192} - \frac{89\nu}{96} \right) - \frac{623\nu}{96} + \frac{293}{192} \right] + \chi_a \chi_s \left[\frac{89\delta\kappa_s}{96} + \frac{293\delta}{96} \right. \right. \right. \\ &\quad \left. \left. \left. + \kappa_a \left(\frac{89}{96} - \frac{89\nu}{48} \right) \right] + \chi_s^2 \left[\frac{89\delta\kappa_a}{192} + \kappa_s \left(\frac{89}{192} - \frac{89\nu}{96} \right) + \frac{37\nu}{96} + \frac{293}{192} \right] \right\} \right), \quad (\text{B4e}) \end{aligned}$$

$$\mathcal{L}_{\text{SO,circ}}^{2.5\text{PN}} = y^5 \left[\chi_a \left(-30\delta\nu \log(y) - \frac{638185\delta \log(y)}{2016} \right) + \chi_s \left(60\nu^2 \log(y) + \frac{177185}{504} \nu \log(y) - \frac{638185 \log(y)}{2016} \right) \right], \quad (\text{B4f})$$

$$\begin{aligned}
\mathcal{L}_{\text{SO,ecc}}^{2.5\text{PN}} = & -e_0^2 \frac{105}{272} \left(\frac{y_0}{y} \right)^{19/3} \left\{ y^5 \left[\chi_a \left(\frac{7612064279\delta}{18098640} - \frac{7610543\delta\nu}{23940} \right) + \left(\frac{56185\nu^2}{513} - \frac{576320281\nu}{1131165} + \frac{7612064279}{18098640} \right) \chi_s \right] \right. \\
& + y_0^5 \left[\chi_a \left(\frac{242719\delta\nu}{9720} - \frac{1279073\delta}{38880} \right) + \left(-\frac{4322\nu^2}{243} + \frac{146807\nu}{2430} - \frac{1279073}{38880} \right) \chi_s \right] + y^2 y_0^3 \left[\chi_a \left(\frac{739313\delta\nu}{21168} \right. \right. \\
& \left. \left. - \frac{367678771\delta}{5334336} \right) + \left(-\frac{258995\nu^2}{10584} + \frac{221958103\nu}{2667168} - \frac{367678771}{5334336} \right) \chi_s \right] + y^3 y_0^2 \left[\chi_a \left(\frac{465511\delta\nu}{85050} - \frac{6694379\delta}{2381400} \right) \right. \\
& \left. + \left(\frac{847297\nu^2}{12150} - \frac{10322689\nu}{340200} - \frac{6694379}{2381400} \right) \chi_s \right] \left. \right\}, \tag{B4g}
\end{aligned}$$

$$\mathcal{L}_{\text{SO,circ}}^{3\text{PN}} = y^6 \left[\frac{1615\pi\delta\chi_a}{6} + \left(\frac{1615\pi}{6} - 170\pi\nu \right) \chi_s \right], \tag{B4h}$$

$$\begin{aligned}
\mathcal{L}_{\text{SO,ecc}}^{3\text{PN}} = & -e_0^2 \frac{105}{272} \left(\frac{y_0}{y} \right)^{19/3} \left\{ y^6 \left[\frac{157779329\pi\delta\chi_a}{870912} + \left(\frac{157779329\pi}{870912} - \frac{6844081\pi\nu}{217728} \right) \chi_s \right] + y_0^6 \left[\left(\frac{37663\pi\nu}{3888} \right. \right. \right. \\
& \left. \left. - \frac{157043\pi}{15552} \right) \chi_s - \frac{157043\pi\delta\chi_a}{15552} \right] + y^3 y_0^3 \left[\left(-\frac{2764421\pi\nu}{42525} - \frac{2617099\pi}{340200} \right) \chi_s - \frac{2617099\pi\delta\chi_a}{340200} \right] \left. \right\}, \tag{B4i}
\end{aligned}$$

$$\begin{aligned}
\mathcal{L}_{\text{SS,circ}}^{3\text{PN}} = & y^6 \left\{ \chi_a^2 \left[\kappa_a \left(\frac{50705\delta}{224} - \frac{505\delta\nu}{6} \right) + \kappa_s \left(-\frac{305\nu^2}{4} - \frac{180395\nu}{336} + \frac{50705}{224} \right) - \frac{305\nu^2}{4} + \frac{273635\nu}{252} - \frac{2951395}{8064} \right] \right. \\
& + \chi_a \chi_s \left[\kappa_s \left(\frac{50705\delta}{112} - \frac{505\delta\nu}{3} \right) + \frac{8725\delta\nu}{72} - \frac{2951395\delta}{4032} + \kappa_a \left(-\frac{305\nu^2}{2} - \frac{180395\nu}{168} + \frac{50705}{112} \right) \right] \\
& \left. + \chi_s^2 \left[\kappa_a \left(\frac{50705\delta}{224} - \frac{505\delta\nu}{6} \right) + \kappa_s \left(-\frac{305\nu^2}{4} - \frac{180395\nu}{336} + \frac{50705}{224} \right) + \frac{880\nu^2}{9} + \frac{1006615\nu}{2016} - \frac{2951395}{8064} \right] \right\}, \tag{B4j}
\end{aligned}$$

$$\begin{aligned}
\mathcal{L}_{\text{SS,ecc}}^{3\text{PN}} = & -e_0^2 \frac{105}{272} \left(\frac{y_0}{y} \right)^{19/3} \left(y^6 \left\{ \chi_a^2 \left[\kappa_a \left(\frac{33341947\delta\nu}{387072} + \frac{398332253\delta}{3612672} \right) + \kappa_s \left(-\frac{40026449\nu^2}{64512} - \frac{728209501\nu}{5419008} \right. \right. \right. \right. \\
& \left. \left. + \frac{398332253}{3612672} \right) - \frac{394111\nu^2}{7168} + \frac{240105088291\nu}{146313216} - \frac{130039497587}{292626432} \right] + \chi_a \chi_s \left[\kappa_s \left(\frac{33341947\delta\nu}{193536} + \frac{398332253\delta}{1806336} \right) \right. \\
& \left. + \frac{68731561\delta\nu}{5225472} - \frac{130039497587\delta}{146313216} + \kappa_a \left(-\frac{40026449\nu^2}{32256} - \frac{728209501\nu}{2709504} + \frac{398332253}{1806336} \right) \right] \\
& + \chi_s^2 \left[\kappa_a \left(\frac{33341947\delta\nu}{387072} + \frac{398332253\delta}{3612672} \right) + \kappa_s \left(-\frac{40026449\nu^2}{64512} - \frac{728209501\nu}{5419008} + \frac{398332253}{3612672} \right) \right. \\
& \left. + \frac{3649860101\nu^2}{5225472} + \frac{3128341513\nu}{20901888} - \frac{130039497587}{292626432} \right] \left. \right\} + y_0^6 \left\{ \chi_a^2 \left[\kappa_a \left(\frac{906103\delta}{193536} - \frac{12877\delta\nu}{2304} \right) + \kappa_s \left(\frac{24271\nu^2}{3456} \right. \right. \right. \\
& \left. \left. - \frac{1446937\nu}{96768} + \frac{906103}{193536} \right) + \frac{169897\nu^2}{3456} - \frac{40961143\nu}{373248} + \frac{17465819}{746496} \right] + \chi_a \chi_s \left[\kappa_s \left(\frac{906103\delta}{96768} - \frac{12877\delta\nu}{1152} \right) \right. \\
& \left. - \frac{5526373\delta\nu}{93312} + \frac{17465819\delta}{373248} + \kappa_a \left(\frac{24271\nu^2}{1728} - \frac{1446937\nu}{48384} + \frac{906103}{96768} \right) \right] + \chi_s^2 \left[\kappa_a \left(\frac{906103\delta}{193536} - \frac{12877\delta\nu}{2304} \right) \right. \\
& \left. + \kappa_s \left(\frac{24271\nu^2}{3456} - \frac{1446937\nu}{96768} + \frac{906103}{193536} \right) + \frac{433639\nu^2}{93312} - \frac{16075987\nu}{373248} + \frac{17465819}{746496} \right] \left. \right\} \\
& + y^2 y_0^4 \left\{ \chi_a^2 \left[\kappa_a \left(\frac{208429367\delta}{18966528} - \frac{419101\delta\nu}{75264} \right) + \kappa_s \left(\frac{419101\nu^2}{37632} - \frac{261236093\nu}{9483264} + \frac{208429367}{18966528} \right) + \frac{419101\nu^2}{5376} \right. \right. \\
& \left. \left. - \frac{33323519\nu}{193536} + \frac{686177579}{18966528} \right] + \chi_a \chi_s \left[\kappa_s \left(\frac{208429367\delta}{9483264} - \frac{419101\delta\nu}{37632} \right) - \frac{1379737\delta\nu}{37632} + \frac{686177579\delta}{9483264} \right. \right. \\
& \left. \left. + \kappa_a \left(\frac{419101\nu^2}{18816} - \frac{261236093\nu}{4741632} + \frac{208429367}{9483264} \right) \right] + \chi_s^2 \left[\kappa_a \left(\frac{208429367\delta}{18966528} - \frac{419101\delta\nu}{75264} \right) \right. \right. \\
& \left. \left. + \kappa_s \left(\frac{419101\nu^2}{37632} - \frac{261236093\nu}{9483264} + \frac{208429367}{18966528} \right) - \frac{174233\nu^2}{37632} - \frac{87196451\nu}{9483264} + \frac{686177579}{18966528} \right] \right\} \\
& + y^3 y_0^3 \left[\chi_a \chi_s \left(\frac{4466869\delta\nu}{127575} + \frac{741982\delta}{127575} \right) + \left(-\frac{94622\nu^2}{3645} + \frac{4466869\nu}{127575} + \frac{370991}{127575} \right) \chi_s^2 + \left(\frac{370991}{127575} \right. \right.
\end{aligned}$$

$$\begin{aligned}
& -\frac{1483964\nu}{127575} \chi_a^2 \Big] + y^4 y_0^2 \left\{ \chi_a^2 \left[\kappa_a \left(\frac{1308486209\delta}{14902272} - \frac{90988981\delta\nu}{532224} \right) + \kappa_s \left(\frac{90988981\nu^2}{266112} - \frac{2582331943\nu}{7451136} \right. \right. \right. \\
& + \left. \left. \frac{1308486209}{14902272} \right) - \frac{6574087\nu^2}{24192} + \frac{2185974971\nu}{7451136} - \frac{1177199323}{14902272} \right] + \chi_a \chi_s \left[\kappa_s \left(\frac{1308486209\delta}{7451136} - \frac{90988981\delta\nu}{266112} \right) \right. \\
& + \left. \frac{81859607\delta\nu}{266112} - \frac{1177199323\delta}{7451136} + \kappa_a \left(\frac{90988981\nu^2}{133056} - \frac{2582331943\nu}{3725568} + \frac{1308486209}{7451136} \right) \right] \\
& + \chi_s^2 \left[\kappa_a \left(\frac{1308486209\delta}{14902272} - \frac{90988981\delta\nu}{532224} \right) + \kappa_s \left(\frac{90988981\nu^2}{266112} - \frac{2582331943\nu}{7451136} + \frac{1308486209}{14902272} \right) - \frac{13057751\nu^2}{38016} \right. \\
& \left. + \frac{351498953\nu}{1064448} - \frac{1177199323}{14902272} \right] \Big\} . \tag{B4k}
\end{aligned}$$

Inverting Eq. (A1g), one obtains u in terms of l . Similarly, once u is obtained as a function of l , v can also be obtained as a function of u through Eq. (A1h). The expressions of u as a function of l and v as a function of u are rather large and have been given in a supplementary file. We also find that out of the set f_ϕ, g_ϕ, i_ϕ , and h_ϕ , only f_ϕ contributes at 3PN for spinning systems. That is,

the rest of the contribution to g_ϕ, i_ϕ , and h_ϕ comes due to the non-spinning (and eccentric) parts of the system, so we ignore them and concentrate on the contribution of the spinning parts. Before calculating W , we find that we have one more quantity to calculate: $K = (1 + k)$. We find K in terms of y as follows

$$K = \mathcal{K}_{\text{NS}} + \mathcal{K}_{\text{SO}} + \mathcal{K}_{\text{SS}}, \tag{B5}$$

where,

$$\mathcal{K}_{\text{NS}} = 1 + \mathcal{O}(y^2, e_0^2 y^4), \tag{B6a}$$

$$\mathcal{K}_{\text{SO,circ}}^{1.5\text{PN}} = y^3 [(2\nu - 4)\chi_s - 4\delta\chi_a], \tag{B6b}$$

$$\mathcal{K}_{\text{SO,ecc}}^{1.5\text{PN}} = 0, \tag{B6c}$$

$$\mathcal{K}_{\text{SS,circ}}^{2\text{PN}} = y^4 \left\{ \chi_a^2 \left[\frac{3\delta\kappa_a}{2} + \kappa_s \left(\frac{3}{2} - 3\nu \right) - 3\nu \right] + \chi_a \chi_s [3\delta\kappa_s + \kappa_a(3 - 6\nu)] + \chi_s^2 \left[\frac{3\delta\kappa_a}{2} + \kappa_s \left(\frac{3}{2} - 3\nu \right) + 3\nu \right] \right\}, \tag{B6d}$$

$$\mathcal{K}_{\text{SS,ecc}}^{2\text{PN}} = 0, \tag{B6e}$$

$$\mathcal{K}_{\text{SO,circ}}^{2.5\text{PN}} = y^5 \left[\chi_a \left(\frac{17\delta\nu}{2} - 34\delta \right) + \left(-2\nu^2 + \frac{81\nu}{2} - 34 \right) \chi_s \right], \tag{B6f}$$

$$\mathcal{K}_{\text{SO,ecc}}^{2.5\text{PN}} = e_0^2 \left(\frac{y_0}{y} \right)^{19/3} y^5 [\chi_a(14\delta\nu - 30\delta) + (-7\nu^2 + 29\nu - 30)\chi_s], \tag{B6g}$$

$$\mathcal{K}_{\text{SO,circ}}^{3\text{PN}} = 0, \tag{B6h}$$

$$\mathcal{K}_{\text{SO,ecc}}^{3\text{PN}} = 0, \tag{B6i}$$

$$\begin{aligned}
\mathcal{K}_{\text{SS,circ}}^{3\text{PN}} = y^6 \left\{ \chi_a^2 \left[\kappa_a \left(\frac{39\delta}{2} - \frac{17\delta\nu}{2} \right) + \kappa_s \left(5\nu^2 - \frac{95\nu}{2} + \frac{39}{2} \right) + 5\nu^2 - 92\nu + 14 \right] + \chi_a \chi_s [\kappa_s(39\delta - 17\delta\nu) - 38\delta\nu \right. \\
\left. + 28\delta + \kappa_a(10\nu^2 - 95\nu + 39)] + \chi_s^2 \left[\kappa_a \left(\frac{39\delta}{2} - \frac{17\delta\nu}{2} \right) + \kappa_s \left(5\nu^2 - \frac{95\nu}{2} + \frac{39}{2} \right) + 9\nu^2 - 2\nu + 14 \right] \right\}, \tag{B6j}
\end{aligned}$$

$$\begin{aligned}
\mathcal{K}_{\text{SS,ecc}}^{3\text{PN}} = e_0^2 \left(\frac{y_0}{y} \right)^{19/3} y^6 \left\{ \chi_a^2 \left[\kappa_a \left(\frac{39\delta}{2} - \frac{35\delta\nu}{4} \right) + \kappa_s \left(\frac{29\nu^2}{2} - \frac{191\nu}{4} + \frac{39}{2} \right) + \frac{29\nu^2}{2} - \frac{249\nu}{4} + 6 \right] \right. \\
+ \chi_a \chi_s \left[\kappa_s \left(39\delta - \frac{35\delta\nu}{2} \right) - \frac{15\delta\nu}{2} + 12\delta + \kappa_a \left(29\nu^2 - \frac{191\nu}{2} + 39 \right) \right] + \chi_s^2 \left[\kappa_a \left(\frac{39\delta}{2} - \frac{35\delta\nu}{4} \right) \right. \\
\left. + \kappa_s \left(\frac{29\nu^2}{2} - \frac{191\nu}{4} + \frac{39}{2} \right) - \frac{29\nu^2}{2} + \frac{123\nu}{4} + 6 \right] \Big\}. \tag{B6k}
\end{aligned}$$

The oscillatory part of the phase W as a function of y is a rather lengthy expression, which we don't show in this text. However, we plot W as a function of the GW frequency f for the spinning case in Fig. 4. It is seen that the value of W decreases rapidly as the binary inspiral progresses towards higher frequencies.

When the spin is not zero, the oscillatory phase is similar to the non-spinning case. We have observed that the behaviour of the oscillatory phase does not depend much on the component spins. In Fig. 4, we have shown the oscillatory phase for different orientations and values of the spins. We noticed that the phase only changes while the amplitude remains constant.

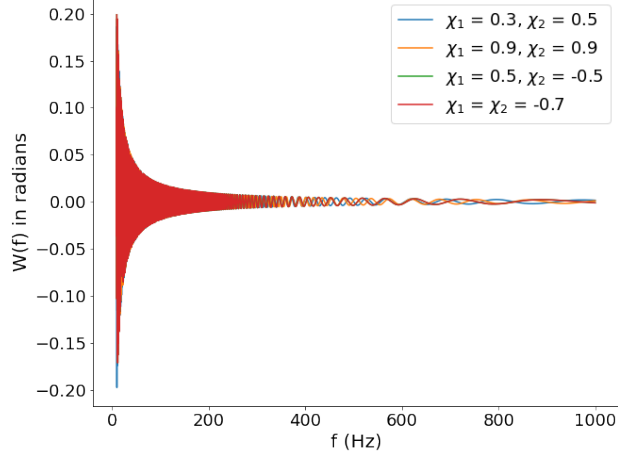


Figure 4. The oscillatory part of the phase $W(f)$ has been plotted as a function of the GW frequency f . We have limited the masses of the components to be $m_1 = m_2 = 1.4 M_\odot$ in this figure and have varied the spins while keeping the initial eccentricity e_0 fixed at 0.1 at 10 Hz. We observed that there was very little difference from the non-spinning system. The amplitude of each scenario remained at 0.2. However, in the $W(f)$ phase, there were shifts when the spins and their orientations were altered.

Detector	LIGO/Virgo		3G			DECIGO		LISA		
Masses (M_\odot)	1.4 + 1.4	10 + 10	1.4 + 1.4	50 + 50	500 + 500	500 + 500	5000 + 5000	$10^5 + 10^5$	$10^7 + 10^7$	
PN order	cumulative number of cycles									
0PN	-4.87×10^{-3}	-1.21×10^{-1}	-2.47×10^{-2}	7.51×10^{-2}	1.31×10^{-1}	4.39×10^{-2}	7.51×10^{-2}	1.28×10^{-1}	-7.48×10^{-2}	
1PN	7.21×10^{-4}	-1.23×10^{-2}	7.62×10^{-4}	-2.29×10^{-3}	3.36×10^{-2}	-1.07×10^{-3}	-2.29×10^{-3}	-2.63×10^{-3}	-3.35×10^{-2}	
1.5PN	-4.84×10^{-4}	3.37×10^{-3}	-1.95×10^{-5}	8.97×10^{-4}	1.04×10^{-2}	6.13×10^{-5}	8.97×10^{-4}	2.48×10^{-4}	4.22×10^{-2}	
2PN	2.55×10^{-4}	-1.83×10^{-3}	-1.17×10^{-5}	-1.05×10^{-3}	5.58×10^{-3}	-6.33×10^{-5}	-1.05×10^{-3}	-1.22×10^{-4}	1.53×10^{-2}	
2.5PN	1.33×10^{-4}	-2.17×10^{-3}	-1.43×10^{-5}	-9.92×10^{-4}	-6.59×10^{-3}	-2.95×10^{-6}	-9.92×10^{-4}	-1.63×10^{-4}	-1.12×10^{-2}	
3PN	-4.94×10^{-5}	2.36×10^{-4}	-3.63×10^{-6}	1.47×10^{-4}	2.09×10^{-3}	-9.37×10^{-6}	1.47×10^{-4}	2.24×10^{-5}	1.42×10^{-3}	
Total	-4.30×10^{-3}	-1.34×10^{-1}	-2.40×10^{-2}	7.18×10^{-2}	1.76×10^{-1}	4.28×10^{-2}	7.18×10^{-2}	1.25×10^{-1}	-6.06×10^{-2}	

Table III. Contribution of each PN order to the total number of accumulated cycles by the oscillatory phase inside the detector's frequency band, for typical eccentric spinning ($e_0 = 0.2$; $\chi_1 = \chi_2 = 0.4$ for BNS and $\chi_1 = \chi_2 = 0.9$ for BBH) compact binaries observed by current and future detectors. We have approximated the frequency bands of LIGO/Virgo A+, Einstein Telescope (ET/CE/3G), DECIGO, and LISA with step functions (as in Table II), respectively between $[10 \text{ Hz}, 10^3 \text{ Hz}]$, $[1 \text{ Hz}, 10^4 \text{ Hz}]$, $[10^{-2} \text{ Hz}, 1 \text{ Hz}]$ and $[10^{-4} \text{ Hz}, 10^{-1} \text{ Hz}]$.

Appendix C: TaylorT1, TaylorT3 and TaylorT4

The orbital binding energy for a spin-aligned system in an eccentric orbit has the following structure in the y parametrization

1. TaylorT1

$$\mathcal{E}(y) = -\frac{y^2}{2} (\mathcal{E}_{\text{NS}} + \mathcal{E}_{\text{SO}}^{1.5\text{PN}} + \mathcal{E}_{\text{SS}}^{2\text{PN}} + \mathcal{E}_{\text{SO}}^{2.5\text{PN}} + \mathcal{E}_{\text{SO}}^{3\text{PN}} + \mathcal{E}_{\text{SS}}^{3\text{PN}}), \quad (\text{C1})$$

where,

$$\mathcal{E}_{\text{NS}} = 1 - e_0^2 \left(\frac{y_0}{y} \right)^{19/3} + \mathcal{O}(y^2, e_0^4), \quad (\text{C2a})$$

$$\mathcal{E}_{\text{SO,circ}}^{1.5\text{PN}} = y^3 \left[\frac{8\delta\chi_a}{3} + \left(\frac{8}{3} - \frac{4\nu}{3} \right) \chi_s \right], \quad (\text{C2b})$$

$$\mathcal{E}_{\text{SO,ecc}}^{1.5\text{PN}} = e_0^2 \left(\frac{y_0}{y} \right)^{19/3} \left\{ y^3 \left[\left(\frac{91\nu}{27} - \frac{301}{54} \right) \chi_s - \frac{301\delta\chi_a}{54} \right] + y_0^3 \left[\frac{157\delta\chi_a}{54} + \left(\frac{157}{54} - \frac{55\nu}{27} \right) \chi_s \right] \right\} + \mathcal{O}(e_0^4), \quad (\text{C2c})$$

$$\mathcal{E}_{\text{SS,circ}}^{2\text{PN}} = y^4 \left\{ \chi_a^2 \left[-\frac{\delta\kappa_a}{2} + \kappa_s \left(\nu - \frac{1}{2} \right) + 2\nu \right] + \chi_a \chi_s [\kappa_a(2\nu - 1) - \delta\kappa_s] + \chi_s^2 \left[-\frac{\delta\kappa_a}{2} + \kappa_s \left(\nu - \frac{1}{2} \right) - 2\nu \right] \right\}, \quad (\text{C2d})$$

$$\begin{aligned} \mathcal{E}_{\text{SS,ecc}}^{2\text{PN}} = & e_0^2 \left(\frac{y_0}{y} \right)^{19/3} \left(y^4 \left\{ \chi_a^2 \left[\frac{185\delta\kappa_a}{192} + \kappa_s \left(\frac{185}{192} - \frac{185\nu}{96} \right) - \frac{815\nu}{96} + \frac{293}{192} \right] + \chi_a \chi_s \left[\frac{185\delta\kappa_s}{96} + \frac{293\delta}{96} \right. \right. \right. \\ & \left. \left. + \kappa_a \left(\frac{185}{96} - \frac{185\nu}{48} \right) \right] + \chi_s^2 \left[\frac{185\delta\kappa_a}{192} + \kappa_s \left(\frac{185}{192} - \frac{185\nu}{96} \right) + \frac{229\nu}{96} + \frac{293}{192} \right] \right\} + y_0^4 \left\{ \chi_a^2 \left[-\frac{89\delta\kappa_a}{192} \right. \right. \\ & \left. \left. + \kappa_s \left(\frac{89\nu}{96} - \frac{89}{192} \right) + \frac{623\nu}{96} - \frac{293}{192} \right] + \chi_a \chi_s \left[-\frac{89\delta\kappa_s}{96} - \frac{293\delta}{96} + \kappa_a \left(\frac{89\nu}{48} - \frac{89}{96} \right) \right] + \chi_s^2 \left[-\frac{89\delta\kappa_a}{192} \right. \right. \\ & \left. \left. + \kappa_s \left(\frac{89\nu}{96} - \frac{89}{192} \right) - \frac{37\nu}{96} - \frac{293}{192} \right] \right\} \right), \quad (\text{C2e}) \end{aligned}$$

$$\mathcal{E}_{\text{SO,circ}}^{2.5\text{PN}} = y^5 \left[\chi_a \left(8\delta - \frac{31\delta\nu}{9} \right) + \left(\frac{2\nu^2}{9} - \frac{121\nu}{9} + 8 \right) \chi_s \right], \quad (\text{C2f})$$

$$\begin{aligned} \mathcal{E}_{\text{SO,ecc}}^{2.5\text{PN}} = & e_0^2 \left(\frac{y_0}{y} \right)^{19/3} \left\{ y^5 \left[\chi_a \left(\frac{1855859\delta}{272160} - \frac{295501\delta\nu}{9720} \right) + \left(\frac{4298\nu^2}{243} - \frac{1211369\nu}{68040} + \frac{1855859}{272160} \right) \chi_s \right] \right. \\ & \left. + y_0^5 \left[\chi_a \left(\frac{1279073\delta}{38880} - \frac{242719\delta\nu}{9720} \right) + \left(\frac{4322\nu^2}{243} - \frac{146807\nu}{2430} + \frac{1279073}{38880} \right) \chi_s \right] + y^2 y_0^3 \left[\chi_a \left(\frac{29987\delta\nu}{1944} \right. \right. \right. \\ & \left. \left. - \frac{365653\delta}{54432} \right) + \left(-\frac{10505\nu^2}{972} + \frac{547913\nu}{27216} - \frac{365653}{54432} \right) \chi_s \right] + y^3 y_0^2 \left[\chi_a \left(\frac{59297\delta\nu}{1944} - \frac{121819\delta}{7776} \right) + \left(-\frac{17927\nu^2}{972} \right. \right. \\ & \left. \left. + \frac{155423\nu}{3888} - \frac{121819}{7776} \right) \chi_s \right] \right\}, \quad (\text{C2g}) \end{aligned}$$

$$\begin{aligned} \mathcal{E}_{\text{SO,ecc}}^{3\text{PN}} = & e_0^2 \left(\frac{y_0}{y} \right)^{19/3} \left\{ y^6 \left[\frac{533621\pi\delta\chi_a}{15552} + \left(\frac{533621\pi}{15552} - \frac{72421\pi\nu}{3888} \right) \chi_s \right] + y_0^6 \left[\frac{157043\pi\delta\chi_a}{15552} + \left(\frac{157043\pi}{15552} \right. \right. \right. \\ & \left. \left. - \frac{37663\pi\nu}{3888} \right) \chi_s \right] + y^3 y_0^3 \left[\left(\frac{27521\pi\nu}{972} - \frac{86333\pi}{1944} \right) \chi_s - \frac{86333\pi\delta\chi_a}{1944} \right] \right\}, \quad (\text{C2h}) \end{aligned}$$

$$\begin{aligned} \mathcal{E}_{\text{SS,circ}}^{3\text{PN}} = & y^6 \left\{ \chi_a^2 \left[\kappa_a \left(\frac{25\delta\nu}{12} - \frac{35\delta}{12} \right) + \kappa_s \left(-\frac{5\nu^2}{6} + \frac{95\nu}{12} - \frac{35}{12} \right) - \frac{5\nu^2}{3} + \frac{10\nu}{9} + \frac{20}{9} \right] + \chi_a \chi_s \left[\kappa_s \left(\frac{25\delta\nu}{6} \right. \right. \right. \\ & \left. \left. - \frac{35\delta}{6} \right) + \frac{70\delta\nu}{9} + \frac{40\delta}{9} + \kappa_a \left(-\frac{5\nu^2}{3} + \frac{95\nu}{6} - \frac{35}{6} \right) \right] + \chi_s^2 \left[\kappa_a \left(\frac{25\delta\nu}{12} - \frac{35\delta}{12} \right) + \kappa_s \left(-\frac{5\nu^2}{6} + \frac{95\nu}{12} - \frac{35}{12} \right) \right. \\ & \left. \left. - \frac{25\nu^2}{9} - \frac{20\nu}{9} + \frac{20}{9} \right] \right\}, \quad (\text{C2i}) \end{aligned}$$

$$\begin{aligned} \mathcal{E}_{\text{SS,ecc}}^{3\text{PN}} = & e_0^2 \left(\frac{y_0}{y} \right)^{19/3} \left[y^6 \left\{ \chi_a^2 \left[\kappa_a \left(\frac{28637\delta\nu}{6912} - \frac{106027\delta}{21504} \right) + \kappa_s \left(-\frac{47605\nu^2}{3456} + \frac{1355161\nu}{96768} - \frac{106027}{21504} \right) \right. \right. \right. \\ & \left. \left. - \frac{146515\nu^2}{3456} + \frac{196667449\nu}{2612736} - \frac{56676329}{5225472} \right] + \chi_a \chi_s \left[\kappa_s \left(\frac{28637\delta\nu}{3456} - \frac{106027\delta}{10752} \right) + \frac{470839\delta\nu}{93312} - \frac{56676329\delta}{2612736} \right. \right. \end{aligned}$$

$$\begin{aligned}
& + \kappa_a \left(-\frac{47605\nu^2}{1728} + \frac{1355161\nu}{48384} - \frac{106027}{10752} \right) + \chi_s^2 \left[\kappa_a \left(\frac{28637\delta\nu}{6912} - \frac{106027\delta}{21504} \right) + \kappa_s \left(-\frac{47605\nu^2}{3456} + \frac{1355161\nu}{96768} \right. \right. \\
& \left. \left. - \frac{106027}{21504} \right) + \frac{2238659\nu^2}{93312} - \frac{10018757\nu}{373248} - \frac{56676329}{5225472} \right] + y_0^6 \left\{ \chi_a^2 \left[\kappa_a \left(\frac{12877\delta\nu}{2304} - \frac{906103\delta}{193536} \right) \right. \right. \\
& \left. \left. + \kappa_s \left(-\frac{24271\nu^2}{3456} + \frac{1446937\nu}{96768} - \frac{906103}{193536} \right) - \frac{169897\nu^2}{3456} + \frac{40961143\nu}{373248} - \frac{17465819}{746496} \right] \right. \\
& \left. + \chi_a \chi_s \left[\kappa_s \left(\frac{12877\delta\nu}{1152} - \frac{906103\delta}{96768} \right) + \frac{5526373\delta\nu}{93312} - \frac{17465819\delta}{373248} + \kappa_a \left(-\frac{24271\nu^2}{1728} + \frac{1446937\nu}{48384} - \frac{906103}{96768} \right) \right] \right. \\
& \left. + \chi_s^2 \left[\kappa_a \left(\frac{12877\delta\nu}{2304} - \frac{906103\delta}{193536} \right) + \kappa_s \left(-\frac{24271\nu^2}{3456} + \frac{1446937\nu}{96768} - \frac{906103}{193536} \right) - \frac{433639\nu^2}{93312} + \frac{16075987\nu}{373248} \right. \right. \\
& \left. \left. - \frac{17465819}{746496} \right] \right\} + y^3 y_0^3 \left\{ \chi_a \chi_s \left(\frac{47257\delta}{1458} - \frac{15421\delta\nu}{729} \right) + \left(\frac{5005\nu^2}{729} - \frac{15421\nu}{729} + \frac{47257}{2916} \right) \chi_s^2 \right. \\
& \left. + \left(\frac{47257}{2916} - \frac{47257\nu}{729} \right) \chi_a^2 \right\} + y^2 y_0^4 \left\{ \chi_a^2 \left[\kappa_a \left(\frac{207281\delta}{193536} - \frac{16999\delta\nu}{6912} \right) + \kappa_s \left(\frac{16999\nu^2}{3456} - \frac{445267\nu}{96768} + \frac{207281}{193536} \right) \right. \right. \\
& \left. \left. + \frac{118993\nu^2}{3456} - \frac{319207\nu}{13824} + \frac{682397}{193536} \right] + \chi_a \chi_s \left[\kappa_s \left(\frac{207281\delta}{96768} - \frac{16999\delta\nu}{3456} \right) - \frac{55963\delta\nu}{3456} + \frac{682397\delta}{96768} \right. \right. \\
& \left. \left. + \kappa_a \left(\frac{16999\nu^2}{1728} - \frac{445267\nu}{48384} + \frac{207281}{96768} \right) \right] + \chi_s^2 \left[\kappa_a \left(\frac{207281\delta}{193536} - \frac{16999\delta\nu}{6912} \right) + \kappa_s \left(\frac{16999\nu^2}{3456} - \frac{445267\nu}{96768} \right. \right. \\
& \left. \left. + \frac{207281}{193536} \right) - \frac{7067\nu^2}{3456} - \frac{697309\nu}{96768} + \frac{682397}{193536} \right] + y^4 y_0^2 \left\{ \chi_a^2 \left[\kappa_a \left(\frac{524105\delta}{193536} - \frac{36445\delta\nu}{6912} \right) + \kappa_s \left(\frac{36445\nu^2}{3456} \right. \right. \right. \\
& \left. \left. - \frac{1034335\nu}{96768} + \frac{524105}{193536} \right) + \frac{160555\nu^2}{3456} - \frac{3116989\nu}{96768} + \frac{830069}{193536} \right] + \chi_a \chi_s \left[\kappa_s \left(\frac{524105\delta}{96768} - \frac{36445\delta\nu}{3456} \right) \right. \\
& \left. - \frac{57721\delta\nu}{3456} + \frac{830069\delta}{96768} + \kappa_a \left(\frac{36445\nu^2}{1728} - \frac{1034335\nu}{48384} + \frac{524105}{96768} \right) \right] + \chi_s^2 \left[\kappa_a \left(\frac{524105\delta}{193536} - \frac{36445\delta\nu}{6912} \right) \right. \\
& \left. \left. + \kappa_s \left(\frac{36445\nu^2}{3456} - \frac{1034335\nu}{96768} + \frac{524105}{193536} \right) - \frac{45113\nu^2}{3456} - \frac{159337\nu}{96768} + \frac{830069}{193536} \right] \right\} \Bigg\} . \tag{C2j}
\end{aligned}$$

Similarly, the energy flux can be written as follows

$$\mathcal{F}(y) = \frac{32\nu^2 y^{10}}{5} (\mathcal{F}_{\text{NS}} + \mathcal{F}_{\text{SO}}^{1.5\text{PN}} + \mathcal{F}_{\text{SS}}^{2\text{PN}} + \mathcal{F}_{\text{SO}}^{2.5\text{PN}} + \mathcal{F}_{\text{SO}}^{3\text{PN}} + \mathcal{F}_{\text{SS}}^{3\text{PN}}) , \tag{C3}$$

where,

$$\mathcal{F}_{\text{NS}} = 1 + \frac{37}{24} \left(\frac{y_0}{y} \right)^{19/3} e_0^2 + \mathcal{O}(y^2, e_0^4) , \tag{C4a}$$

$$\mathcal{F}_{\text{SO,circ}}^{1.5\text{PN}} = y^3 \left[\left(3\nu - \frac{11}{4} \right) \chi_s - \frac{11\delta\chi_a}{4} \right] , \tag{C4b}$$

$$\mathcal{F}_{\text{SO,ecc}}^{1.5\text{PN}} = \frac{37}{24} \left(\frac{y_0}{y} \right)^{19/3} e_0^2 \left\{ y^3 \left[\left(\frac{7613\nu}{999} - \frac{41099}{1998} \right) \chi_s - \frac{41099\delta\chi_a}{1998} \right] + y_0^3 \left[\left(\frac{55\nu}{27} - \frac{157}{54} \right) \chi_s - \frac{157\delta\chi_a}{54} \right] \right\} , \tag{C4c}$$

$$\begin{aligned}
\mathcal{F}_{\text{SS,circ}}^{2\text{PN}} &= y^4 \left\{ \chi_a^2 \left[2\delta\kappa_a + \kappa_s(2 - 4\nu) - 4\nu + \frac{1}{16} \right] + \chi_a \chi_s \left[4\delta\kappa_s + \frac{\delta}{8} + \kappa_a(4 - 8\nu) \right] + \chi_s^2 \left[2\delta\kappa_a + \kappa_s(2 - 4\nu) \right. \right. \\
&\left. \left. + \frac{15\nu}{4} + \frac{1}{16} \right] \right\} , \tag{C4d}
\end{aligned}$$

$$\begin{aligned}
\mathcal{F}_{\text{SS,ecc}}^{2\text{PN}} &= \frac{37}{24} \left(\frac{y_0}{y} \right)^{19/3} e_0^2 \left(y^4 \left\{ \chi_a^2 \left[\frac{99235\delta\kappa_a}{7104} + \kappa_s \left(\frac{99235}{7104} - \frac{99235\nu}{3552} \right) - \frac{79477\nu}{3552} - \frac{8537}{7104} \right] + \chi_a \chi_s \left[\frac{99235\delta\kappa_s}{3552} \right. \right. \right. \\
&\left. \left. - \frac{8537\delta}{3552} + \kappa_a \left(\frac{99235}{3552} - \frac{99235\nu}{1776} \right) \right] + \chi_s^2 \left[\frac{99235\delta\kappa_a}{7104} + \kappa_s \left(\frac{99235}{7104} - \frac{99235\nu}{3552} \right) + \frac{96551\nu}{3552} - \frac{8537}{7104} \right] \right\} \right) , \tag{C4e}
\end{aligned}$$

$$\mathcal{F}_{\text{SO,circ}}^{2.5\text{PN}} = y^5 \left[\chi_a \left(\frac{701\delta\nu}{36} - \frac{59\delta}{16} \right) + \left(-\frac{157\nu^2}{9} + \frac{227\nu}{9} - \frac{59}{16} \right) \chi_s \right] , \tag{C4f}$$

$$\begin{aligned}
\mathcal{F}_{\text{SO,ecc}}^{2.5\text{PN}} = & \frac{37}{24} \left(\frac{y_0}{y}\right)^{19/3} e_0^2 \left\{ y^5 \left[\chi_a \left(\frac{26398327\delta\nu}{359640} - \frac{892925123\delta}{10069920} \right) + \left(-\frac{826165\nu^2}{17982} + \frac{643447193\nu}{2517480} - \frac{892925123}{10069920} \right) \chi_s \right] \right. \\
& + y_0^5 \left[\chi_a \left(\frac{242719\delta\nu}{9720} - \frac{1279073\delta}{38880} \right) + \left(-\frac{4322\nu^2}{243} + \frac{146807\nu}{2430} - \frac{1279073}{38880} \right) \chi_s \right] + y^2 y_0^3 \left[\chi_a \left(\frac{2335375\delta\nu}{71928} \right. \right. \\
& - \frac{63891935\delta}{2013984} \left. \left. + \left(-\frac{818125\nu^2}{35964} + \frac{55077775\nu}{1006992} - \frac{63891935}{2013984} \right) \chi_s \right] + y^3 y_0^2 \left[\chi_a \left(\frac{8096503\delta\nu}{71928} - \frac{116433467\delta}{2013984} \right) \right. \right. \\
& \left. \left. + \left(-\frac{1499761\nu^2}{35964} + \frac{134918671\nu}{1006992} - \frac{116433467}{2013984} \right) \chi_s \right] \right\}, \tag{C4g}
\end{aligned}$$

$$\mathcal{F}_{\text{SO,circ}}^{3\text{PN}} = y^6 \left[\left(\frac{34\pi\nu}{3} - \frac{65\pi}{6} \right) \chi_s - \frac{65\pi\delta\chi_a}{6} \right], \tag{C4h}$$

$$\begin{aligned}
\mathcal{F}_{\text{SO,ecc}}^{3\text{PN}} = & \frac{37}{24} \left(\frac{y_0}{y}\right)^{19/3} e_0^2 \left\{ y^6 \left[\left(\frac{1300057\pi\nu}{143856} - \frac{18439049\pi}{575424} \right) \chi_s - \frac{18439049\pi\delta\chi_a}{575424} \right] + y_0^6 \left[\left(\frac{37663\pi\nu}{3888} - \frac{157043\pi}{15552} \right) \chi_s \right. \right. \\
& \left. \left. - \frac{157043\pi\delta\chi_a}{15552} \right] + y^3 y_0^3 \left[\left(\frac{2127583\pi\nu}{35964} - \frac{9724027\pi}{71928} \right) \chi_s - \frac{9724027\pi\delta\chi_a}{71928} \right] \right\}, \tag{C4i}
\end{aligned}$$

$$\begin{aligned}
\mathcal{F}_{\text{SS,circ}}^{3\text{PN}} = & y^6 \left\{ \chi_a^2 \left[\kappa_a \left(\frac{\delta}{7} - \frac{127\delta\nu}{8} \right) + \kappa_s \left(\frac{43\nu^2}{2} - \frac{905\nu}{56} + \frac{1}{7} \right) + \frac{43\nu^2}{2} - \frac{25\nu}{63} + \frac{77}{72} \right] + \chi_a \chi_s \left[\kappa_s \left(\frac{2\delta}{7} - \frac{127\delta\nu}{4} \right) \right. \right. \\
& - \frac{475\delta\nu}{36} + \frac{77\delta}{36} + \kappa_a \left(43\nu^2 - \frac{905\nu}{28} + \frac{2}{7} \right) \left. \left. + \chi_s^2 \left[\kappa_a \left(\frac{\delta}{7} - \frac{127\delta\nu}{8} \right) + \kappa_s \left(\frac{43\nu^2}{2} - \frac{905\nu}{56} + \frac{1}{7} \right) - \frac{107\nu^2}{9} \right. \right. \right. \\
& \left. \left. - \frac{4303\nu}{252} + \frac{77}{72} \right] \right\}, \tag{C4j}
\end{aligned}$$

$$\begin{aligned}
\mathcal{F}_{\text{SS,ecc}}^{3\text{PN}} = & \frac{37}{24} \left(\frac{y_0}{y}\right)^{19/3} e_0^2 \left\{ y^6 \left\{ \chi_a^2 \left[\kappa_a \left(\frac{38752555\delta}{340992} - \frac{33416267\delta\nu}{255744} \right) + \kappa_s \left(\frac{14989123\nu^2}{127872} - \frac{183090199\nu}{511488} \right. \right. \right. \right. \\
& \left. \left. + \frac{38752555}{340992} \right] + \frac{150001\nu^2}{3456} - \frac{38341393513\nu}{96671232} + \frac{11991613877}{193342464} \right\} + \chi_a \chi_s \left[\kappa_s \left(\frac{38752555\delta}{170496} - \frac{33416267\delta\nu}{127872} \right) \right. \\
& - \frac{609975481\delta\nu}{3452544} + \frac{11991613877\delta}{96671232} + \kappa_a \left(\frac{14989123\nu^2}{63936} - \frac{183090199\nu}{255744} + \frac{38752555}{170496} \right) \left. \left. + \chi_s^2 \left[\kappa_a \left(\frac{38752555\delta}{340992} \right. \right. \right. \right. \\
& - \frac{33416267\delta\nu}{255744} \left. \left. + \kappa_s \left(\frac{14989123\nu^2}{127872} - \frac{183090199\nu}{511488} + \frac{38752555}{340992} \right) - \frac{113766965\nu^2}{3452544} - \frac{388735387\nu}{13810176} \right. \right. \right. \\
& \left. \left. + \frac{11991613877}{193342464} \right] \right\} + y_0^6 \left\{ \chi_a^2 \left[\kappa_a \left(\frac{906103\delta}{193536} - \frac{12877\delta\nu}{2304} \right) + \kappa_s \left(\frac{24271\nu^2}{3456} - \frac{1446937\nu}{96768} + \frac{906103}{193536} \right) + \frac{169897\nu^2}{3456} \right. \right. \\
& - \frac{40961143\nu}{373248} + \frac{17465819}{746496} \left. \left. + \chi_a \chi_s \left[\kappa_s \left(\frac{906103\delta}{96768} - \frac{12877\delta\nu}{1152} \right) - \frac{5526373\delta\nu}{93312} + \frac{17465819\delta}{373248} + \kappa_a \left(\frac{24271\nu^2}{1728} \right. \right. \right. \right. \\
& - \frac{1446937\nu}{48384} + \frac{906103}{96768} \left. \left. + \chi_s^2 \left[\kappa_a \left(\frac{906103\delta}{193536} - \frac{12877\delta\nu}{2304} \right) + \kappa_s \left(\frac{24271\nu^2}{3456} - \frac{1446937\nu}{96768} + \frac{906103}{193536} \right) \right. \right. \right. \\
& \left. \left. + \frac{433639\nu^2}{93312} - \frac{16075987\nu}{373248} + \frac{17465819}{746496} \right] \right\} + y^2 y_0^4 \left\{ \chi_a^2 \left[\kappa_a \left(\frac{36218995\delta}{7160832} - \frac{1323875\delta\nu}{255744} \right) + \kappa_s \left(\frac{1323875\nu^2}{127872} \right. \right. \right. \\
& - \frac{54753245\nu}{3580416} + \frac{36218995}{7160832} \left. \left. + \frac{9267125\nu^2}{127872} - \frac{44935745\nu}{511488} + \frac{119237815}{7160832} \right] + \chi_a \chi_s \left[\kappa_s \left(\frac{36218995\delta}{3580416} \right. \right. \right. \\
& - \frac{1323875\delta\nu}{127872} \left. \left. - \frac{4358375\delta\nu}{127872} + \frac{119237815\delta}{3580416} + \kappa_a \left(\frac{1323875\nu^2}{63936} - \frac{54753245\nu}{1790208} + \frac{36218995}{3580416} \right) \right] \right. \\
& \left. \left. + \chi_s^2 \left[\kappa_a \left(\frac{36218995\delta}{7160832} - \frac{1323875\delta\nu}{255744} \right) + \kappa_s \left(\frac{1323875\nu^2}{127872} - \frac{54753245\nu}{3580416} + \frac{36218995}{7160832} \right) - \frac{14875\nu^2}{3456} \right. \right. \right. \\
& - \frac{45959915\nu}{3580416} + \frac{119237815}{7160832} \left. \left. \right] \right\} + y^3 y_0^3 \left[\chi_a \chi_s \left(\frac{6452543\delta}{53946} - \frac{1727843\delta\nu}{26973} \right) + \left(\frac{418715\nu^2}{26973} - \frac{1727843\nu}{26973} \right. \right. \\
& \left. \left. + \frac{6452543}{107892} \right] \chi_s^2 + \left(\frac{6452543}{107892} - \frac{6452543\nu}{26973} \right) \chi_a^2 + y^4 y_0^2 \left\{ \chi_a^2 \left[\kappa_a \left(\frac{281132755\delta}{7160832} - \frac{19549295\delta\nu}{255744} \right) \right. \right. \right.
\end{aligned}$$

$$\begin{aligned}
& + \kappa_s \left(\frac{19549295\nu^2}{127872} - \frac{554822885\nu}{3580416} + \frac{281132755}{7160832} \right) + \frac{15656969\nu^2}{127872} - \frac{201613295\nu}{3580416} - \frac{24185321}{7160832} \\
& + \chi_a \chi_s \left[\kappa_s \left(\frac{281132755\delta}{3580416} - \frac{19549295\delta\nu}{127872} \right) + \frac{1681789\delta\nu}{127872} - \frac{24185321\delta}{3580416} + \kappa_a \left(\frac{19549295\nu^2}{63936} - \frac{554822885\nu}{1790208} \right. \right. \\
& \left. \left. + \frac{281132755}{3580416} \right) \right] + \chi_s^2 \left[\kappa_a \left(\frac{281132755\delta}{7160832} - \frac{19549295\delta\nu}{255744} \right) + \kappa_s \left(\frac{19549295\nu^2}{127872} - \frac{554822885\nu}{3580416} + \frac{281132755}{7160832} \right) \right. \\
& \left. - \frac{19020547\nu^2}{127872} + \frac{42439147\nu}{511488} - \frac{24185321}{7160832} \right] \Big\} \Big\} . \tag{C4k}
\end{aligned}$$

We also give here dE/dy for the convenience of the reader

$$\frac{dE}{dy} = -y \left(\mathcal{G}_{\text{NS}} + \mathcal{G}_{\text{SO}}^{1.5\text{PN}} + \mathcal{G}_{\text{SS}}^{2\text{PN}} + \mathcal{G}_{\text{SO}}^{2.5\text{PN}} + \mathcal{G}_{\text{SO}}^{3\text{PN}} + \mathcal{G}_{\text{SS}}^{3\text{PN}} \right) , \tag{C5}$$

where,

$$\mathcal{G}_{\text{NS}} = 1 - e_0^2 \left(\frac{y_0}{y} \right)^{19/3} + \mathcal{O}(y^2, e_0^4) , \tag{C6a}$$

$$\mathcal{G}_{\text{SO,circ}}^{1.5\text{PN}} = y^3 \left[\frac{20\delta\chi_a}{3} + \left(\frac{20}{3} - \frac{10\nu}{3} \right) \chi_s \right] , \tag{C6b}$$

$$\mathcal{G}_{\text{SO,ecc}}^{1.5\text{PN}} = -e_0^2 \left(\frac{y_0}{y} \right)^{19/3} \left\{ y^3 \left[\frac{517\delta\chi_a}{54} + \left(\frac{517}{54} - \frac{145\nu}{27} \right) \chi_s \right] + y_0^3 \left[\left(\frac{55\nu}{27} - \frac{157}{54} \right) \chi_s - \frac{157\delta\chi_a}{54} \right] \right\} , \tag{C6c}$$

$$\mathcal{G}_{\text{SS,circ}}^{2\text{PN}} = y^4 \left\{ \chi_a^2 \left[-\frac{3\delta\kappa_a}{2} + \kappa_s \left(3\nu - \frac{3}{2} \right) + 6\nu \right] + \chi_a \chi_s \left[\kappa_a(6\nu - 3) - 3\delta\kappa_s \right] + \chi_s^2 \left[-\frac{3\delta\kappa_a}{2} + \kappa_s \left(3\nu - \frac{3}{2} \right) - 6\nu \right] \right\} , \tag{C6d}$$

$$\begin{aligned}
\mathcal{G}_{\text{SS,ecc}}^{2\text{PN}} = & -e_0^2 \left(\frac{y_0}{y} \right)^{19/3} \left(y^4 \left\{ \chi_a^2 \left[-\frac{377\delta\kappa_a}{192} + \kappa_s \left(\frac{377\nu}{96} - \frac{377}{192} \right) + \frac{1199\nu}{96} - \frac{293}{192} \right] + \chi_a \chi_s \left[-\frac{377\delta\kappa_s}{96} - \frac{293\delta}{96} \right. \right. \right. \\
& \left. \left. + \kappa_a \left(\frac{377\nu}{48} - \frac{377}{96} \right) \right] + \chi_s^2 \left[-\frac{377\delta\kappa_a}{192} + \kappa_s \left(\frac{377\nu}{96} - \frac{377}{192} \right) - \frac{613\nu}{96} - \frac{293}{192} \right] \right\} + y_0^4 \left\{ \chi_a^2 \left[\frac{89\delta\kappa_a}{192} \right. \right. \\
& \left. \left. + \kappa_s \left(\frac{89}{192} - \frac{89\nu}{96} \right) - \frac{623\nu}{96} + \frac{293}{192} \right] + \chi_a \chi_s \left[\frac{89\delta\kappa_s}{96} + \frac{293\delta}{96} + \kappa_a \left(\frac{89}{96} - \frac{89\nu}{48} \right) \right] + \chi_s^2 \left[\frac{89\delta\kappa_a}{192} + \kappa_s \left(\frac{89}{192} \right. \right. \right. \\
& \left. \left. \left. - \frac{89\nu}{96} \right) + \frac{37\nu}{96} + \frac{293}{192} \right] \right\} , \tag{C6e}
\end{aligned}$$

$$\mathcal{G}_{\text{SO,circ}}^{2.5\text{PN}} = y^5 \left[\chi_a \left(28\delta - \frac{217\delta\nu}{18} \right) + \left(\frac{7\nu^2}{9} - \frac{847\nu}{18} + 28 \right) \chi_s \right] , \tag{C6f}$$

$$\begin{aligned}
\mathcal{G}_{\text{SO,ecc}}^{2.5\text{PN}} = & -e_0^2 \left(\frac{y_0}{y} \right)^{19/3} \left\{ y^5 \left[\chi_a \left(\frac{733051\delta\nu}{9720} - \frac{16313459\delta}{272160} \right) + \left(-\frac{10655\nu^2}{243} + \frac{3030787\nu}{34020} - \frac{16313459}{272160} \right) \chi_s \right] \right. \\
& \left. + y_0^5 \left[\chi_a \left(\frac{242719\delta\nu}{9720} - \frac{1279073\delta}{38880} \right) + \left(-\frac{4322\nu^2}{243} + \frac{146807\nu}{2430} - \frac{1279073}{38880} \right) \chi_s \right] + y^2 y_0^3 \left[\chi_a \left(\frac{286525\delta}{54432} \right. \right. \right. \\
& \left. \left. - \frac{29045\delta\nu}{1944} \right) + \left(\frac{10175\nu^2}{972} - \frac{507005\nu}{27216} + \frac{286525}{54432} \right) \chi_s \right] + y^3 y_0^2 \left[\chi_a \left(\frac{1464661\delta}{54432} - \frac{101849\delta\nu}{1944} \right) + \left(\frac{28565\nu^2}{972} \right. \right. \\
& \left. \left. - \frac{1836671\nu}{27216} + \frac{1464661}{54432} \right) \chi_s \right] \right\} , \tag{C6g}
\end{aligned}$$

$$\mathcal{G}_{\text{SO,circ}}^{3\text{PN}} = 0 , \tag{C6h}$$

$$\begin{aligned}
\mathcal{G}_{\text{SO,ecc}}^{3\text{PN}} = & -e_0^2 \left(\frac{y_0}{y} \right)^{19/3} \left\{ y^6 \left[\left(\frac{113137\pi\nu}{3888} - \frac{859349\pi}{15552} \right) \chi_s - \frac{859349\pi\delta\chi_a}{15552} \right] + y_0^6 \left[\left(\frac{37663\pi\nu}{3888} - \frac{157043\pi}{15552} \right) \chi_s \right. \right. \\
& \left. \left. - \frac{157043\pi\delta\chi_a}{15552} \right] + y^3 y_0^3 \left[\frac{127049\pi\delta\chi_a}{1944} + \left(\frac{127049\pi}{1944} - \frac{9425\pi\nu}{243} \right) \chi_s \right] \right\} , \tag{C6i}
\end{aligned}$$

$$\mathcal{G}_{\text{SS,circ}}^{3\text{PN}} = y^6 \left\{ \chi_a^2 \left[\kappa_a \left(\frac{25\delta\nu}{3} - \frac{35\delta}{3} \right) + \kappa_s \left(-\frac{10\nu^2}{3} + \frac{95\nu}{3} - \frac{35}{3} \right) - \frac{20\nu^2}{3} + \frac{40\nu}{9} + \frac{80}{9} \right] + \chi_a \chi_s \left[\kappa_s \left(\frac{50\delta\nu}{3} \right. \right. \right.$$

$$-\frac{70\delta}{3} + \frac{280\delta\nu}{9} + \frac{160\delta}{9} + \kappa_a \left(-\frac{20\nu^2}{3} + \frac{190\nu}{3} - \frac{70}{3} \right) + \chi_s^2 \left[\kappa_a \left(\frac{25\delta\nu}{3} - \frac{35\delta}{3} \right) + \kappa_s \left(-\frac{10\nu^2}{3} + \frac{95\nu}{3} - \frac{35}{3} \right) - \frac{100\nu^2}{9} - \frac{80\nu}{9} + \frac{80}{9} \right] \}, \quad (\text{C6j})$$

$$\begin{aligned} \mathcal{G}_{\text{SS,ecc}}^{3\text{PN}} = & -e_0^2 \left(\frac{y_0}{y} \right)^{19/3} \left(y^6 \left\{ \chi_a^2 \left[\kappa_a \left(\frac{1613401\delta}{64512} - \frac{107399\delta\nu}{6912} \right) + \kappa_s \left(\frac{140191\nu^2}{3456} - \frac{6343789\nu}{96768} + \frac{1613401}{64512} \right) \right. \right. \right. \\ & + \frac{329017\nu^2}{3456} - \frac{847050901\nu}{2612736} + \frac{273707297}{5225472} \left. \right] + \chi_a \chi_s \left[\kappa_s \left(\frac{1613401\delta}{32256} - \frac{107399\delta\nu}{3456} \right) - \frac{4587853\delta\nu}{93312} + \frac{273707297\delta}{2612736} \right. \\ & + \kappa_a \left(\frac{140191\nu^2}{1728} - \frac{6343789\nu}{48384} + \frac{1613401}{32256} \right) \left. \right] + \chi_s^2 \left[\kappa_a \left(\frac{1613401\delta}{64512} - \frac{107399\delta\nu}{6912} \right) + \kappa_s \left(\frac{140191\nu^2}{3456} - \frac{6343789\nu}{96768} \right. \right. \\ & + \frac{1613401}{64512} \left. \right) - \frac{7005401\nu^2}{93312} + \frac{171176423\nu}{2612736} + \frac{273707297}{5225472} \left. \right] \left. \right\} + y_0^6 \left\{ \chi_a^2 \left[\kappa_a \left(\frac{906103\delta}{193536} - \frac{12877\delta\nu}{2304} \right) \right. \right. \\ & + \kappa_s \left(\frac{24271\nu^2}{3456} - \frac{1446937\nu}{96768} + \frac{906103}{193536} \right) + \frac{169897\nu^2}{3456} - \frac{40961143\nu}{373248} + \frac{17465819}{746496} \left. \right] + \chi_a \chi_s \left[\kappa_s \left(\frac{906103\delta}{96768} - \right. \right. \\ & \frac{12877\delta\nu}{1152} \left. \right) - \frac{5526373\delta\nu}{93312} + \frac{17465819\delta}{373248} + \kappa_a \left(\frac{24271\nu^2}{1728} - \frac{1446937\nu}{48384} + \frac{906103}{96768} \right) \left. \right] + \chi_s^2 \left[\kappa_a \left(\frac{906103\delta}{193536} \right. \right. \\ & - \frac{12877\delta\nu}{2304} \left. \right) + \kappa_s \left(\frac{24271\nu^2}{3456} - \frac{1446937\nu}{96768} + \frac{906103}{193536} \right) + \frac{433639\nu^2}{93312} - \frac{16075987\nu}{373248} + \frac{17465819}{746496} \left. \right] \left. \right\} \\ & + y^2 y_0^4 \left\{ \chi_a^2 \left[\kappa_a \left(\frac{16465\delta\nu}{6912} - \frac{162425\delta}{193536} \right) + \kappa_s \left(-\frac{16465\nu^2}{3456} + \frac{392935\nu}{96768} - \frac{162425}{193536} \right) - \frac{115255\nu^2}{3456} + \frac{270835\nu}{13824} \right. \right. \\ & - \frac{534725}{193536} \left. \right] + \chi_a \chi_s \left[\kappa_s \left(\frac{16465\delta\nu}{3456} - \frac{162425\delta}{96768} \right) + \frac{54205\delta\nu}{3456} - \frac{534725\delta}{96768} + \kappa_a \left(-\frac{16465\nu^2}{1728} + \frac{392935\nu}{48384} \right. \right. \\ & - \frac{162425}{96768} \left. \right] + \chi_s^2 \left[\kappa_a \left(\frac{16465\delta\nu}{6912} - \frac{162425\delta}{193536} \right) + \kappa_s \left(-\frac{16465\nu^2}{3456} + \frac{392935\nu}{96768} - \frac{162425}{193536} \right) + \frac{6845\nu^2}{3456} \right. \\ & + \frac{691345\nu}{96768} - \frac{534725}{193536} \left. \right] \left. \right\} + y^3 y_0^3 \left[\chi_a \chi_s \left(\frac{25600\delta\nu}{729} - \frac{81169\delta}{1458} \right) + \left(-\frac{7975\nu^2}{729} + \frac{25600\nu}{729} - \frac{81169}{2916} \right) \chi_s \right. \\ & + \left(\frac{81169\nu}{729} - \frac{81169}{2916} \right) \chi_a^2 \left. \right] + y^4 y_0^2 \left\{ \chi_a^2 \left[\kappa_a \left(\frac{74269\delta\nu}{6912} - \frac{1068041\delta}{193536} \right) + \kappa_s \left(-\frac{74269\nu^2}{3456} + \frac{2107807\nu}{96768} \right. \right. \right. \\ & - \frac{1068041}{193536} \left. \right) - \frac{236203\nu^2}{3456} + \frac{4204861\nu}{96768} - \frac{830069}{193536} \left. \right] + \chi_a \chi_s \left[\kappa_s \left(\frac{74269\delta\nu}{3456} - \frac{1068041\delta}{96768} \right) + \frac{57721\delta\nu}{3456} \right. \\ & - \frac{830069\delta}{96768} + \kappa_a \left(-\frac{74269\nu^2}{1728} + \frac{2107807\nu}{48384} - \frac{1068041}{96768} \right) \left. \right] + \chi_s^2 \left[\kappa_a \left(\frac{74269\delta\nu}{6912} - \frac{1068041\delta}{193536} \right) + \kappa_s \left(-\frac{74269\nu^2}{3456} \right. \right. \\ & \left. \left. + \frac{2107807\nu}{96768} - \frac{1068041}{193536} \right) + \frac{120761\nu^2}{3456} - \frac{928535\nu}{96768} - \frac{830069}{193536} \right] \left. \right\} \left. \right). \quad (\text{C6k}) \end{aligned}$$

2. TaylorT3

$$F = \frac{\theta^3}{8M\pi} \left\{ F_{\text{circ}} - \frac{471}{344} e_0^2 \left(\frac{\theta_0}{\theta} \right)^{19/3} \left[F_{\text{SO,ecc}} + F_{\text{SS,ecc}} \right] \right\}, \quad (\text{C7})$$

where,

$$F_{\text{NS}} = 1 - \frac{471}{344} e_0^2 \left(\frac{\theta_0}{\theta} \right)^{19/3} + \mathcal{O}(e_0^4), \quad (\text{C8a})$$

$$F_{\text{SO,ecc}}^{1.5\text{PN}} = \theta_0^3 \left[\frac{4871\delta\chi_A}{4320} + \frac{4871}{4320} \left(1 - \frac{3232\nu}{4871} \right) \chi_s \right] + \theta^3 \left[-\frac{1893215\delta\chi_a}{2306016} - \frac{1893215}{2306016} \left(1 - \frac{739666\nu}{1893215} \right) \chi_s \right], \quad (\text{C8b})$$

$$F_{\text{SS,ecc}}^{2\text{PN}} = \theta_0^4 \left\{ \left[\frac{7}{3072} \left(1 + \frac{2328\nu}{7} \right) - \frac{97\delta\kappa_a}{256} - \frac{97}{256} (1 - 2\nu)\kappa_s \right] \chi_a^2 + \left[-\frac{97}{128} (1 - 2\nu)\kappa_a + \delta \left(\frac{7}{1536} - \frac{97\kappa_s}{128} \right) \right] \chi_a \chi_s \right\}$$

$$\begin{aligned}
& + \left[\frac{7}{3072} \left(1 - \frac{2356\nu}{7} \right) - \frac{97\delta\kappa_a}{256} - \frac{97}{256} (1 - 2\nu)\kappa_s \right] \chi_s^2 \Big\} + \theta^4 \left\{ \left[-\frac{11179}{3737856} \left(1 + \frac{2102946\nu}{11179} \right) + \frac{350491\delta\kappa_a}{1245952} \right. \right. \\
& + \frac{350491}{1245952} (1 - 2\nu)\kappa_s \Big] \chi_a^2 + \left[\frac{350491}{622976} (1 - 2\nu)\kappa_a + \delta \left(-\frac{11179}{1868928} + \frac{350491\kappa_s}{622976} \right) \right] \chi_a \chi_s \\
& + \left. \left[-\frac{11179}{3737856} \left(1 - \frac{2147662\nu}{11179} \right) + \frac{350491\delta\kappa_a}{1245952} + \frac{350491}{1245952} (1 - 2\nu)\kappa_s \right] \chi_s^2 \right\}, \tag{C8c}
\end{aligned}$$

$$\begin{aligned}
F_{\text{SO,ecc}}^{2.5\text{PN}} &= \theta_0^5 \left[\frac{69146501}{13063680} \left(1 - \frac{79387834\nu}{69146501} + \frac{7548240\nu^2}{69146501} \right) \chi_s + \frac{69146501}{13063680} \left(1 - \frac{19488462\nu}{69146501} \right) \delta\chi_a \right] \\
& + \theta^3 \theta_0^2 \left[-\frac{8415340675}{7969591296} \left(1 - \frac{444\nu}{889} \right) \delta\chi_a - \frac{8415340675}{7969591296} \left(1 - \frac{1498150534\nu}{1683068135} + \frac{328411704\nu^2}{1683068135} \right) \chi_s \right] \\
& - \theta^2 \theta_0^3 \left[\frac{37248834131}{303547668480} \left(1 - \frac{17585652\nu}{7647061} \right) \delta\chi_a + \frac{37248834131}{303547668480} \left(1 - \frac{110375012044\nu}{37248834131} + \frac{56836827264\nu^2}{37248834131} \right) \chi_s \right] \\
& + \theta^5 \left[-\frac{7261740747155}{3612217254912} \left(1 - \frac{80220876078\nu}{1452348149431} \right) \delta\chi_a - \frac{7261740747155}{3612217254912} \left(1 - \frac{17211071085917\nu}{14523481494310} \right. \right. \\
& \left. \left. - \frac{521561712378\nu^2}{36308703735775} \right) \chi_s \right], \tag{C8d}
\end{aligned}$$

$$\begin{aligned}
F_{\text{SO,ecc}}^{3\text{PN}} &= \theta_0^6 \left[-\frac{22358051\pi\delta\chi_a}{24883200} - \frac{22358051\pi}{24883200} \left(1 - \frac{16608892\nu}{22358051} \right) \chi_s \right] + \theta^3 \theta_0^3 \left[-\frac{1482249323\pi\delta\chi_a}{13282652160} \right. \\
& \left. - \frac{1482249323\pi}{13282652160} \left(1 - \frac{920485108\nu}{1482249323} \right) \chi_s \right] + \theta^6 \left[\frac{55371553\pi\delta\chi_a}{84602880} + \frac{55371553\pi}{84602880} \left(1 - \frac{29754273364\nu}{43466669105} \right) \chi_s \right], \tag{C8e}
\end{aligned}$$

$$\begin{aligned}
F_{\text{SS,ecc}}^{3\text{PN}} &= \theta^2 \theta_0^4 \left\{ \chi_a \chi_s \left[-\frac{7647061\delta}{15418294272} \left(1 - \frac{17585652\nu}{7647061} \right) + \frac{741764917}{8994004992} \left(1 - \frac{32879774\nu}{7647061} + \frac{35171304\nu^2}{7647061} \right) \kappa_a \right. \right. \\
& + \frac{741764917\delta}{8994004992} \left(1 - \frac{17585652\nu}{7647061} \right) \kappa_s \Big] + \chi_s^2 \left[\frac{741764917}{17988009984} \left(1 - \frac{32879774\nu}{7647061} + \frac{35171304\nu^2}{7647061} \right) \kappa_s \right. \\
& - \frac{7647061}{30836588544} \left(1 - \frac{18139575280\nu}{53529427} + \frac{5918828016\nu^2}{7647061} \right) + \frac{741764917\delta}{17988009984} \left(1 - \frac{17585652\nu}{7647061} \right) \kappa_a \Big] \\
& + \chi_a^2 \left[\frac{741764917}{17988009984} \left(1 - \frac{32879774\nu}{7647061} + \frac{35171304\nu^2}{7647061} \right) \kappa_s + \frac{741764917\delta}{17988009984} \left(1 - \frac{17585652\nu}{7647061} \right) \kappa_a \right. \\
& \left. - \frac{7647061}{30836588544} \left(1 + \frac{17679258444\nu}{53529427} - \frac{5848485408\nu^2}{7647061} \right) \right] \Big\} + \theta^4 \theta_0^2 \left\{ \chi_a \chi_s \left[\frac{1557932495}{2153005056} \left(1 - \frac{2222\nu}{889} \right. \right. \right. \\
& + \frac{888\nu^2}{889} \Big) \kappa_a + \frac{1557932495\delta}{2153005056} \left(1 - \frac{444\nu}{889} \right) \kappa_s - \frac{49690655\delta}{6459015168} \left(1 - \frac{444\nu}{889} \right) \Big] + \chi_s^2 \left[\frac{1557932495}{4306010112} \left(1 - \frac{2222\nu}{889} \right. \right. \\
& + \frac{888\nu^2}{889} \Big) \kappa_s + \frac{1557932495\delta}{4306010112} \left(1 - \frac{444\nu}{889} \right) \kappa_a - \frac{49690655}{12918030336} \left(1 - \frac{273462142\nu}{1419733} + \frac{953561928\nu^2}{9938131} \right) \Big] \\
& + \chi_a^2 \left[\frac{1557932495}{4306010112} \left(1 - \frac{2222\nu}{889} + \frac{888\nu^2}{889} \right) \kappa_s + \frac{1557932495\delta}{4306010112} \left(1 - \frac{444\nu}{889} \right) \kappa_a - \frac{49690655}{12918030336} \left(1 \right. \\
& + \frac{266365074\nu}{1419733} - \frac{933708024\nu^2}{9938131} \Big) \Big] \Big\} + \theta^3 \theta_0^3 \left\{ -\frac{1844370053}{1992397824} (1 - 4\nu) \chi_a^2 - \frac{1844370053}{1992397824} \left(1 - \frac{9721783966\nu}{9221850265} \right. \right. \\
& + \frac{2390600512\nu^2}{9221850265} \Big) \chi_s^2 - \frac{1844370053\delta}{996198912} \left(1 - \frac{4860891983\nu}{9221850265} \right) \chi_a \chi_s \Big\} + \theta_0^6 \left\{ \chi_s^2 \left[-\frac{15796363}{6193152} \left(1 - \frac{38091274\nu}{15796363} \right. \right. \right. \\
& + \frac{3292968\nu^2}{15796363} \Big) \kappa_s - \frac{15796363\delta}{6193152} \left(1 - \frac{6498548\nu}{15796363} \right) \kappa_a + \frac{29393895511}{16721510400} \left(1 - \frac{84309055624\nu}{29393895511} + \frac{4422254704\nu^2}{29393895511} \right) \Big] \\
& + \chi_a \chi_s \left[-\frac{15796363}{3096576} \left(1 - \frac{38091274\nu}{15796363} + \frac{3292968\nu^2}{15796363} \right) \kappa_a - \frac{15796363\delta}{3096576} \left(1 - \frac{6498548\nu}{15796363} \right) \kappa_s \right. \\
& + \frac{29393895511\delta}{8360755200} \left(1 - \frac{3294795812\nu}{29393895511} \right) \Big] + \chi_a^2 \left[-\frac{15796363}{6193152} \left(1 - \frac{38091274\nu}{15796363} + \frac{3292968\nu^2}{15796363} \right) \kappa_s \right. \\
& \left. - \frac{15796363\delta}{6193152} \left(1 - \frac{6498548\nu}{15796363} \right) \kappa_a + \frac{29393895511}{16721510400} \left(1 - \frac{39856118044\nu}{29393895511} - \frac{8891013600\nu^2}{29393895511} \right) \right] \Big\}
\end{aligned}$$

$$\begin{aligned}
& + \theta^6 \left\{ \chi_a^2 \left[\frac{5865969154439}{4646902579200} \left(1 - \frac{41973254021326\nu}{17597907463317} - \frac{974298467240\nu^2}{5865969154439} \right) \kappa_s + \frac{5865969154439\delta}{4646902579200} \left(1 \right. \right. \right. \\
& \left. \left. \left. - \frac{6777439094692\nu}{17597907463317} \right) \kappa_a - \frac{1206460449012419}{2559513940623360} \left(1 + \frac{2979651431961776\nu}{6032302245062095} + \frac{536643595755792\nu^2}{1206460449012419} \right) \right] \right. \\
& + \chi_s^2 \left[\frac{5865969154439}{4646902579200} \left(1 - \frac{41973254021326\nu}{17597907463317} - \frac{974298467240\nu^2}{5865969154439} \right) \kappa_s + \frac{5865969154439\delta}{4646902579200} \left(1 \right. \right. \\
& \left. \left. \left. - \frac{6777439094692\nu}{17597907463317} \right) \kappa_a - \frac{1206460449012419}{2559513940623360} \left(1 - \frac{3624177344679476\nu}{1206460449012419} - \frac{1846637721438496\nu^2}{1206460449012419} \right) \right] \right. \\
& + \chi_a \chi_s \left[\frac{5865969154439\delta}{2323451289600} \left(1 - \frac{6777439094692\nu}{17597907463317} \right) \kappa_s + \frac{5865969154439}{2323451289600} \left(1 - \frac{41973254021326\nu}{17597907463317} \right. \right. \\
& \left. \left. - \frac{974298467240\nu^2}{5865969154439} \right) \kappa_a - \frac{1206460449012419\delta}{1279756970311680} \left(1 + \frac{4493986844406388\nu}{6032302245062095} \right) \right] \left. \right\}. \tag{C8f}
\end{aligned}$$

This solution is now used on Eq. (23) to provide the time domain phasing ϕ as a function of time, $\langle\phi\rangle(t) = \langle\phi\rangle[y = y(t)]$. The secular section of the orbital phasing $\langle\phi\rangle$ as a function of θ is then given by

$$\langle\phi\rangle - \phi_c = -\frac{1}{\nu\theta^5} \left\{ \phi_{\text{circ}} - \frac{7065}{11696} e_0^2 \left(\frac{\theta_0}{\theta} \right)^{19/3} \left[\phi_{\text{SO,ecc}} + \phi_{\text{SS,ecc}} \right] \right\}, \tag{C9}$$

where,

$$\phi_{\text{NS}} = 1 - \frac{7065}{11696} e_0^2 \left(\frac{\theta_0}{\theta} \right)^{19/3} + \mathcal{O}(e_0^4), \tag{C10a}$$

$$\phi_{\text{SO,ecc}}^{1.5\text{PN}} = \theta_0^3 \left[\frac{4871\delta\chi_a}{4320} + \frac{4871}{4320} \left(1 - \frac{3232\nu}{4871} \right) \chi_s \right] + \theta^3 \left[-\frac{378643\delta\chi_a}{339120} - \frac{378643}{339120} \left(1 - \frac{739666\nu}{1893215} \right) \chi_s \right], \tag{C10b}$$

$$\begin{aligned}
\phi_{\text{SS,ecc}}^{2\text{PN}} = & \theta_0^4 \left\{ \left[\frac{7}{3072} \left(1 + \frac{2328\nu}{7} \right) - \frac{97\delta\kappa_a}{256} - \frac{97}{256} (1 - 2\nu)\kappa_s \right] \chi_a^2 + \left[-\frac{97}{128} (1 - 2\nu)\kappa_a + \delta \left(\frac{7}{1536} - \frac{97\kappa_S}{128} \right) \right] \chi_a \chi_s \right. \\
& + \left[\frac{7}{3072} \left(1 - \frac{2356\nu}{7} \right) - \frac{97\delta\kappa_a}{256} - \frac{97}{256} (1 - 2\nu)\kappa_s \right] \chi_s^2 \left. \right\} + \theta^4 \left\{ \left[-\frac{190043}{41116416} \left(1 + \frac{2102946\nu}{11179} \right) + \frac{5958347\delta\kappa_a}{13705472} \right. \right. \\
& + \frac{5958347}{13705472} (1 - 2\nu)\kappa_s \left. \right] \chi_a^2 + \left[\frac{5958347}{6852736} (1 - 2\nu)\kappa_a + \delta \left(-\frac{190043}{20558208} + \frac{5958347\kappa_s}{6852736} \right) \right] \chi_a \chi_s \right. \\
& \left. + \left[-\frac{190043}{41116416} \left(1 - \frac{2147662\nu}{11179} \right) + \frac{5958347\delta\kappa_a}{13705472} + \frac{5958347}{13705472} (1 - 2\nu)\kappa_s \right] \chi_s^2 \right\}, \tag{C10c}
\end{aligned}$$

$$\begin{aligned}
\phi_{\text{SO,ecc}}^{2.5\text{PN}} = & \theta_0^5 \left[\frac{69146501}{13063680} \left(1 - \frac{79387834\nu}{69146501} + \frac{7548240\nu^2}{69146501} \right) \chi_s + \frac{69146501}{13063680} \left(1 - \frac{19488462\nu}{69146501} \right) \delta\chi_a \right] \\
& + \theta^3 \theta_0^2 \left[-\frac{336613627}{234399744} \left(1 - \frac{444\nu}{889} \right) \delta\chi_a - \frac{336613627}{234399744} \left(1 - \frac{1498150534\nu}{1683068135} + \frac{328411704\nu^2}{1683068135} \right) \chi_s \right] \\
& + \theta^5 \left[\frac{5033550410711}{1009295997696} \left(1 + \frac{14362504401\nu}{117059311877} \right) \delta\chi_a + \frac{5033550410711}{1009295997696} \left(1 - \frac{346680975625\nu}{468237247508} \right. \right. \\
& \left. \left. - \frac{111702828657\nu^2}{585296559385} \right) \chi_s \right] + \theta^2 \theta_0^3 \left[-\frac{633230180227}{4249667358720} \left(1 - \frac{110375012044\nu}{37248834131} + \frac{56836827264\nu^2}{37248834131} \right) \chi_s \right. \\
& \left. - \frac{633230180227}{4249667358720} \left(1 - \frac{17585652\nu}{7647061} \right) \delta\chi_a \right], \tag{C10d}
\end{aligned}$$

$$\begin{aligned}
\phi_{\text{SO,ecc}}^{3\text{PN}} = & \theta_0^6 \left[-\frac{22358051\pi\delta\chi_a}{24883200} - \frac{22358051\pi}{24883200} \left(1 - \frac{16608892\nu}{22358051} \right) \chi_s \right] + \theta^6 \left[\frac{55371553\pi\delta\chi_a}{39813120} \right. \\
& + \frac{55371553\pi}{39813120} \left(1 - \frac{29754273364\nu}{43466669105} \right) \chi_s \left. \right] - \theta^3 \theta_0^3 \left[\frac{1482249323\pi\delta\chi_a}{9766656000} + \frac{1482249323\pi}{9766656000} \left(1 - \frac{920485108\nu}{1482249323} \right) \chi_s \right], \tag{C10e}
\end{aligned}$$

$$\phi_{\text{SS,ecc}}^{3\text{PN}} = \theta^2 \theta_0^4 \left\{ \chi_a \chi_s \left[\frac{12610003589}{125916069888} \left(1 - \frac{32879774\nu}{7647061} + \frac{35171304\nu^2}{7647061} \right) \kappa_a + \frac{12610003589\delta}{125916069888} \left(1 - \frac{17585652\nu}{7647061} \right) \kappa_s \right. \right.$$

$$\begin{aligned}
& - \frac{130000037\delta}{215856119808} \left(1 - \frac{17585652\nu}{7647061} \right) \Big] + \chi_s^2 \left[\frac{12610003589}{251832139776} \left(1 - \frac{32879774\nu}{7647061} + \frac{35171304\nu^2}{7647061} \right) \kappa_s \right. \\
& - \frac{130000037}{431712239616} \left(1 - \frac{18139575280\nu}{53529427} + \frac{5918828016\nu^2}{7647061} \right) + \frac{12610003589\delta}{251832139776} \left(1 - \frac{17585652\nu}{7647061} \right) \kappa_a \Big] \\
& + \chi_a^2 \left[\frac{12610003589}{251832139776} \left(1 - \frac{32879774\nu}{7647061} + \frac{35171304\nu^2}{7647061} \right) \kappa_s + \frac{12610003589\delta}{251832139776} \left(1 - \frac{17585652\nu}{7647061} \right) \kappa_a \right. \\
& - \frac{130000037}{431712239616} \left(1 + \frac{17679258444\nu}{53529427} - \frac{5848485408\nu^2}{7647061} \right) \Big] \Big\} + \theta^4 \theta_0^2 \left\{ \chi_a \chi_s \left[\frac{26484852415}{23683055616} \left(1 - \frac{2222\nu}{889} \right. \right. \right. \\
& + \frac{888\nu^2}{889} \Big) \kappa_a + \frac{26484852415\delta}{23683055616} \left(1 - \frac{444\nu}{889} \right) \kappa_s - \frac{844741135\delta}{71049166848} \left(1 - \frac{444\nu}{889} \right) \Big] + \chi_s^2 \left[\frac{26484852415}{47366111232} \left(1 - \frac{2222\nu}{889} \right. \right. \\
& + \frac{888\nu^2}{889} \Big) \kappa_s + \frac{26484852415\delta}{47366111232} \left(1 - \frac{444\nu}{889} \right) \kappa_a - \frac{844741135}{142098333696} \left(1 - \frac{273462142\nu}{1419733} + \frac{953561928\nu^2}{9938131} \right) \Big] \\
& + \chi_a^2 \left[\frac{26484852415}{47366111232} \left(1 - \frac{2222\nu}{889} + \frac{888\nu^2}{889} \right) \kappa_s + \frac{26484852415\delta}{47366111232} \left(1 - \frac{444\nu}{889} \right) \kappa_a - \frac{844741135}{142098333696} \left(1 \right. \\
& + \frac{266365074\nu}{1419733} - \frac{933708024\nu^2}{9938131} \Big) \Big] \Big\} + \theta^3 \theta_0^3 \left[- \frac{1844370053}{1464998400} (1 - 4\nu) \chi_a^2 - \frac{1844370053}{1464998400} \left(1 - \frac{9721783966\nu}{9221850265} \right. \right. \\
& + \frac{2390600512\nu^2}{9221850265} \Big) \chi_s^2 - \frac{1844370053\delta}{732499200} \left(1 - \frac{4860891983\nu}{9221850265} \right) \chi_a \chi_s \Big] + \theta_0^6 \left\{ \chi_s^2 \left[- \frac{15796363}{6193152} \left(1 - \frac{38091274\nu}{15796363} \right. \right. \right. \\
& + \frac{3292968\nu^2}{15796363} \Big) \kappa_s - \frac{15796363\delta}{6193152} \left(1 - \frac{6498548\nu}{15796363} \right) \kappa_a + \frac{29393895511}{16721510400} \left(1 - \frac{84309055624\nu}{29393895511} + \frac{4422254704\nu^2}{29393895511} \right) \Big] \\
& + \chi_a \chi_s \left[- \frac{15796363}{3096576} \left(1 - \frac{38091274\nu}{15796363} + \frac{3292968\nu^2}{15796363} \right) \kappa_a - \frac{15796363\delta}{3096576} \left(1 - \frac{6498548\nu}{15796363} \right) \kappa_s \right. \\
& + \frac{29393895511\delta}{8360755200} \left(1 - \frac{3294795812\nu}{29393895511} \right) \Big] + \chi_a^2 \left[- \frac{15796363}{6193152} \left(1 - \frac{38091274\nu}{15796363} + \frac{3292968\nu^2}{15796363} \right) \kappa_s \right. \\
& - \frac{15796363\delta}{6193152} \left(1 - \frac{6498548\nu}{15796363} \right) \kappa_a + \frac{29393895511}{16721510400} \left(1 - \frac{39856118044\nu}{29393895511} - \frac{8891013600\nu^2}{29393895511} \right) \Big] \Big\} \\
& + \theta^6 \left\{ \chi_a^2 \left[\frac{99721475625463}{37175220633600} \left(1 - \frac{41973254021326\nu}{17597907463317} - \frac{974298467240\nu^2}{5865969154439} \right) \kappa_s + \frac{99721475625463\delta}{37175220633600} \left(1 \right. \right. \\
& - \frac{6777439094692\nu}{17597907463317} \Big) \kappa_a - \frac{1206460449012419}{1204477148528640} \left(1 + \frac{2979651431961776\nu}{6032302245062095} + \frac{536643595755792\nu^2}{1206460449012419} \right) \Big] \\
& + \chi_s^2 \left[\frac{99721475625463}{37175220633600} \left(1 - \frac{41973254021326\nu}{17597907463317} - \frac{974298467240\nu^2}{5865969154439} \right) \kappa_s + \frac{99721475625463\delta}{37175220633600} \left(1 \right. \\
& - \frac{6777439094692\nu}{17597907463317} \Big) \kappa_a - \frac{1206460449012419}{1204477148528640} \left(1 - \frac{3624177344679476\nu}{1206460449012419} - \frac{1846637721438496\nu^2}{1206460449012419} \right) \Big] \\
& + \chi_a \chi_s \left[\frac{99721475625463}{18587610316800} \left(1 - \frac{41973254021326\nu}{17597907463317} - \frac{974298467240\nu^2}{5865969154439} \right) \kappa_a \right. \\
& + \frac{99721475625463\delta}{18587610316800} \left(1 - \frac{6777439094692\nu}{17597907463317} \right) \kappa_s - \frac{1206460449012419\delta}{602238574264320} \left(1 + \frac{4493986844406388\nu}{6032302245062095} \right) \Big] \Big\}. \quad (\text{C10f})
\end{aligned}$$

3. TaylorT4

$$\begin{aligned}
\frac{dy}{dt} = \frac{32y^9\nu}{5M} \left\{ \rho_{\text{circ}} - \frac{5}{8} e_0^2 \left(\frac{y_0}{y} \right)^{19/3} \left[\rho_{\text{SO,ecc}} + \rho_{\text{SS,ecc}} \right] \right. \\
\left. - \frac{725}{2432} e_0^4 \left(\frac{y_0}{y} \right)^{19/3} \left[\dots + \mathcal{O}(y^6) + \frac{311}{145} \left(\frac{y_0}{y} \right)^{19/3} \left[\dots + \mathcal{O}(y^6) \right] \right] + \mathcal{O}(e_0^8) \right\}, \quad (\text{C11})
\end{aligned}$$

where,

$$\rho_{\text{NS}} = 1 - \frac{5}{8} e_0^2 \left(\frac{y_0}{y} \right)^{19/3} - \frac{725}{2432} e_0^4 \left(\frac{y_0}{y} \right)^{19/3} \left[1 + \frac{311}{145} \left(\frac{y_0}{y} \right)^{19/3} \right] + \mathcal{O}(e_0^6), \quad (\text{C12a})$$

$$\rho_{\text{SO,ecc}}^{1.5\text{PN}} = y^3 \left[\frac{4691\delta\chi_A}{270} + \frac{4691}{270} \left(1 + \frac{782\nu}{4691} \right) \chi_s \right] + y_0^3 \left[-\frac{157\delta\chi_a}{54} - \frac{157}{54} \left(1 - \frac{110\nu}{157} \right) \chi_s \right], \quad (\text{C12b})$$

$$\begin{aligned} \rho_{\text{SS,ecc}}^{2\text{PN}} = & y_0^4 \left\{ \chi_a \chi_s \left[\delta \left(\frac{13}{48} + \frac{89\kappa_s}{24} \right) + \frac{89}{24} (1 - 2\nu) \kappa_a \right] + \chi_a^2 \left[\frac{13}{96} + \frac{89\delta\kappa_a}{48} - \frac{89\nu}{24} + \frac{89}{48} (1 - 2\nu) \kappa_s \right] \right. \\ & + \chi_s^2 \left[\frac{13}{96} + \frac{89\delta\kappa_a}{48} + \frac{19\nu}{6} + \frac{89}{48} (1 - 2\nu) \kappa_s \right] \left. \right\} + y^4 \left\{ \chi_a \chi_s \left[\delta \left(-\frac{137}{240} - \frac{2749\kappa_s}{120} \right) - \frac{2749}{120} (1 - 2\nu) \kappa_a \right] \right. \\ & - \chi_s^2 \left[\frac{137}{480} + \frac{2749\delta\kappa_a}{240} + \frac{653\nu}{30} + \frac{2749}{240} (1 - 2\nu) \kappa_s \right] + \chi_a^2 \left[-\frac{137}{480} - \frac{2749\delta\kappa_a}{240} + \frac{2749\nu}{120} - \frac{2749}{240} (1 - 2\nu) \kappa_s \right] \left. \right\}, \quad (\text{C12c}) \end{aligned}$$

$$\begin{aligned} \rho_{\text{SO,ecc}}^{2.5\text{PN}} = & -y_0^5 \left[\frac{1279073}{38880} \left(1 - \frac{2348912\nu}{1279073} + \frac{691520\nu^2}{1279073} \right) \chi_s + \frac{1279073}{38880} \left(1 - \frac{970876\nu}{1279073} \right) \delta\chi_a \right] \\ & + y^2 y_0^3 \left[\frac{5917801}{54432} \left(1 - \frac{28308\nu}{37693} \right) \delta\chi_a + \frac{5917801}{54432} \left(1 - \frac{8590586\nu}{5917801} + \frac{3113880\nu^2}{5917801} \right) \chi_s \right] \\ & + y^3 y_0^2 \left[\frac{13289603}{272160} \left(1 - \frac{5516\nu}{2833} \right) \delta\chi_a + \frac{13289603}{272160} \left(1 - \frac{23660150\nu}{13289603} - \frac{4313512\nu^2}{13289603} \right) \chi_s \right] \\ & + y^5 \left[\frac{105998407}{272160} \left(1 - \frac{84843948\nu}{105998407} \right) \delta\chi_a + \frac{105998407}{272160} \left(1 - \frac{193354904\nu}{105998407} + \frac{53724048\nu^2}{105998407} \right) \chi_s \right], \quad (\text{C12d}) \end{aligned}$$

$$\begin{aligned} \rho_{\text{SO,ecc}}^{3\text{PN}} = & y_0^6 \left[-\frac{157043\pi\delta\chi_a}{15552} - \frac{157043\pi}{15552} \left(1 - \frac{150652\nu}{157043} \right) \chi_s \right] + y^3 y_0^3 \left[\frac{654587\pi\delta\chi_a}{4860} \right. \\ & + \left. \frac{654587\pi}{4860} \left(1 - \frac{75154\nu}{654587} \right) \chi_s \right] + y^6 \left[\frac{13328783\pi\delta\chi_a}{77760} + \frac{13328783\pi}{77760} \left(1 - \frac{367804\nu}{1025291} \right) \chi_s \right], \quad (\text{C12e}) \end{aligned}$$

$$\begin{aligned} \rho_{\text{SS,ecc}}^{3\text{PN}} = & -y^4 y_0^2 \left\{ \chi_a \chi_s \left[\frac{7787917}{120960} \left(1 - \frac{11182\nu}{2833} + \frac{11032\nu^2}{2833} \right) \kappa_a + \frac{7787917\delta}{120960} \left(1 - \frac{5516\nu}{2833} \right) \kappa_s + \frac{388121\delta}{241920} \left(1 - \frac{5516\nu}{2833} \right) \right] \right. \\ & + \chi_a^2 \left[\frac{7787917}{241920} \left(1 - \frac{11182\nu}{2833} + \frac{11032\nu^2}{2833} \right) \kappa_s + \frac{7787917\delta}{241920} \left(1 - \frac{5516\nu}{2833} \right) \kappa_a + \frac{388121}{483840} \left(1 - \frac{31907360\nu}{388121} \right) \right. \\ & + \left. \frac{60653936\nu^2}{388121} \right] + \chi_s^2 \left[\frac{7787917}{241920} \left(1 - \frac{11182\nu}{2833} + \frac{11032\nu^2}{2833} \right) \kappa_s + \frac{7787917\delta}{241920} \left(1 - \frac{5516\nu}{2833} \right) \kappa_A + \frac{388121}{483840} \left(1 - \frac{28843492\nu}{388121} - \frac{57631168\nu^2}{388121} \right) \right] \left. \right\} - y^2 y_0^4 \left\{ \chi_a \chi_s \left[\frac{3354677}{24192} \left(1 - \frac{103694\nu}{37693} + \frac{56616\nu^2}{37693} \right) \kappa_a + \frac{3354677\delta}{24192} \left(1 - \frac{28308\nu}{37693} \right) \kappa_s + \frac{490009\delta}{48384} \left(1 - \frac{28308\nu}{37693} \right) \right] \right. \\ & + \chi_a^2 \left[\frac{3354677}{48384} \left(1 - \frac{103694\nu}{37693} + \frac{56616\nu^2}{37693} \right) \kappa_s + \frac{3354677\delta}{48384} \left(1 - \frac{28308\nu}{37693} \right) \kappa_a + \frac{490009}{96768} \left(1 - \frac{13786712\nu}{490009} + \frac{10077648\nu^2}{490009} \right) \right] + \chi_s^2 \left[\frac{3354677}{48384} \left(1 - \frac{103694\nu}{37693} + \frac{56616\nu^2}{37693} \right) \kappa_s \right. \\ & + \left. \frac{3354677\delta}{48384} \left(1 - \frac{28308\nu}{37693} \right) \kappa_a + \frac{490009}{96768} \left(1 + \frac{11090668\nu}{490009} - \frac{8605632\nu^2}{490009} \right) \right] \left. \right\} + y_0^6 \left\{ \chi_a^2 \left[\frac{906103}{48384} \left(1 - \frac{2893874\nu}{906103} \right) \right. \right. \\ & + \left. \frac{1359176\nu^2}{906103} \right] \kappa_s + \frac{906103\delta}{48384} \left(1 - \frac{1081668\nu}{906103} \right) \kappa_a + \frac{24433195}{2612736} \left(1 - \frac{169526104\nu}{24433195} + \frac{73395504\nu^2}{24433195} \right) \right] \\ & + \chi_a \chi_s \left[\frac{906103}{24192} \left(1 - \frac{2893874\nu}{906103} + \frac{1359176\nu^2}{906103} \right) \kappa_a + \frac{906103\delta}{24192} \left(1 - \frac{1081668\nu}{906103} \right) \kappa_s + \frac{24433195\delta}{1306368} \left(1 - \frac{33561668\nu}{24433195} \right) \right] + \chi_s^2 \left[\frac{906103}{48384} \left(1 - \frac{2893874\nu}{906103} + \frac{1359176\nu^2}{906103} \right) \kappa_s + \frac{906103\delta}{48384} \left(1 - \frac{1081668\nu}{906103} \right) \kappa_a \right. \\ & + \left. \frac{24433195}{2612736} \left(1 + \frac{4669988\nu}{24433195} - \frac{42904736\nu^2}{24433195} \right) \right] \left. \right\} + y^6 \left\{ \chi_a^2 \left[-\frac{7161173\delta}{26880} \left(1 - \frac{2082500\nu}{2222433} \right) \kappa_a - \frac{7161173}{26880} \left(1 \right. \right. \right. \end{aligned}$$

$$\begin{aligned}
& - \frac{6527366\nu + 9540328\nu^2}{2222433} + \frac{9540328\nu^2}{7161173} \Big) \kappa_s - \frac{599862209}{2612736} \left(1 - \frac{17949354544\nu}{2999311045} + \frac{4636599408\nu^2}{2999311045} \right) \Big] + \chi_a \chi_s \left[- \frac{7161173\delta}{13440} \right. \\
& \times \left(1 - \frac{2082500\nu}{2222433} \Big) \kappa_s - \frac{7161173}{13440} \left(1 - \frac{6527366\nu}{2222433} + \frac{9540328\nu^2}{7161173} \Big) \kappa_a - \frac{599862209\delta}{1306368} \left(1 - \frac{1572186644\nu}{2999311045} \right) \right] \\
& + \chi_s^2 \left[- \frac{7161173\delta}{26880} \left(1 - \frac{2082500\nu}{2222433} \Big) \kappa_a - \frac{7161173}{26880} \left(1 - \frac{6527366\nu}{2222433} + \frac{9540328\nu^2}{7161173} \Big) \kappa_s \right. \right. \\
& \left. \left. - \frac{599862209}{2612736} \left(1 + \frac{2807737076\nu}{2999311045} - \frac{4131331232\nu^2}{2999311045} \right) \right] \right\} - y^3 y_0^3 \left[\frac{736487\delta}{7290} \left(1 - \frac{196618\nu}{736487} \right) \chi_a \chi_s \right. \\
& \left. + \frac{736487}{14580} \left(1 - \frac{393236\nu}{736487} - \frac{86020\nu^2}{736487} \right) \chi_s^2 + \frac{736487}{14580} (1 - 4\nu) \chi_a^2 \right]. \tag{C12f}
\end{aligned}$$

-
- [1] B. P. Abbott *et al.* (LIGO Scientific, Virgo), *Phys. Rev. Lett.* **116**, 061102 (2016), arXiv:1602.03837 [gr-qc].
- [2] B. P. Abbott *et al.* (LIGO Scientific, Virgo), *Phys. Rev. Lett.* **119**, 161101 (2017), arXiv:1710.05832 [gr-qc].
- [3] B. P. Abbott *et al.* (LIGO Scientific, Virgo), *Astrophys. J. Lett.* **892**, L3 (2020), arXiv:2001.01761 [astro-ph.HE].
- [4] R. Abbott *et al.* (LIGO Scientific, KAGRA, VIRGO), *Astrophys. J. Lett.* **915**, L5 (2021), arXiv:2106.15163 [astro-ph.HE].
- [5] J. Aasi *et al.* (LIGO Scientific), *Class. Quant. Grav.* **32**, 074001 (2015), arXiv:1411.4547 [gr-qc].
- [6] F. Acernese *et al.* (VIRGO), *Class. Quant. Grav.* **32**, 024001 (2015), arXiv:1408.3978 [gr-qc].
- [7] B. P. Abbott *et al.* (LIGO Scientific, Virgo), *Phys. Rev. X* **9**, 031040 (2019), arXiv:1811.12907 [astro-ph.HE].
- [8] R. Abbott *et al.* (LIGO Scientific, Virgo), *Phys. Rev. X* **11**, 021053 (2021), arXiv:2010.14527 [gr-qc].
- [9] R. Abbott *et al.* (LIGO Scientific, VIRGO), *Phys. Rev. D* **109**, 022001 (2024), arXiv:2108.01045 [gr-qc].
- [10] R. Abbott *et al.* (KAGRA, VIRGO, LIGO Scientific), *Phys. Rev. X* **13**, 041039 (2023), arXiv:2111.03606 [gr-qc].
- [11] C. Cutler and E. E. Flanagan, *Phys. Rev. D* **49**, 2658 (1994), arXiv:gr-qc/9402014.
- [12] E. Poisson and C. M. Will, *Phys. Rev. D* **52**, 848 (1995), arXiv:gr-qc/9502040.
- [13] A. Krolak, K. D. Kokkotas, and G. Schaefer, *Phys. Rev. D* **52**, 2089 (1995), arXiv:gr-qc/9503013.
- [14] B. P. Abbott *et al.* (LIGO Scientific, Virgo), *Phys. Rev. D* **93**, 122003 (2016), arXiv:1602.03839 [gr-qc].
- [15] L. Blanchet, *Living Rev. Rel.* **17**, 2 (2014), arXiv:1310.1528 [gr-qc].
- [16] <http://www.black-holes.org/waveforms>.
- [17] J. Healy and C. O. Lousto, *Phys. Rev. D* **105**, 124010 (2022), arXiv:2202.00018 [gr-qc].
- [18] D. Ferguson *et al.*, (2023), arXiv:2309.00262 [gr-qc].
- [19] A. Pound and B. Wardell, (2021), 10.1007/978-981-15-4702-7_38-1, arXiv:2101.04592 [gr-qc].
- [20] P. C. Peters and J. Mathews, *Phys. Rev.* **131**, 435 (1963).
- [21] P. C. Peters, *Phys. Rev.* **136**, B1224 (1964).
- [22] Y. Kozai, *Astron. J.* **67**, 591 (1962).
- [23] M. Lidov, *Planetary and Space Science* **9**, 719 (1962).
- [24] J. Samsing, M. MacLeod, and E. Ramirez-Ruiz, *Astrophys. J.* **784**, 71 (2014), arXiv:1308.2964 [astro-ph.HE].
- [25] C. L. Rodriguez, S. Chatterjee, and F. A. Rasio, *Phys. Rev. D* **93**, 084029 (2016), arXiv:1602.02444 [astro-ph.HE].
- [26] F. Antonini, S. Chatterjee, C. L. Rodriguez, M. Morscher, B. Pattabiraman, V. Kalogera, and F. A. Rasio, *Astrophys. J.* **816**, 65 (2016), arXiv:1509.05080 [astro-ph.GA].
- [27] L. Chomiuk, J. Strader, T. J. Maccarone, J. C. A. Miller-Jones, C. Heinke, E. Noyola, A. C. Seth, and S. Ransom, *Astrophys. J.* **777**, 69 (2013), arXiv:1306.6624 [astro-ph.HE].
- [28] J. Strader, L. Chomiuk, T. Maccarone, J. Miller-Jones, and A. Seth, *Nature* **490**, 71 (2012), arXiv:1210.0901 [astro-ph.HE].
- [29] T. Osburn, N. Warburton, and C. R. Evans, *Phys. Rev. D* **93**, 064024 (2016), arXiv:1511.01498 [gr-qc].
- [30] J. H. VanLandingham, M. C. Miller, D. P. Hamilton, and D. C. Richardson, *Astrophys. J.* **828**, 77 (2016), arXiv:1604.04948 [astro-ph.HE].
- [31] B.-M. Hoang, S. Naoz, B. Kocsis, F. A. Rasio, and F. Dosopoulou, *Astrophys. J.* **856**, 140 (2018), arXiv:1706.09896 [astro-ph.HE].
- [32] L. Gondán, B. Kocsis, P. Raffai, and Z. Frei, *Astrophys. J.* **855**, 34 (2018), arXiv:1705.10781 [astro-ph.HE].
- [33] L. Gondán and B. Kocsis, *Mon. Not. Roy. Astron. Soc.* **506**, 1665 (2021), arXiv:2011.02507 [astro-ph.HE].
- [34] J. Kumamoto, M. S. Fujii, and A. Tanikawa, *Mon. Not. Roy. Astron. Soc.* **486**, 3942 (2019), arXiv:1811.06726 [astro-ph.HE].
- [35] G. Fragione and B. Kocsis, *Mon. Not. Roy. Astron. Soc.* **486**, 4781 (2019), arXiv:1903.03112 [astro-ph.GA].
- [36] R. M. O’Leary, F. A. Rasio, J. M. Fregeau, N. Ivanova, and R. W. O’Shaughnessy, *Astrophys. J.* **637**, 937 (2006), arXiv:astro-ph/0508224.
- [37] B. Allen, W. G. Anderson, P. R. Brady, D. A. Brown, and J. D. E. Creighton, *Phys. Rev. D* **85**, 122006 (2012), arXiv:gr-qc/0509116.
- [38] S. A. Bhat, P. Saini, M. Favata, and K. G. Arun, *Phys. Rev. D* **107**, 024009 (2023), arXiv:2207.13761 [gr-qc].
- [39] A. Chattaraj, T. Roychowdhury, Divyajyoti, C. K. Mishra, and A. Gupta, *Phys. Rev. D* **106**, 124008 (2022), arXiv:2204.02377 [gr-qc].
- [40] M. Favata, *Phys. Rev. Lett.* **112**, 101101 (2014), arXiv:1310.8288 [gr-qc].

- [41] Divyajyoti, S. Kumar, S. Tibrewal, I. M. Romero-Shaw, and C. K. Mishra, *Phys. Rev. D* **109**, 043037 (2024), [arXiv:2309.16638 \[gr-qc\]](#).
- [42] Y. Cui *et al.*, *Nature* **621**, 711 (2023), [arXiv:2310.09015 \[astro-ph.HE\]](#).
- [43] A. Taracchini, Y. Pan, A. Buonanno, E. Barausse, M. Boyle, T. Chu, G. Lovelace, H. P. Pfeiffer, and M. A. Scheel, *Phys. Rev. D* **86**, 024011 (2012), [arXiv:1202.0790 \[gr-qc\]](#).
- [44] A. Ramos-Buades, S. Husa, G. Pratten, H. Estellés, C. García-Quirós, M. Mateu-Lucena, M. Colleoni, and R. Jaume, *Phys. Rev. D* **101**, 083015 (2020), [arXiv:1909.11011 \[gr-qc\]](#).
- [45] E. O’Shea and P. Kumar, *Phys. Rev. D* **108**, 104018 (2023), [arXiv:2107.07981 \[astro-ph.HE\]](#).
- [46] A. Klein, N. Cornish, and N. Yunes, *Phys. Rev. D* **88**, 124015 (2013), [arXiv:1305.1932 \[gr-qc\]](#).
- [47] E. A. Huerta, P. Kumar, S. T. McWilliams, R. O’Shaughnessy, and N. Yunes, *Phys. Rev. D* **90**, 084016 (2014), [arXiv:1408.3406 \[gr-qc\]](#).
- [48] B. Moore, T. Robson, N. Loutrel, and N. Yunes, *Class. Quant. Grav.* **35**, 235006 (2018), [arXiv:1807.07163 \[gr-qc\]](#).
- [49] A. Klein, Y. Boetzel, A. Gopakumar, P. Jetzer, and L. de Vittori, *Phys. Rev. D* **98**, 104043 (2018), [arXiv:1801.08542 \[gr-qc\]](#).
- [50] S. Tanay, A. Klein, E. Berti, and A. Nishizawa, *Phys. Rev. D* **100**, 064006 (2019), [arXiv:1905.08811 \[gr-qc\]](#).
- [51] X. Liu, Z. Cao, and L. Shao, *Phys. Rev. D* **101**, 044049 (2020), [arXiv:1910.00784 \[gr-qc\]](#).
- [52] S. Tiwari and A. Gopakumar, *Phys. Rev. D* **102**, 084042 (2020), [arXiv:2009.11333 \[gr-qc\]](#).
- [53] A. Klein, (2021), [arXiv:2106.10291 \[gr-qc\]](#).
- [54] K. Paul and C. K. Mishra, *Phys. Rev. D* **108**, 024023 (2023), [arXiv:2211.04155 \[gr-qc\]](#).
- [55] E. A. Huerta *et al.*, *Phys. Rev. D* **95**, 024038 (2017), [arXiv:1609.05933 \[gr-qc\]](#).
- [56] T. Hinderer and S. Babak, *Phys. Rev. D* **96**, 104048 (2017), [arXiv:1707.08426 \[gr-qc\]](#).
- [57] I. Hinder, L. E. Kidder, and H. P. Pfeiffer, *Phys. Rev. D* **98**, 044015 (2018), [arXiv:1709.02007 \[gr-qc\]](#).
- [58] E. A. Huerta *et al.*, *Phys. Rev. D* **97**, 024031 (2018), [arXiv:1711.06276 \[gr-qc\]](#).
- [59] Z. Chen, E. A. Huerta, J. Adamo, R. Haas, E. O’Shea, P. Kumar, and C. Moore, *Phys. Rev. D* **103**, 084018 (2021), [arXiv:2008.03313 \[gr-qc\]](#).
- [60] D. Chiaramello and A. Nagar, *Phys. Rev. D* **101**, 101501 (2020), [arXiv:2001.11736 \[gr-qc\]](#).
- [61] P. Manna, T. RoyChowdhury, and C. K. Mishra, (2024), [arXiv:2409.10672 \[gr-qc\]](#).
- [62] K. Paul, A. Maurya, Q. Henry, K. Sharma, P. Satheesh, Divyajyoti, P. Kumar, and C. K. Mishra, (2024), [arXiv:2409.13866 \[gr-qc\]](#).
- [63] C. K. Mishra, K. G. Arun, and B. R. Iyer, *Phys. Rev. D* **91**, 084040 (2015), [arXiv:1501.07096 \[gr-qc\]](#).
- [64] K. G. Arun, A. Buonanno, G. Faye, and E. Ochsner, *Phys. Rev. D* **79**, 104023 (2009), [Erratum: *Phys.Rev.D* 84, 049901 (2011)], [arXiv:0810.5336 \[gr-qc\]](#).
- [65] A. Buonanno, G. Faye, and T. Hinderer, *Phys. Rev. D* **87**, 044009 (2013), [arXiv:1209.6349 \[gr-qc\]](#).
- [66] Q. Henry, S. Marsat, and M. Khalil, *Phys. Rev. D* **106**, 124018 (2022), [arXiv:2209.00374 \[gr-qc\]](#).
- [67] L. E. Kidder, C. M. Will, and A. G. Wiseman, *Phys. Rev. D* **47**, R4183 (1993), [arXiv:gr-qc/9211025](#).
- [68] L. E. Kidder, *Phys. Rev. D* **52**, 821 (1995), [arXiv:gr-qc/9506022](#).
- [69] M. Vasuth and J. Majar, *Int. J. Mod. Phys. A* **22**, 2405 (2007), [arXiv:0705.3481 \[gr-qc\]](#).
- [70] J. Majar and M. Vasuth, *Phys. Rev. D* **77**, 104005 (2008), [arXiv:0806.2273 \[gr-qc\]](#).
- [71] M. Khalil, A. Buonanno, J. Steinhoff, and J. Vines, *Phys. Rev. D* **104**, 024046 (2021), [arXiv:2104.11705 \[gr-qc\]](#).
- [72] Q. Henry and M. Khalil, *Phys. Rev. D* **108**, 104016 (2023), [arXiv:2308.13606 \[gr-qc\]](#).
- [73] L. Blanchet, T. Damour, and B. R. Iyer, *Phys. Rev. D* **51**, 5360 (1995), [Erratum: *Phys.Rev.D* 54, 1860 (1996)], [arXiv:gr-qc/9501029](#).
- [74] L. Blanchet, T. Damour, G. Esposito-Farese, and B. R. Iyer, *Phys. Rev. Lett.* **93**, 091101 (2004), [arXiv:gr-qc/0406012](#).
- [75] L. Blanchet, G. Faye, Q. Henry, F. Larrouturou, and D. Trestini, *Phys. Rev. Lett.* **131**, 121402 (2023), [arXiv:2304.11185 \[gr-qc\]](#).
- [76] B. Moore, M. Favata, K. G. Arun, and C. K. Mishra, *Phys. Rev. D* **93**, 124061 (2016), [arXiv:1605.00304 \[gr-qc\]](#).
- [77] B. Moore and N. Yunes, *Class. Quant. Grav.* **36**, 185003 (2019), [arXiv:1903.05203 \[gr-qc\]](#).
- [78] N. V. Krishnendu, K. G. Arun, and C. K. Mishra, *Phys. Rev. Lett.* **119**, 091101 (2017), [arXiv:1701.06318 \[gr-qc\]](#).
- [79] Divyajyoti, N. V. Krishnendu, M. Saleem, M. Colleoni, A. Vijaykumar, K. G. Arun, and C. K. Mishra, *Phys. Rev. D* **109**, 023016 (2024), [arXiv:2311.05506 \[gr-qc\]](#).
- [80] L. Blanchet and G. Schaefer, *Mon. Not. Roy. Astron. Soc.* **239**, 845 (1989), [Erratum: *Mon.Not.Roy.Astron.Soc.* 242, 704 (1990)].
- [81] Y. Boetzel, A. Susobhanan, A. Gopakumar, A. Klein, and P. Jetzer, *Phys. Rev. D* **96**, 044011 (2017), [arXiv:1707.02088 \[gr-qc\]](#).
- [82] C. Van Den Broeck and A. S. Sengupta, *Class. Quantum Grav.* **24**, 1089 (2007), [arXiv:gr-qc/0610126](#).
- [83] R. Memmesheimer, A. Gopakumar, and G. Schäfer, *Phys. Rev. D* **70**, 104011 (2004), [gr-qc/0407049](#).
- [84] A. Buonanno, B. R. Iyer, E. Ochsner, Y. Pan, and B. S. Sathyaprakash, *Phys. Rev. D* **80**, 084043 (2009), [arXiv:0907.0700 \[gr-qc\]](#).
- [85] M. Pürrer, *Class. Quant. Grav.* **31**, 195010 (2014), [arXiv:1402.4146 \[gr-qc\]](#).